Aus der Augenklinik und Poliklinik

der Universitätsmedizin der Johannes Gutenberg-Universität Mainz

Identification of clinical biomarkers in dry eye disease using a targeted proteomics approach

Identifizierung klinischer Biomarker für das trockene Augen-Syndrom mithilfe eines gezielten proteomischen Ansatzes

Inauguraldissertation

zur Erlangung des Doktorgrades der Medizin

der Universitätsmedizin

der Johannes Gutenberg-Universität Mainz

Vorgelegt von

Alexandra Tschäbunin

aus Ludwigsburg

Mainz, 2020

Tag der Promotion: 08. Dezember 2020

TABLE OF CONTENTS

LIST OF ABBREVIATIONS

%	percentage
&	and
<	less than
>	more than
°C	degree Celsius
µg	microgram
µl	microliter
2DE	two-dimensional electrophoresis
ACN	acetonitrile
AIMS	accurate inclusion mass screening
a.u.	arbitrary unit
CHCA	α-cyano-4- hydroxy cinnamic acid
CTRL	healthy subjects/control group
DAP	differentially abundant proteins
DES	dry eye syndrome
DRYaq	aqueous deficient DES
DRYaqlip	aqueous and lipid deficient DES
DRYlip	lipid deficient DES
e.g.	for example
FDR	false discovery rate
GOBP	gene ontology biological process
GOCC	gene ontology cellular components
GOMF	gene ontology molecular functions
LC	liquid chromatography
LFQ	label-free quantification
m/z	mass to charge ratio
MALDI	matrix-assisted laser desorption/ionization
min	minute
ml	milliliter
MS	mass spectrometry
MS/MS	tandem mass spectrometry
n.s.	non-significant
PBS	phosphate-buffered saline

PTM	post-translational modification
SELDI	surface enhanced laser desorption ionization
TBUT	tear film break-up time
TFA	trifluoroacetic acid
TFOS	tear film and ocular surface
TOF	time of flight

LIST OF FIGURES

LIST OF TABLES

1. **INTRODUCTION**

The dry eye syndrome (DES) is a common disease that affects as much as one-third of the world's population with symptoms like ocular pain, visual impairment and inflammation of the eye [1-5]. While its relevance for patients' welfare and clinical practice has been underestimated in the past, recent studies have identified it as one of the most frequent reasons for patients to see an ophthalmologist, emphasizing both the distress caused by DES for the patient and its clinical importance for medicine [5, 6]. Though there is a staggering prevalence of DES patients, diagnostics and treatments remain a challenge to this day.

This is partly due to the DES being in fact not one single disease, but an assortment of conditions leading to similar ocular symptoms revolving around hyperosmolarity and inflammation [5]. In order to differentiate this variety of conditions, the syndrome is most commonly divided into DES caused by a lack of tear production and DES induced by the instability of the tear film lipid layer, as well as a combination of the two. These disease states lead to changes in the tear film which can be measured by several clinical tests, most of which are based on patient questionnaires or descriptive parameters, leading to poor correlations between the level of symptoms, diagnostic test results, and actual DES disease stage [7, 8]. Unfortunately, treatments are therefore based on symptom control rather than causal therapy due to a lack of knowledge about its pathophysiology.

In an effort to understand the mechanism behind the DES and hence, improve clinical diagnostics and treatments, scientific research has focused on measuring differentially expressed molecules in tears of DES patients, especially proteins [9]. Mass spectrometry-based (MS) approaches are widely used for this purpose because of their precision and versatility [10]. In so-called MS discovery stage studies, researchers were able to establish protein profiles of DES subgroups and identify potential biomarker candidates by measuring as many proteins in pooled samples as possible [11-23]. For clinical purposes, these potential biomarker candidates need to be verified in a larger cohort of individual samples. Considering the immense time span it takes to measure an entire sample's protein content, researchers have been employing several targeted methods for this intent, including the Accurate Inclusion Mass Screening (AIMS) [24]. This method allows the identification and quantification of a previously specified list of peptides, which makes

these measurements fast as well as highly specific. Moreover, measuring individual samples enables investigations for interpersonal protein changes and their underlying mechanisms, especially concerning age and gender, since DES is known to occur more frequently in women and higher ages, which is a vital step toward personalized medicine in DES and disease prevention [3, 25, 26].

Nevertheless, some highly abundant proteins in tears are not measured well with the currently used MS methods, leading to false negative results in preceding studies. Consequently, the methods used need to be optimized. Particularly in the case of proline-rich protein 4 (PRR4), which is one of the most abundant proteins in tears, identification and quantification *via* MS has proven to be an ongoing challenge [27, 28]. Presumably, this is due to its amino acid sequence not being fully uncovered and each person expressing a distinct combination of PRR4 isoforms. Protein identification in targeted MS measurements, as well as statistical comparisons between samples, is therefore challenging. Gaining more information about this protein and its behavior in MS is therefore crucial in order to optimize currently used measurement techniques.

The situation, therefore, calls for a different view on PRR4, preferably one that involves as little sample manipulation as possible. An easy and fast proteomics method that presents itself in this matter is the matrix-assisted laser desorption time-of-flight mass spectrometry (MALDI-TOF-MS), which separates a sample's peptides according to their mass and charge. Resulting spectra can then be used to evaluate the previously established isoforms of PRR4, their abundance and their performance in complex samples. Since individual tear samples have not been measured in this way before, a MALDI-TOF-MS method needs to be established for this purpose.

The aims of this study are therefore as follows:

1. To optimize a robust targeted proteomics strategy for clinical biomarker discovery and to further unravel the underlying pathophysiological mechanisms of the dry eye syndrome.

2. To establish a rapid and reliable MS-based analysis utilizing MALDI-TOF to identify the highly abundant tear protein PRR4.

2. LITERATURE DISCUSSION

2.1 Dry eye syndrome (DES)

According to the revised definition of the Tear Film and Ocular Surface Society Dry Eye Workshop II (TFOS DEWS II), the DES is a multifactorial disease of the ocular surface that causes loss of tear film homeostasis, which ultimately leads to ocular symptoms [5]. Rather than seeing DES as one single disease, this new definition recognizes it as a term representing a multitude of conditions that result in a common pathway of hyperosmolarity and inflammation.

Depending on diagnosis criteria, age, gender, and ethnicity, prevalence varies from 5 to 50% [2-4, 25, 29-33]. While it is most common among Asians, women, and patients over 50 years of age, an increased incidence in office workers and younger populations can be noted recently, presumably because of the expanding use of digital devices [25, 34, 35], making DES a widespread and growing ophthalmological concern. It diminishes the patient's quality of life substantially by ocular symptoms such as discomfort, foreign body sensation, visual disturbances and an unstable tear film resulting in damage and inflammation of the eye [36, 37]. Sixty percent of dry eye patients report reduced quality of life in everyday activities, which is comparable to people suffering from angina pectoris [38-40], while 38% even state reduced levels of work efficiency because of their symptoms [41, 42]. Even neurosensory abnormalities [5], psychosomatic symptoms like depression and anxiety [43-45] and sleep disorders have been correlated to the disease [46, 47]. Both the abundance of cases and the potential severity of symptoms make DES not only a burden for patients but the healthcare system as well with direct costs per dry eye patient ranging from 270 to 1100 USD a year globally [48] and an estimated annual 55 billion USD DES-related financial burden in the United States alone [49].

2.2 Tear film

The tear film is a fluid harboring many crucial functions such as nourishing, protecting and moisturizing the ocular surface, while also being the primary refracting surface for light entering the eye. Amongst other things, it contains metabolites, electrolytes, antimicrobial peptides, proteins and soluble immunoglobins [50]. Tear film homeostasis was found to be of extensive importance for the maintenance of physiological eye functions [5, 51]. It represents a balance between all tear film

components and therefore their respective production or regulation sites. The intricate system maintaining tear integrity is often referred to as the lacrimal functional unit, consisting of the cornea, conjunctiva, lacrimal gland, accessory lacrimal glands, meibomian glands, and an interconnecting innervation regulating the entire coordination [51-53]. The complex system behind tear film production and balancing is not yet fully discovered and remains a topic of intensive research [51].

In order to simplify this intricacy, the tear film is often illustrated as consisting of three layers, comprising a lipid, an aqueous and a mucous one, as shown in **Figure 1;** even though there was found to be no distinct separation between them in clinical settings [54]. The lipid layer is mostly understood as a manifold mixture of polar phospholipids and non-polar lipids primarily derived from the meibomian glands, preventing evaporation of the mucin and aqueous layers. However, more current studies indicate that the lipid layer is only responsible for a small fraction of evaporation prevention [55]. It is believed to essentially assume a similar role to surfactant, breaking down surface tension to allow the hydrophilic layers to spread out more thinly and prevent it from collapsing [56-58]. As the outermost layer, it also protects the ocular surface from debris and microbial agents alike.

Making up most of the tear volume, the aqueous layer is predominantly produced by the lacrimal gland. It provides the ocular surface with vital substances such as oxygen, electrolytes, hormones, cytokines, and proteins and therefore nourishes, protects and cleanses the epithelium. Additionally, it also ensures proper lubrication of the cornea by leveling out any imperfections in the ocular surface [50].

Finally, covering the ocular surface itself, the mucin layer consists of membrane-anchored and secreted glycoproteins, produced by conjunctival and corneal goblet cells. While lowering the hydrophobicity of the aqueous layer and therefore assuring proper adhesion of the tear film, the mucins provide moisture as well as a protective barrier to the eye [59]. They are also believed to possess a function in immune tolerance and signaling pathways [60-62]. If any of those layers or their components fall out of balance, the level of tear evaporation is increased, leading to hyperosmolarity, while tear break up time is decreased due to tear film instability– the clinical symptoms of dry eye.

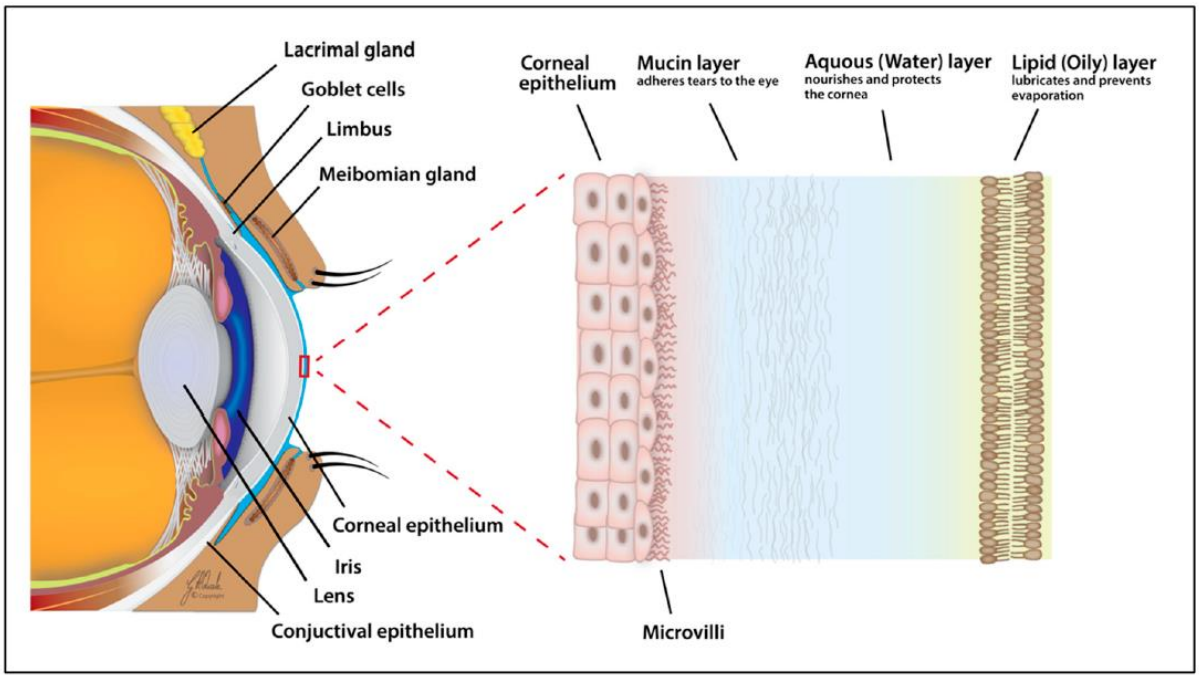

Figure 1: Tear film model (adapted from [63]).

2.3 DES subgroups

2.3.1 Etiology and classification

The deficiency of tear film homeostasis resulting in dry eye syndrome can be initiated by multiple factors that eventually end in a common pathway creating a vicious circle of DES progression [51, 64, 65]. This circle focuses on hyperosmolarity through evaporation as an underlying origin for all types of dry eye disease [51]. Based on the cause of said evaporation, DES can be further subclassified into two major groups. As shown in **Figure 2,** it is either a result of volume loss *via* tear film instability (Evaporative Dry Eye, EDE or DRYlip) or a decrease in lacrimal secretion (Aqueous-Deficient Dry Eye, ADDE or DRYaq). Since both of them end in the same self-amplifying pathophysiological cycle, these conditions have the potential to initiate each other and exist side by side. Especially over time said mechanism can lead to a combined dry eye syndrome (DRYaqlip) which frequently induces severe symptoms since there is no more compensation leeway [66]. Because of this transition, conclusively assigning patients to one specific DES subgroup is not always possible [67].

ADDE is caused by numerous factors and can be induced by any disruption in the aqueous layer's balance. Historically it can be subclassified in Sjögren's syndrome

dry eye, one of the first conditions described including DES symptoms, and non-Sjögren's Syndrome dry eye. Since the secretion of the lacrimal gland is triggered and controlled by nerves, any restriction of sensory, sympathetic or parasympathetic interconnections can lead to a reflex block or decreased blinking rate. The main origins of this are refractive surgery, contact lens wear, systemic drugs like beta-blockers and statins or conditions with a neurological impairment such as diabetes mellitus [68-73]. Further crucial causes are lacrimal gland dysfunctions through physical damage, infiltration or fibrosis. While any kind of local or systemic inflammation can lead to said implications [74, 75], autoimmune triggered diseases like Sjögren's Syndrome or Systemic lupus erythematosus promote major lacrimal gland damage [76, 77] often resulting in combined aqueous deficient and evaporative dry eye [78]. Aging on the other hand mainly prompts dry eye through fibrotic conversions, hormone changes declining blood supply to the glands and altered immune system regulations [79-81]. Finally, there are flaws in tear draining, such as tear flow obstructions, Graft-versus-Host-reactions after transplantations or neoplasia, to name some of the rarer reasons for aqueous deficient dry eye.

EDE is mainly evoked by lipid layer dysfunctions generating tear film instability and evaporation. Much like lacrimal gland dysfunctions, those can be subclassified, firstly into lid-related EDE which is mostly caused by Meibomian gland dysfunction (MGD) [51]. Since meibomian gland secreted lipids are greatly responsible for the physiological uphold of lipid layer functions, any kind of meibomian gland dysfunction results in said evaporative stress. They can be brought on by similar risk factors as ADDE, such as age, hormonal changes, systemic and local medications, contact lens wear, surgery or inflammation [82-86]. Tear film instability can also occur without prior increased osmolarity levels through conditions primarily affecting the ocular surface, therefore allowing for a second subgroup called ocular surface-related EDE. Causes include allergies, topical preservatives or xeropthalmia e.g. brought about by vitamin A deficiency [51].

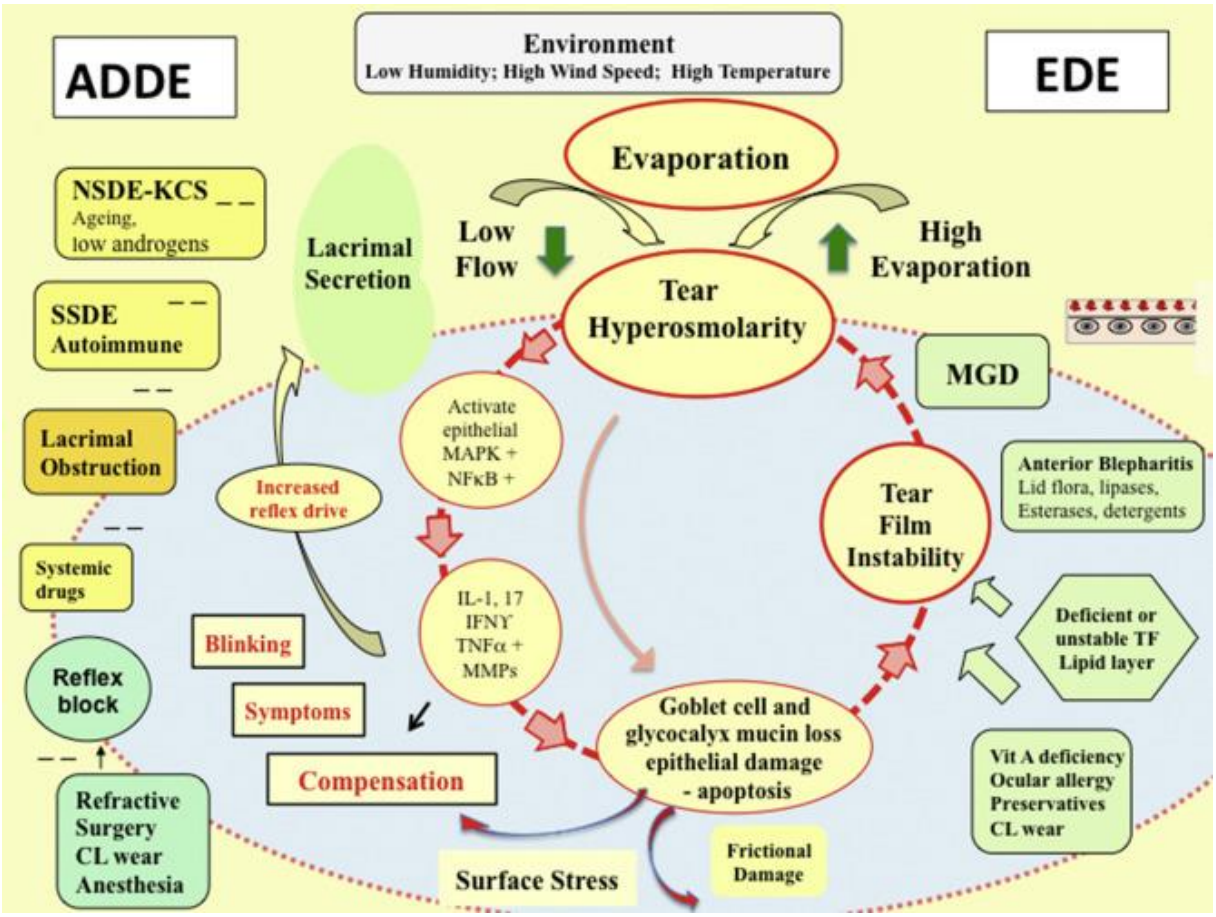

Figure 2: Pathophysiology of aqueous deficient dry eye (ADDE) and evaporative dry eye (EDE) (adapted from [1]). **NSDE-KCS** = non Sjögren's Syndrome dry eye – Keratoconjunctivitis sicca, **SSDE** = Sjögren's Syndrome dry eye, **CL** = contact lense, **MGD** = Meibomian gland dysfunction, **TF** = tear film

2.3.2 Vicious cycle of inflammation

Once tear hyperosmolarity is established through mechanisms mentioned above, inflammatory cascades involving mitogen-activated protein kinases (MAPK), nuclear factor 'kappa-light-chain-enhancer' of activated B-cells (NFκB) and metalloproteinases trigger epithelial cells to produce cytokines like interleukin-1 (IL-1), interleukin-2 (IL-2), interleukin-6 (IL-6), tumor necrosis factor-α (TNFα) and matrix metallopeptidase 9 (MMP9) [87-90]. Provided that those mediators initiate goblet and epithelial cell demise through apoptosis, they eventually result in decreased abundances of mucins and therefore lead to tear film instability, where the cycle of evaporation and now intensified hyperosmolarity starts anew.

Inflammatory mediators and extracellular DNA set free through cell apoptosis and invading neutrophils may also lead to direct ocular surface damage [51]. The proceeding surface stress and neurosensory triggering develop symptoms like increased blinking rates and reflex drives, pain, foreign body sensation or itching [91]. In turn, those factors elicit an increased lacrimal gland secretion rate in order to compensate tear film hyperosmolarity. Moreover, there are recent findings of both increased [92] and decreased corneal sensation in dry eye patients, depending on disease etiology [93]. Provided that sensory provoked compensation methods greatly reduce symptom intensity, these aspects could explain the discrepancy between subjective symptom severity and measurable DES biomarkers in clinical settings. Especially symptoms in early disease stages can be obscured through compensatory mechanisms, hindering a correct diagnosis [94].

2.4 DES diagnosis

While there are several approaches to it, DES diagnostics still remain a challenge due to the previously mentioned poor correlations between symptoms, disease stage, and clinical test results [7, 8, 95]. Established methods vary from symptom questionnaires to evaluations of tear film volume (Schirmer's test and meniscometry) and quality (tear break-up time), while there are also ways of unveiling existing effects of DES like ocular surface damage through staining techniques or hyperosmolarity *via* osmometry [96-98]. But since sensitivity and specificity of these tests are often not satisfying, while most established methods also lack reproducibility, there is no gold standard for the diagnosis of dry eyes yet [50, 99-102]. Therefore, to make diagnostics and evaluation of severity grading more reliable and objective, research focused on quantifiable entities in tears related to DES, especially proteins. Early on, there have been considerable efforts in protein assay development for lysozyme C (LYZ) and lactotransferrin (LTF), which are significantly reduced in dry eye patients. Coupled with Schirmer's tests they show diagnostic sensitivities of 85% and 70% respectively [103, 104]. Furthermore, matrix metalloproteinase 9 is increased in DES as part of inflammatory responses to corneal epithelial cell damage and showed a sensitivity of 80% to 85% in DES diagnosis, depending on study design and population, and a specificity of 98% when combined with other established tests [105-107].

While these developments were built upon the vast potential of immunoassays as being highly specific, fast and inexpensive clinical tests, the currently selected proteins lack sensitivity. Due to most of them being part of regular inflammatory pathways, their abundance in tears can easily be influenced by reactions to infection, other ocular diseases, surgery, contact lens use, allergies, medication, environmental stress et cetera. This could explain why the presented clinical assays are seldom used without additional testing and do not determine milder disease stages well [107, 108].

In search of unique or more sensitive proteins for enzyme-linked immunosorbent assay (ELISA) development and in order to further unravel the underlying pathophysiological mechanism of DES, research needed to focus on preceding steps in biomarker discovery. As shown in **Figure 3,** normal and disease protein profiles of tears needed to be established through the measurement of their entire protein content first. Subsequently, suitable proteins that distinguish those profiles could be verified by targeted approaches in larger study populations. Using the most uniquely expressed ones for validation *via* immunoassay measurements presumably delivers the most reliable biomarkers for highly sensitive and specific assays that could be adapted for inexpensive and fast clinical use. In recent years, measurements of individual proteins or protein panels employing discovery and targeted proteomics strategies for DES diagnostics have been thoroughly expanded and an extensive review of all related studies, including their sensitivity and specificity, can be found in the TFOS DEWS II Tear Film Report [50].

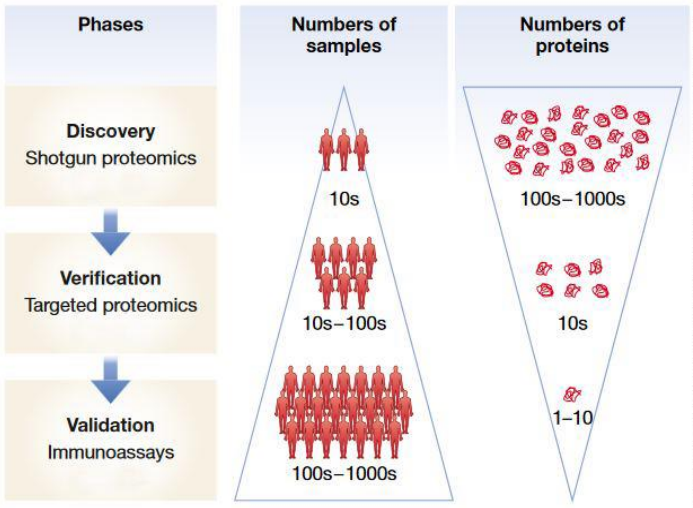

Figure 3: Exemplary biomarker discovery workflow in proteomics (adapted from [109])

2.5 Tear proteome analysis

2.5.1 Personalized medicine

Modern medicine as we know it is currently experiencing a paradigm shift. Due to current advances in science, doctors are moving away from generalized ideas of diseases and their treatment. Instead, each patient is believed to display a unique set of internal and external factors that may lead to pathology or a specific reaction to medication [26, 110]. In recent years, major advances have been made in an effort to unravel further internal factors and cellular pathways that influence individual disease progressions including the identification and quantification of many cellular components like genes, lipids, metabolites and proteins [111].

Medicine focused on genetics after the human genome was uncovered, since it is the cell's 'blueprint' and therefore affects all other previously mentioned entities. And while several diseases are based on genetic alterations or at least have a genetic component, many conditions cannot be attributed to this etiology alone since even complementary DNA sets in identical twins can lead to altering protein expressions, e.g. through epigenetics and mutations [112, 113]. To expand our understanding of cell physiology and pathology, scientific focus, therefore, shifted to other previously mentioned components, especially proteins because of their unique standing between the DNA's 'blueprint' and the cell's activities [9, 114]. Proteomics, the determination of a sample's protein content, is additionally of eminent importance for the concept of personalized medicine since proteins are also not exact derivatives of their respective DNA, but are altered throughout protein synthesis according to the cell's needs [115]. Effectively this means that proteomics reflects the inner workings of the cell including post-translational modifications (PTMs), acute or chronic cellular conditions (e.g. disease), protein-protein interactions et cetera and help to identify diagnostic and treatment steps most fit for each patient [116].

For example in case of cancer, protein expressions may vary in between patients suffering from the same condition, which suggests that they are based on divergent cellular pathways and would e.g. benefit from different medications [117-119]. A clinically established example would be programmed death ligand 1 (PD-L1) which is a protein expressed by some tumors and negatively influences the patient's outcome [120]. Nevertheless, due to the development of antibody treatments against the PD-1 receptor, so-called checkpoint inhibitors, the treatment of those tumors has drastically improved, which makes testing for the protein's expression vital [121, 122].

In case of DES, personalized medicine approaches could greatly influence the way this disease is diagnosed and therefore also a patient's outcome. Instead of determining and treating unspecific symptoms, proteomics could help to identify the cause for them and help to bring forth new advances in pharmaceutical research.

2.5.2 Age and gender-related changes in tear proteins

Some factors of personalized medicine are already well known about DES. As has been mentioned in previous chapters, DES occurs more often with women and older patients, which makes age and gender important elements to consider when measuring individual tear samples.

Age has been correlated to dry eye through many prevalence-based studies. An extensive comparison of them can be found in the TFOS DEWS II Epidemiology Report [25]. Regarding symptoms and the number of DES diagnoses, there is a linear increase after the age of 50, with an even elevated regression factor beyond 80 in those studies. The most significant diagnostic factors that correlated with age included subjective symptoms or an Ocular Surface Disease Index (OSDI) score over 22, Schirmer strip length and TBUT with p-values ≤ 0.01 [25]. Most commonly those changes are connected to fibrosis and atrophy, as well as lymphocytic and fatty infiltration of the lacrimal functional unit, especially the lacrimal gland [123]. Utilizing several different measurement methods, alterations have likewise been identified on the protein level of aged specimens not diagnosed with DES (**Table 1**). While IgA was found to be increased *via* single radial immunodiffusion by Sen *et al.* [124], it was decreased in ELISA measurements, along with other inflammatory mediators like LYZ and LTF [125]. At the same time IgG and ceruloplasmin, which is involved in the copper metabolism and acts as an acute-phase protein, were found to be increased in the latter study. Other proteins involved in inflammation were also discovered to be elevated in protein array and sequential window acquisition of all theoretical mass spectra (SWATH-MS) measurements, such as interleukins, TNF-α, S100 calcium-binding protein A8 (S100-A8), S100 calcium-binding protein A9 (S100A9) and lipocalin. Furthermore, markers of cell death like matrix metalloproteinase-1 (MMP-1), actin, serum albumin and annexin A1 were found to be increased, while ubiquitin-like modifier-activating enzyme 1 (UBA1), which is also associated with cell death, and golgi membrane protein 1 (GOLM1) were decreased [126, 127]. Additionally, age was correlated to a decrease in neuromediators [128].

Conclusively, even though the patients in these studies were not diagnosed with DES, the significantly elevated proteins are similar to the ones in DES. Even though there is still a need for decisive information on this topic, age seems to promote inflammatory mechanisms and cell demise, which might be an entry point for the pathophysiological cycle of DES described in previous chapters.

Table 1: Summary of studies on age-related protein changes in tears

Group	Study population	Measurement technique	Protein	Expression profile with age
Sen *et al.*, 1978 [124]	220	Single radial immunodiffusion	IgA	Increased
McGill *et al.*, 1984[125]	55	ELISA	IgA, LYZ, LTF	Decreased
			CP, IgG	Increased
Micera *et al.*, 2018 [126]	75	Chip-based protein array	CCL5, IL-3, IL-6, IL-8, MMP-1, TNF-α,	Increased
Nättinen *et al.*, 2019 [127]	115	NanoLC-TripleTOF SWATH MS	ACTB, ACTG1, ALB, ANXA1, CEACAM7, DEFA1, GSN, LCN2, PFN1, RARRES1, SCGB2A2, S100A8, S100A9, TF	Increased
			GOLM1, UBA1	Decreased
Tummanapalli *et al.*, 2019 [128]	26	ELISA	CGRP, TAC1	Decreased

Gender, especially the female sex, has been known to be a risk factor for several eye diseases for more than 100 years [129]. Even though there are many influences responsible for this phenomenon like sex-specific autosomal factors, epigenetics, and general hormonal changes (e.g. thyroid and hypothalamic-pituitary hormones), scientific research focuses mainly on the difference of sex steroids between genders [130-133]. Androgens, estrogens, and progestins have distinct effects on the entire lacrimal functional unit and influence protein synthesis rate, aqueous tear output, lipid production, mucous secretion, tear film stability, blink rate and immune functions amongst other things in several animal model studies [134-139]. Estrogens, in particular, are believed to induce pro-inflammatory substances in animals, while androgens were found to be beneficial, especially for the lacrimal and meibomian glands and therefore tear film lipid layer balance [140, 141]. Nonetheless, the exact workings of sex steroids on the human eye have not been uncovered yet. While there are some contradictory results in recent studies, especially regarding hormone therapy and its benefits for DES patients, most publications esteem low levels of

circulating androgens, high levels of estrogens and an unbalanced ratio of sex steroids as risk factors for dry eyes [134, 142-144]. Women especially would be affected by these elements and therefore show a higher prevalence of DES after menopause and during pregnancy, while men and women show equal risks for DES in higher ages when men's androgen levels begin to decrease [142, 145, 146]. Furthermore, sex steroid changes or imbalances have been linked to the occurrence of autoimmune diseases and depression [147-149]. Both are linked to DES and have a higher prevalence in women, particularly after puberty, with females making up as much as 86% of autoimmune-related DES or Sjögren's syndrome patients, depending on study design and population [147, 150]. Additionally, women were found to have an increased level of sensitivity to ocular pain and therefore also a higher score in symptom evaluation tests compared to men suffering from the same objectively measured disease severity [151]. They were, therefore, more likely to express symptoms of DES, even in early disease stages. Nevertheless, many studies focusing on gender-specific protein changes in human tears fail to come up with reliable biomarkers. Even though there is no definite answer to this problem yet, scientists believe it may be due to interpersonal differences in local ocular hormone production and enzyme distribution. This leads to most sex steroids in women after menopause to be conducted in peripheral tissue, while studies often focus on measuring systemic hormone levels [152-155]. Studies that successfully established differences in tears of altering genders not diagnosed with DES (summary in **Table 2**) found females to possess increased levels of inflammatory proteins like IgA, LCN1, LF and haptoglobin (HP) [124, 156, 157]. Interestingly, cystatin 4 (CST4), mammaglobin-B (SCGB2A1) and α-1-antitrypsin (SERPINA1), proteins that were previously found to be decreased in DES, were increased in LC-MS/MS measurements of females' tears compared to males' [20, 156]. On the other hand, proteins involved in cell renewal like epidermal growth factor (EGF) and transforming growth factor-alpha (TGF-α) were increased in men [158, 159]. With mostly inconsistent settings in terms of the study population, measurement techniques as well as inclusion and exclusion parameters, the exploration of gender-specific differences in tears still need further unraveling in order to bring forth the concept of personalized medicine in DES.

Table 2: Summary of studies on sex-related protein changes in tears

Group	Study population	Measurement technique	Protein	Expression profile in males/females
Sen *et al.*, 1978 [124]	220	Single radial immunodiffusion	IgA	Increased in females
Mii *et al.*, 1992 [157]	36	2D electrophoresis	LF	Increased in females
Van Setten *et al.*, 1994 [158]	?	radioimmunoassay	TGF-α	Increased in males
Nava *et al.*, 1997 [159]	68	ELISA	EGF	Increased in males
Ananthi *et al.*, 2011 [156]	40	2D electrophoresis, LC-MS/MS	CST4, HP, LACRT, LCN1, LF, SCGB2A1, SERPINA1	Increased in females

2.5.3 Normal tear proteome

Human tears are a complex and dynamic mixture of proteins. As described before, there are particular protein patterns in an individual's samples, but through discovery stage experiments, consensus patterns for physiological and DES tear samples could be determined. This was achieved by pooling samples and therefore accentuating shared characteristics of the two conditions, which were then identified.

Depending on the tear collection method and analyzation technique, up to around 1500 proteins were measured in healthy and sick subjects hitherto (a summary of total proteins measured in recent studies can be found in **Table 3**) [160, 161]. While this stresses the intricacy of this fluid, the majority of the total protein amount is only made up of a handful of them. LYZ, LTF, lipocalin-1 (LCN1), lacritin (LACRT), secretory immunoglobin A and proline-rich proteins make up more than 90% of the overall tear protein content [15, 162, 163]. They are involved in coagulation, as well as metabolic and protective immune pathways that ensure a healthy ocular surface equilibrium [161]. Other major groups involved in those mechanisms include the 14-3-3, trefoil factor and S100 protein families, mucins and cystatins [160].

In comparison to other diagnostic body fluid measurements, for example, blood serum or urine, tears show a lower protein concentration and total number of measurable proteins [164, 165]. While this may seem like a disadvantage at first, other fluids are often too complex for protein measurements or heavily influenced by an inconceivable number of factors to give decisive diagnostic information when no unique proteins are involved. Also, even though tears, urine, and cerebrospinal fluid

are ultimately filtrated from blood and therefore share proteins, their contents and amounts vary from it and in between themselves to some extent [160, 166]. That is why the eye, having evolved from and being in constant communication with the brain, is believed to show proteomic tear composition differences in neurological conditions in addition to local and systemic diseases [167, 168].

2.5.4 Dry eye syndrome proteome and biomarkers

Overall, in comparison to the tears of healthy subjects, the total protein amount is reduced in all DES subtypes, while osmolarity is increased by mechanisms explained in previous chapters [169]. In recent years, there have been considerable efforts in uncovering the protein profiles not only of DES itself, but also its subgroups – DRYlip, DRYaq, and DRYaqlip. A summary of differently expressed proteins in previous studies, as well as this one, can be found in **Table 9.**

Employing surface-enhanced laser desorption/ionization (SELDI-TOF), Grus *et al.* managed to verify an increase in S100-A8 in DES when compared to control samples, while other major proteins like LYZ, proline-rich protein 3, proline-rich protein 4 (PRR4) and α-1-antitrypsin (SERPINA1) were found to be decreased [12]. Using similar methods, Boehm *et al*. identified the same expression changes in all DES subgroups in addition to an increase in mammaglobin-B (SCGB2A1) and lipophilin A. While DRYaq and DRYaqlip showed vast alterations in the expression of those proteins when compared to healthy subject, DRYlip presented only slight differences, which suggests a stronger impairment of tear film homeostasis in DRYaq [11].

In the following years, various studies used LC-MS/MS techniques for discovery and targeted proteome measurements of tears. Many previously mentioned proteins and their expression levels were verified in those studies, like S100-family proteins (S100A4, S100A8, S100A9, S100A11), PRR4 and LYZ. Furthermore, they indicated an increase of LTF, 14-3-3 proteins (YWHAB), aldehyde dehydrogenase (ALDH3A1), alpha-2-HS-glycoprotein, annexins (ANXA1, ANXA2), complement C3 (C3), glutathione S-transferase P (GSTP1), keratins (KRT4, KRT10), mucin-5 AC precursor, plasminogen activator inhibitor 2 (SERPINB2), phospholipase A2 (PLA2G2A), and zymogen granule protein 16 homolog B (ZG16B) in DES [16, 17, 20, 21, 160, 170]. DRYaq and DRYaqlip subgroups showed heightened expressions

of alpha-enolase (ENO1), serotransferrin (TF), phosphatidylethanolamine-binding protein 1 (PEBP1) and α-1-acid glycoprotein 1 (ORM1), while aldehyde dehydrogenase, dimeric NADP-preferring (ALDH3A1) was only increased in DRYaqlip [20]. Lipid deficient dry eye was again not as affected by proteomic changes as the other subgroups.

In addition to the previously mentioned proteins that were found to be decreased in DES, LC-MS/MS approaches also discovered cystatins (CST1, CST4), growth-inhibiting protein 12, immunoglobulins (J chain, Ig alpha-1 chain C region, immunoglobulin heavy constant mu, polymeric immunoglobulin receptor), keratin (KRT5), lipocalin-1 (LCN-1), prolactin-inducible protein (PIP), proline-rich protein 1 (PROL1), ubiquitin (UBA52) and ZG16B to be diminished in primary and secondary dry eye patients [14, 20, 21, 28, 160, 170]. Aqueous deficient and combination DES additionally possessed lowered levels of SCGB2A1 and deleted in malignant brain tumor 1 protein (DMBT1). Lacritin (LACRT) on the other hand was only decreased in DRYaqlip patients, while overall DRYlip expressions were not as negatively affected as the other subgroups once more.

It is interesting to note, that most significantly expressed proteins measured by LC-MS/MS-based methods were classified as low abundant proteins, even though those make up only a fraction of the total tear protein amount [20]. It remains to be verified by different analysis techniques if that reflects the actual changes in DES or if major tear proteins are mismeasured because of methodical problems (e.g. signature peptide recognition or sample preparation) since considerable proteins like PRR4 have been known to be more accurately represented by other proteomics approaches [27].

Other methods used to contribute to DES protein profiling include a MALDI-TOF/TOF approach by Soria *et al.*, which one the one hand gave complementary results to already discussed studies while on the other hand demonstrating an increase in glutathione S-transferase P and a decrease in zinc-alpha-2-glycoprotein (AZGP1) and galectin-7 [17]. Furthermore, Funke *et al.* and Nichols *et al.* investigated dry eye-induced by contact lens wear *via* MALDI-TOF and LC-MS/MS. They found S100A8 and S100A9 levels to be heightened, along with a decrement of LCN-1, LTF and LYZ [13, 171].

Overall, those additional biomarker candidates further contribute to the idea of inflammation and resulting tissue damage being the central aspects of dry eyes since

they are active in immune, metabolic and cell renewal pathways. For this reason, e.g. LACRT, an eye specific growth factor, that may be involved in tear secretion and ocular epithelial renewal, has been of special interest to recent research and treatment development [172, 173]. A topical synthetic LACRT derived peptide could potentially restore tear film homeostasis and is currently being evaluated in a clinical trial [174]. Since there is currently no causal therapy for DES, approaches like these are of crucial importance to the field of ophthalmology and could be significantly expanded by further proteomic research on this disease.

2.5.5 Proline-rich-protein 4 (PRR4)

One of the highly abundant tear proteins, which has been mentioned several times up until this point is PRR4. Lacrimal PRR4 is produced in the lacrimal gland and is believed to play crucial parts in tear film stability, lubrication and antimicrobial mechanism because of its parallel involvement in saliva and submucosal glands [27, 175]. Nevertheless, the functions and peptide sequence of lacrimal proline-rich protein 4 is yet to be fully uncovered, which complicates not only our understanding of its biological function but also MS-based measurements. Previous studies employing mass spectrometry found PRR4 to be decreased in all subgroups of DES [27, 28] including dry eyes through contact lens use [13], and other diseases secondarily involving the eye like thyroid-associated orbitopathy [19] or diabetic proliferative retinopathy [167, 176]. A decrement could also be established in the sputum of smokers [177, 178], as well as esophageal and laryngeal tumors [179, 180], whereas keratoconus patients showed a similar PRR4 abundance to healthy control patients [181]. The decrement in multiple disease forms is believed to be based on gland deficiencies and compensatory downregulation in chronic processes [27]. In contrast, reflex tears were found to harbor increased levels of PRR4, presumably because of its antimicrobial function [182].

In a nutshell, PRR4 harbors vast potential as a biomarker in multiple diseases and pathophysiological pathways, while it is not easily measured in most proteomic techniques and therefore may not be rightly represented in MS-based studies. In an effort to determine its peptide sequence, Perumal *et al.* employed discovery and targeted MS approaches in order to find a total of four isoforms making up PRR4 derived from different point mutations and PTMs [27, 183]. These isoforms are present in specific patterns, resulting in six possible combinations found in individuals

via LC-ESI-LTQ-Orbitrap. The resulting changes caused by these isoform expressions are yet to be explored. That is why improvements of PRR4 MS measurements techniques as well as functional analysis of this protein and its isoforms are promising subjects for further scientific research.

2.5.6 Protein measurement

2.5.6.1 Mass spectrometry (MS)

Mass spectrometry is an analytical technique used to characterize various biomolecules including proteins. It is an expeditiously evolving field that became the method of choice for identifying and quantifying complex biological samples because of its ability to measure large numbers of proteins and PTMs in a short amount of time while keeping up high levels of accuracy [116, 184, 185]. It is based on the concept of breaking down molecules into ions and sorting them by their mass-to-charge-ratio (*m/z*) in magnetic or electrical fields of so-called mass analyzers. Subsequently, a detector measures the quantity of each ion fragment, which enables statements about the content of analytes and their relative abundance [10]. When measuring proteins one can either choose a “top-down” approach that ionizes intact proteins or introduce enzymatically digested peptides to the MS in a “bottom-up” strategy [186, 187].

Depending on sample characteristics and desired data output, each step of this measurement workflow can be altered or expanded. For example, fluid samples can be ionized *via* electrospray ionization (ESI), whereas matrix-assisted laser desorption/ionization (MALDI) sublimates samples out of a dried, crystallized, energy-absorbing matrix by using laser shots [10]. A variation of MALDI is surface-enhanced laser desorption/ionization (SELDI), in which samples are bound to a surface acting as a solid-phase chromatographic separation prior to laser pulsing [188]. In order to obtain higher accuracy levels, samples can undergo an extra separation step before ionization by gel electrophoresis (1DE or 2DE), liquid or gas chromatography (LC, GC). Making use of other ion characteristics ion mobility spectrometry (IMS) separates ions by their *m/z* in addition to their gas phase mobility [189]. More compact ions, therefore, travel faster than open structures, allowing for an extra dimension of separation. Newest advances also allow ions to be detained in the gas chamber and be eluted at a desired time in trapped IMS (TIMS) [190]. After

ionization, the key point of MS measurements ensues - the mass analyzer. The simplest way of sorting ions is by time-of-flight (TOF), which is based on the acceleration of ions using an electric field. Heavy or lower charged ions will then reach a lower velocity than lighter or higher charged ones. By measuring how long it takes ions to travel a specified distance to the detector, their mass can be determined [191]. Following achievements in sample separation were attained with the development of ion trap mass analyzers that allowed ions not only to be sorted by their *m/z* but also to be captured in an electric or magnetic field to be released and measured at specific time points. These analyzers can either be aligned as a linear quadrupole ion trap (LTQ) or in an orbit of magnetic (Fourier transform ion cyclotron resonance, FT) or electrical fields (Orbitrap) [192-194]). Because all those different techniques harbor specific advantages and disadvantages, they can be combined to perform workflows best befitting any given sample type. A combination of mass analyzers also allows for so-called MS/MS or tandem MS measurements which separate ions of interest in a first MS step, for them to be broken into distinct fragments, most commonly *via* collision energy [195]. Those fragments can then be sorted by *m/z* in a second MS step, resulting in a characteristic pattern and ultimately providing information about the ion of interest's amino acid sequence and can, therefore, identify the peptide and protein the ion originated from [10, 196]. Consequently, MS/MS methods can be used in discovery stage studies by determining as many peptides contained in a sample as possible or in targeted experiments using Accurate Inclusion Mass Screening (AIMS). This concept uses a so-called inclusion list that specifies *m/z*, z and if required, estimated retention time values of ions. If a mass spectral peak matches those specifications during the first MS step, the associated ion is automatically selected for MS/MS measurements [24]. Peptides not included on the list are not quantified. Therefore, AIMS is a powerful tool for a fast protein of interest determination. Recently, MS/MS measurements have reached new efficiency levels with the development of parallel accumulation-serial fragmentation (PASEF), a scan mode that allows for simultaneous measurements of multiple precursor ions. Especially in combination with TIMS, these methods are able to measure up to 15 times more MS/MS spectra than others in short amounts of time with attomole sensitivity [197].

In conclusion, many different mass spectrometry-based techniques can be used in the identification and quantification of proteins. A summary of studies utilizing said methods in tear proteomics including their study population, sampling and number of

identified proteins can be found in **Table 3**. If one desires a fast and fairly untampered with representation of a sample's peptide profile, MALDI-TOF is the method of choice, since it requires only enzymatic digestion before MS measurement. However, it lacks specificity due to different proteins sharing the same peptide sequences, which leads to an overlay of peaks, and only quantifies them in relative abundances [198]. In case of discovery and targeted proteomics, MS/MS techniques combined with further separation e.g. LC are frequently used and can be applied to absolute quantification and protein sequencing. Meanwhile, they also require extensive purification steps and measurements, especially of entire protein profiles during the discovery stage, are time-consuming [10]. Recent achievements in TIMS PASEF measurements could solve many of these problems since it is a fast and highly sensitive method of protein quantification [197]. Nevertheless, sample type, as well as hard- and software optimization steps still need to be established for this technique. Knowledge of sample and MS characteristics is therefore crucial for successful proteomic studies.

Table 3: Summary of tear proteome measurements utilizing mass spectrometry techniques

Group	Sample	MS system	Discovery/ Targeted	Study population	Identified proteins	Disease
Grus *et al*., 2005 [12]	Schirmer-Strip & Microcapillary	SELDI-TOF-MS	Discovery	159	7 highlighted	DES
de Souza *et al*., 2006 [199]	Microcapillary	LTQ-FT & LTQ-Orbitrap	Discovery	1	491	/
Green-Church *et al*., 2008 [200]	Schirmer-Strip & Microcapillary	Nano-LC-MS/MS	Discovery	8	97	/
Nichols JJ *et al*., 2009 [13]	Microcapillary	Nano-LC-MS/MS	Discovery	21	11	DES & contact lense use
Zhou *et al*., 2009 [15]	Schirmer-Strip	2D-nanoLC-nano-ESI-MS/MS	Discovery	96	93	DES
Lema *et al*., 2010 [201]	Schirmer-Strip	MALDI-TOF-MS	Discovery	44	3 highlighted	Keratoconus
Pong *et al*., 2010 [202]	Microcapillary	MALDI-TOF-MS	Discovery	14	6 highlighted	Allergic Kerato-conjunctivitis
Srinivasan *et al*., 2012 [14]	Schirmer-Strip	LC/MS/MS with LTQ-Orbitrap-XL, iTRAQ	Discovery	24	386	DES
Funke *et al*., 2012 [171]	Schirmer-Strip	MALDI-TOF-MS	Discovery	12	267	DES & contact lense use
Pieragostino *et al*., 2012 [203]	Schirmer-Strip	LC-MS & MALDI-TOF-MS	Discovery	14 / 31	PXG *vs.* Control: 45, POAG *vs.* Control: 33, PXG *vs.* POAG: 15	Primary open angle glaucoma & pseudo-exfoliative glaucoma
Zhou *et al*., 2012 [160]	Schirmer-Strip	Nano-RPLC-MS/MS	Discovery	4	1543	/
Csosz *et al*., 2012 [176]	Microcapillary	Nano-LC-(ESI)-MS/MS with 4000 QTRAP MS, iTRAQ	Discovery	145	53	Diabetic retinopathy
Pieragostino *et al*., 2013 [204]	Schirmer-Strip	Nano-LC-MS with Q-TOF Premier MS	Discovery	19	POAG *vs.* Control: 27	Primary open angle glaucoma
Boehm *et al*., 2013 [11]	Schirmer-Strip	SELDI-TOF-, MALDI-TOF-, TOF-MS	Discovery	169	300, 6 highlighted	DES (DRYlip, DRYaq)
Soria *et al*., 2013 [17]	Merocel sponge	MALDI-TOF/TOF-MS	Discovery/Targeted	144	15 highlighted	DES, Meibomian gland dysfunction
Li *et al*., 2014 [205]	Schirmer-Strip	2D-Nano-LC-MS/MS	Discovery	32	435	DES, Sjögren's-Syndrome

Table 3: (continued)

Group	Sample	MS system	Discovery/ Targeted	Study population	Identified proteins	Disease
Salvisberg *et al.*, 2014 [206]	Microcapillary	LC-MS/MS & LTQ Orbitrap Velos	Discovery	55	185	Multiple Sclerosis
Masoudi *et al.*, 2014 [207]	Microcapillary	Nano-LC Ultimate 3000 HPLC MS/MS	Targeted	7	5	Contact lense
Leonardi et al., 2014 [208]	Microcapillary	AB 4800 MALDI TOF/TOF, iTRAQ	Discovery	20	78	Allergic Keratoconjunktivitis
Perumal *et al.*, 2014 [27]	Microcapillary	LC-MALDI-MS & LC-ESI-LTQ-Orbitrap-XL-MS	Discovery/Targeted	10 / 61	200 / 3	/
Tong *et al.*, 2015 [209]	Schirmer-Strip	Nano-LC-MS/MS with Dionex UltiMate 3000 and AB Sciex Triple TOF 5600	Targeted	1000	47	/
Perumal *et al.*, 2015 [182]	Microcapillary	LC-ESI-MS/MS	Discovery/Targeted	20	78 / 13	/
Matheis *et al.*, 2015 [19]	Schirmer-Strip	MALDI-TOF/TOF-MS	Discovery	120	69	Endocrine orbitopathy, DES
Funke et al., 2016 [210]	Schirmer-Strip	LC-ESI-LTQ-Orbitrap-XL-MS	Discovery	3 / 31	1039	Primary open angle glaucoma
Perumal et al., 2016 [20]	Schirmer-Strip	LC-ESI-LTQ-Orbitrap-XL-MS	Discovery/Targeted	80	DRYlip *vs.* CTRL: 22, DRYaq *vs.* CTRL: 58, DRYaqlip *vs.* CTRL: 67, Targeted: 13 highlighted	DES (DRYlip, DRYaq)
Kalló *et al.*, 2016 [168]	Microcapillary	EasynLCII nano HPLC	Targeted	23	10	Alzheimer's disease
Aluru *et al.*, 2016 [211]	Schirmer-Strip	nano LC- MS/MS	Targeted	202	8 highlighted	Rheumatoid Arthritis, DES
Aass *et al.*, 2016 [212]	Schirmer-Strip	2D LC-MS/MS	Discovery	42	1212	Graves' disease
Scieranski, 2017 [213]	Schirmer-Strip	LC-ESI-LTQ-Orbitrap-XL-MS, AIMS	Targeted	72	62	DES, Glaucoma
Aqrawi *et al.*, 2017 [214]	Schirmer-Strip	QExactive mass spectrometer	Discovery	59	500	Sjögren's syndrome

Table 3: (continued)

Group	Sample	MS system	Discovery/ Targeted	Study population	Identified proteins	Disease
Jung *et al.*, 2017 [21]	Transorb Wicks	Q ExactiveTM Orbitrap Hybrid MS coupled with EASY-nLC 1000	Discovery / Targeted	10 / 35	1165 / 3	DES
Soria *et al.*, 2017 [16]	Microcapillary	LC-MS/MS	Discovery / Targeted	37 / 33	135 / 26	DES, Meibomian gland dysfunction
Yenihayat *et al.*, 2018 [215]	Microcapillary	ABSCIEX MALDI-TOF/TOF 5800	Discovery	33	9 highlighted	Keratoconus
Gerber-Hollbach *et al.*, 2018 [216]	Schirmer-Strip	LC-MS/MS	Discovery	20	282	Graft versus host disease
Nättinen *et al.*, 2018 [217]	Schirmer-Strip	SWATH-MS	Discovery	28	785	Glaucoma
Manicam *et al.*, 2018 [218]	Schirmer-Strip	LC-ESI-MS/MS	Discovery	28	230	Contact lens use
Dor *et al.*, 2019 [161]	Schirmer-Strip	LTQ-Orbitrap Velos Pro	Discovery	8	1351	/
Boerger *et al.*, 2019 [219]	Schirmer-Strip	LC-ESI-MS/MS	Discovery	54	571	Parkinson's disease
Eidet, 2019 [220]	Schirmer Strip	LC-MS/MS	Discovery	35	AAU: 235 BK: 198	Acute anterior uveitis (AAU), Bacterial keratitis (BK)
Ji *et al.*, 2019 [221]	Microcapillary	Q Exactive orbitrap hybrid MS	Discovery	153	CsA: 54 DQS: 106	DES treatments (cyclosporine A & diquafosol tetrasodium)
Kenny *et al.*, 2019 [222]	Schirmer Strip	RP-LC-MS/MS	Discovery	32	CTRL: 358 AD: 442	Alzheimer's disease
Chen *et al.*, 2019 [22]	Schirmer Strip	nanoLC/Q-TOF-MS/M	Discovery	37	CTRL: 1031 DES: 190	DES
Kolman *et al.*, 2019 [23]	Micropipetts & Schirmer Strip	timsTOF Pro	Discovery	5	CTRL: 446 DES: 1034	DES

2.5.6.2 Protein quantification

Protein quantification proves to be an ongoing challenge in mass spectrometry. As mentioned beforehand, some MS strategies only qualify for relative quantification. For them to still be used in more extensive ways two different strategies have been developed – labeling and label-free quantification, as depicted in **Figure 4**. The concept of labeling is built around introducing isotopes of distinctly different molecular weights to various samples, which leads to identical peptide fragments having different masses in particular labeled samples. The samples are combined and measured with a MS system that detects the mass differences, which makes them comparable and usable for quantifications. Isotopes can be introduced to the samples in cell cultures or animal models through providing them during growth or cell division (metabolic labeling, e.g. stable isotope labeling by amino acids in cell culture (SILAC) [223]) or on the protein or peptide level by chemical and enzymatic attachment (chemical labeling, e.g. isotope-coded affinity tag (ICAT) [224], isotope tags for relative and absolute quantification (iTRAQ) [225]). Besides actually attaching the isotopes to or including them in samples, one can also add a known quantity of an isotopic-labeled standard peptide to the mix and therefore, in comparing peptide signals, reach absolute quantification (spiked standards, e.g. absolute quantification of proteins (AQUA) [226]). All of those labeling techniques deliver highly accurate and specific quantification results but require extra preparation steps including highly expensive reagents and further add to already complex protein mixtures. Moreover, they do not work as well for all proteins, especially low abundant ones, which are of high interest in tear samples [227]. Instead of focusing on labeling methods, scientific interest, therefore, shifted to quantification in label-free approaches. Bantscheff *et al*. extensively covered the advantages and disadvantages of different label-free methods, which are for the most part using MS/MS data sets to count specific parameters and use them for relative quantification with the help of algorithms and databases [227]. Naturally, those methods cannot achieve the same exceeding level of accuracy as labeled ones, but they are simple, fast, and comparatively cheap methods that have been greatly improved in past years. Especially software like MaxQuant has helped label-free quantifications to become highly accurate in all mass ranges and fold changes, with quality standards comparable to other quantification methods [184, 185, 198, 227, 228]. Using said optimized strategies, Label-free quantification has been

successfully applied to many proteomics studies in recent years [10, 20, 27, 116, 218, 229].

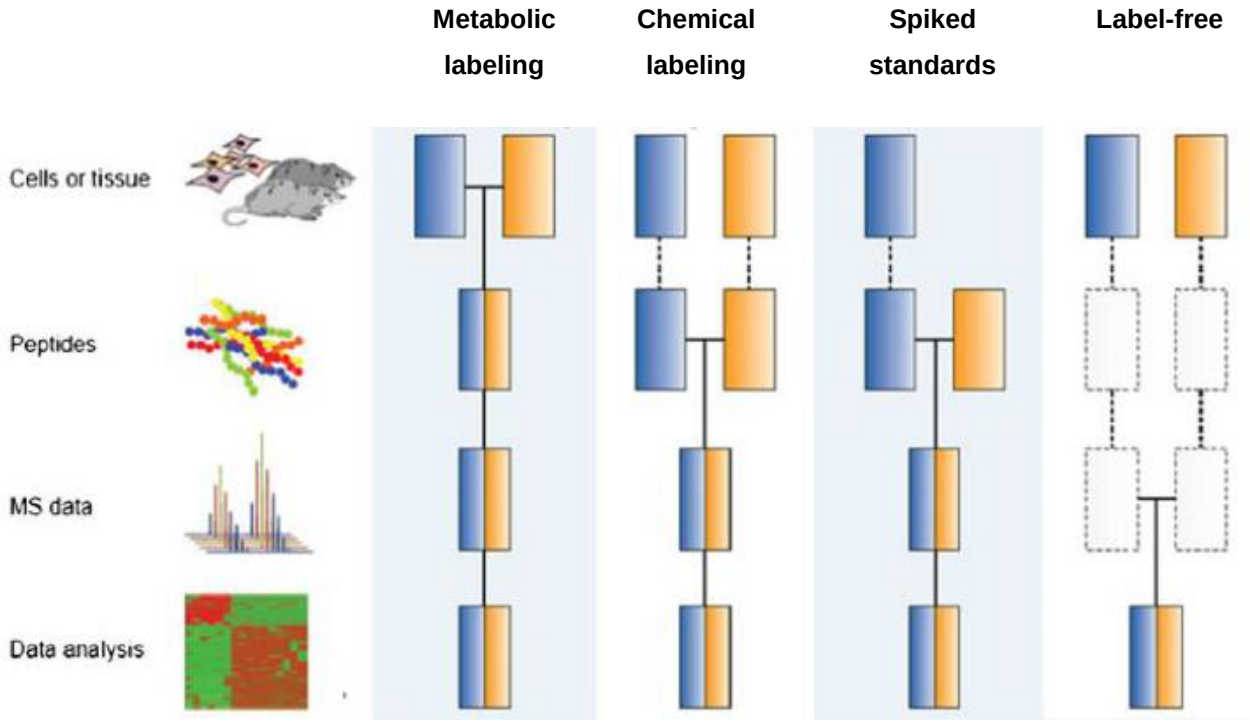

Figure 4: Overview of labeling techniques in proteomics. The blue and yellow boxes represent different experimental conditions (e.g. CTRL *vs.* disease). Dashed lines illustrate possible variations in the workflow. Horizontal lines highlight the step in which sample combination occurs (adapted from [227]).

3. MATERIALS AND METHODS

3.1 Materials

3.1.1 Chemicals

Acetonitrile for LC-MS (ACN)	AppliChem GmbH, Darmstadt, Germany
Ammonium bicarbonate	Sigma-Aldrich, Co., St. Louis, USA
Formic acid 98-100 %	AppliChem GmbH, Darmstadt, Germany
Methanol for LC-MS	AppliChem GmbH, Darmstadt, Germany
Peptide Calibration Standard 2	Bruker Daltonics, Bremen, Germany
Phosphate buffered saline (PBS)	Sigma-Aldrich, Co., St. Louis, USA
Pierce™ BCA-Protein Assay Kit	Thermo Fisher Scientific Inc., Waltham, USA
Pierce™ Reserpine Standard for LC-MS, 100 pg/µl	Thermo Fisher Scientific Inc., Waltham, USA
Sequencing Grade Modified Trypsin	Promega Corporation, Madison, USA
Trifluoroacetic acid (TFA)	Merck KGaA, Darmstadt, Germany
Water for LC-MS	AppliChem GmbH, Darmstadt, Germany

3.1.2 Supplies

96 well cell culture cluster, flat bottom	Costar 3595, Corning Incorporated
96 well cell culture cluster, v-bottom	Costar 3595, Corning Incorporated
C18 ZipTips, Millipore	Merck Millipore Ltd, Tullagreen, Carrigtwohill, Co. Cork, IRL
Eppendorf pipettes	Eppendorf, Hamburg, Germany
Eppendorf pipetting tips	Eppendorf, Hamburg, Germany
Eppendorf tubes 1,5/2.0 ml	Eppendorf, Hamburg, Germany
Microcapillary tubes, 5 µl	Blaubrand, IntraEND, Wertheim,

	Germany
PCR tubes, 0,2 ml	Ratiolab GmbH, Dreieich, Germany
Polyethylene peeling cover film	Ratiolab GmbH, Dreieich, Germany
Schirmer strips	Rolf Babbe Vertriebs GmbH, Augsburg, Germany

3.1.3 Appliances

386 MTP PolishedSteel™ MALDI target plate	Bruker Daltonics, Bremen, Germany
BioBasic C18 column	Thermo Scientific, Rockford, USA
BioBasic Phenyl column	Phenomenex, Torrence, USA
Bruker Ultraflex 2 MALDI TOF	Bruker, Billerica, USA
ESI-LTQ-Orbitrap-XL MS	Thermo Scientific, Bremen, Germany
HTS PAL Autosampler	CTC Analytics AG, Zwinge, Switzerland
Intelli Mixer	neoLab, Heidelberg, Germany
Jupiter C4 column	Phenomenex, Torrence, USA
Rheos Allegro pump	Thermo Scientific, Rockford, USA
Speed Vac Concentrator 5301	Eppendorf, Hamburg, Germany
Ultrasonic unit, Sonorex RK31	Bandelin, Berlin, Germany

3.1.4 Software

Endnote X8	Thomson Reuters, New York City, NY
Flex Analysis Version 2.4	Bruker Daltonics, Bremen, Germany
FlexControl Version 2.4	Bruker Daltonics, Bremen, Germany
Ingenuity Pathway Analysis Software Version v01-04	Qiagen, Redwood City, USA
MASCOT Version 2.2.07	Matrix Science, London, UK
MaxQuant 1.5.2.8	Max Planck Institute of Biochemistry, Cox und Mann 2008
MaxQuant Version 1.5.2.8	Max Planck Institute of Biochemistry (Cox, Mann), Martinsried, Germany
Microsoft Office 2016	Microsoft Cooperation, Redmond, USA
Perseus Version 1.6.5.0	Computational Systems Biochemistry, Max Planck Institute of Biochemistry, Martinsried, Germany
Proteome Discoverer Version 1.1.0.263	Thermo Fisher Scientific Inc., Waltham, USA
Statistica 13	Statsoft, Tulsa, USA
Thermo Proteome Discoverer Version 1.1.0.263	Thermo Scientific, Bremen, Germany

3.2. Methods

3.2.1 DES clinical biomarker discovery employing AIMS in a targeted proteomics strategy

3.2.1.1 Study samples

A total of 162 patients were included in this study, consisting of 106 women (median age: 58.0±16.1) and 56 men (median age: 55.5±14.9). A detailed age distribution for each gender can be found in **Figure 5**. Patients were recruited by the Department of Ophthalmology at the University Medical Center of the Johannes Gutenberg-University, Mainz, when they displayed initial subjective symptoms of dry eyes, while not being diagnosed with DES. Additionally, a group of control patients without dry eye symptoms was recruited. Samples were conducted *via* Schirmer strips on eyes treated with Novesine eye drops, which is a light anesthetic, to ensures less influence of reflex induced mechanisms on sampling [182]. Afterwards, study samples were immediately stored at -80 °C. This study was conducted in exact compliance with the guidelines of the Declaration of Helsinki (1964) and with ethical clearance by the institutional ethics committee of the "Landesärztekammer Rheinland-Pfalz". In accordance with the Declaration of Helsinki, all patients were informed about risks, privacy policy and the general aim of this study. Patients were excluded if one of the following aspects applied to them: previous diagnosis of DES or Sjögren's syndrome, allergy to local anesthetics, contact lens wear, ophthalmic surgery in the last 6 months, age under 18, pregnancy.

Subsequently, all study subjects underwent thorough diagnostic steps according to distinct inclusion and exclusion criteria. These consisted of symptom anamnesis employing the OSDI questionnaire, basic secretory tests (BST) and tear break up time (TBUT). According to each patient's collected data during diagnostics, they were separated into 4 groups in conformance to previous proteomic studies [20, 229-231] – lipid layer dysfunctional DES (DRYlip), aqueous-deficient DES (DRYaq), DES with a combination of lipid and aqueous layer dysfunctions (DRYaqlip) and control (CTRL). An overview of grouping criteria can be found in **Table 4**.

Table 4: Classification criteria for study groups

	BST [mm / 5min]	TBUT [s]
CTRL	> 10 mm	> 10 s
DRYlip	> 10 mm	≤ 10 s
DRYaq	≤ 10 mm	> 10 s
DRYaqlip	≤ 10 mm	≤ 10 s

A dysfunctional lipid layer will lessen tear film stability, which reduces the time the tear film is intact when it is not reorganized by blinking. Therefore the tear break up time is decreased in those cases [232, 233]. A TBUT under 10 seconds hence indicates a lipid layer deficiency in this study.

The patient's tear volume was evaluated *via* BST; in this case a Schirmer's test II. If the lacrimal gland does not produce or secrete sufficient tear fluid, the wetting length of the Schirmer Strip is reduced [51, 234]. A lacking aqueous layer production was therefore classified as ≤ 10 millimeters of wetting length in 5 minutes, conforming to other studies [169, 229]. Accordingly, patients were grouped into DRYaq if they presented values ≤10 millimeters in the BST, but normal lipid layer parameters.

If the BST and TBUT indicated pathologies at the same time, the participant was listed as DRYaqlip. Meanwhile, if all parameters were found to be normal, the patient became part of CTRL. These grouping criteria resulted in the subgroups containing the following number of patients: CTRL – 50, DRYlip – 34, DRYaq – 46 and DRYaqlip – 32. A detailed rendering of groupings including an age and gender-specific distribution within study groups can be found in **Figure 6** and **7**.

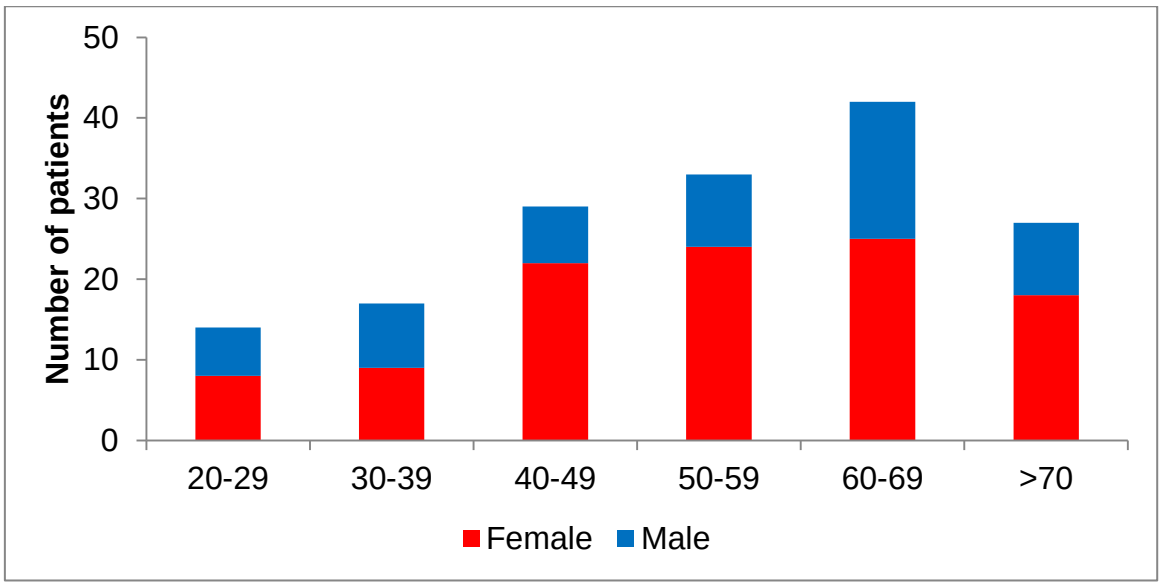

Figure 5: Age and sex distribution of patients

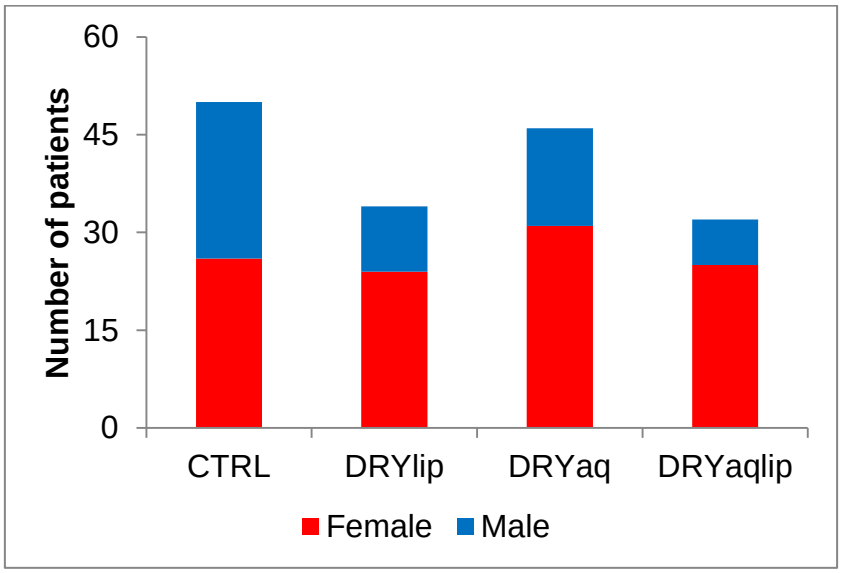

Figure 6: Gender distribution in study groups

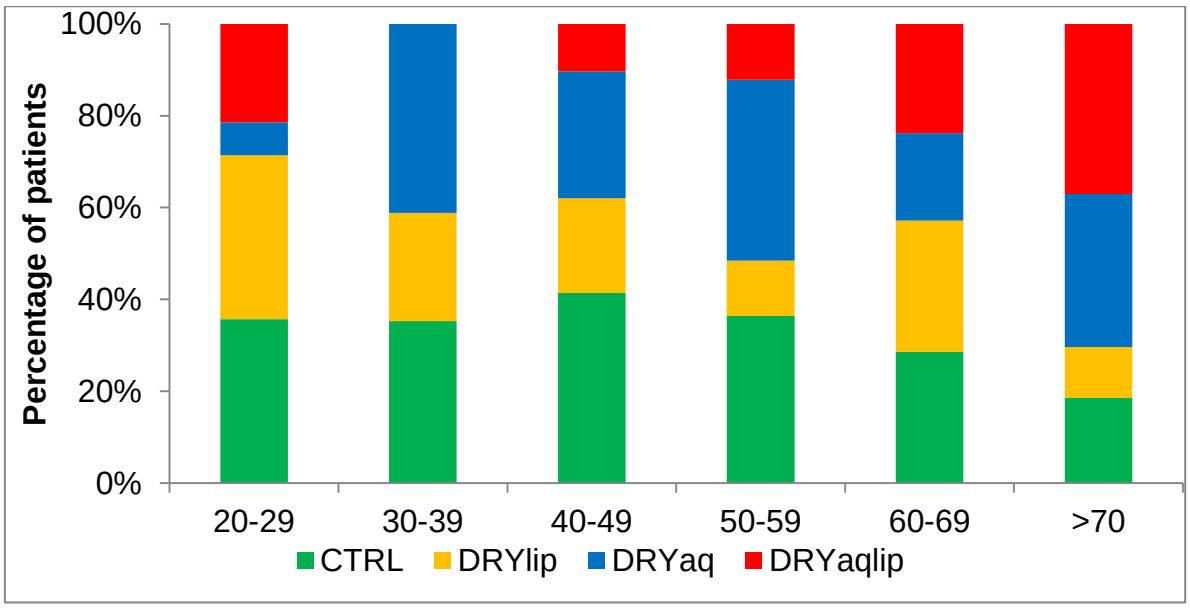

Figure 7: Age distribution in study groups

3.2.1.2 Sample preparation

In order to extract tear proteins, the Schirmer strips were put into a 2ml Eppendorf tube with 300 µl PBS and shaken for 3 hours by an Intelli Mixer at 4 °C. Protein concentrations were subsequently measured *via* BCA Protein Assay Kit, determining the individual tear volume needed for a total of 15 µg and thus normalizing all samples by protein amount. Since proteins need to be broken down to peptides for ensuing proteomic measurements, the samples were processed by in-solution trypsin digestion. The corresponding trypsin digestion buffer consists of 10 mM Ammonium bicarbonate in 10 % ACN. To achieve a trypsin to protein ration of 1:20 during digestion, each vial containing 20 µg of trypsin was filled with 800 µl of digestion buffer, resulting in a total trypsin stock concentration of 0.025 µg/µl. Consequently, 30 µl of trypsin stock was added to each sample before incubation at 37 °C for at least 16 hours. The thus digested samples were then dried down in a SpeedVac Concentrator and stored at -20 °C. For the sake of peptide purification, ZipTip C18 columns were used repeating their manufacturer's instructions for a total of four cycles per sample, before using the SpeedVac Concentrator again to evaporate all liquid to dryness. Prior to AIMS measurement samples were resuspended by 0.1 % TFA solution using sonification.

3.2.1.3 LC-ESI-MS/MS AIMS measurement

To obtain targeted MS/MS data from tear samples, a previously optimized ESI-LTQ-Orbitrap-XL-MS system was extensively adapted for individual tear samples [20, 27, 182, 229]. Peptide fractionation was conducted in the liquid chromatography (LC) system, which consisted of a Rheos Allegro pump (Thermo Scientific, Rockford, USA) and an HTS PAL autosampler (CTC Analytics AG, Zwingen, Switzerland) equipped with a BioBasic C18, 30 x 0.5 mm precolumn (Thermo Scientific, Rockford, USA) connected to a BioBasic C18, 150 x 0.5 mm analytical column (Thermo Scientific, Rockford, USA). The system was run with two solvents, A and B, with solvent A consisting of LC-MS grade water with 0.1% (v/v) formic acid and solvent B of LC-MS grade acetonitrile with 0.1% (v/v) formic acid. During each measurement a 120-minute gradient of the two solvents was run as follows: 0-7 min: 10-15 % B, 7-85 min: 15-30 % B, 85-95 min: 30-35 % B, 95-100 min: 35-90 % B, 100-105 min: 90 % B, 105-110 min: 90-10 % B: 110-120 min: 10 % B.

The general mass spectrometric conditions were as follows: positive-ion electronspray ionization mode, spray voltage set to 2.15 kV, heated capillary temperature set at 220 °C. The system was used in the data-dependent mode of acquisition, enabling automatic switches between MS and MS/MS modes. In MS mode the lock mass option was enabled. Internal recalibration was acquired in real time *via* polydimethylcyclosiloxane (PCM) ions (*m/z* 445.120025). Spectra were conducted from a *m/z* of 300 to 2000 with a target automatic gain control (AGC) set to 5 x 10^5 ions. Tandem data was obtained by selecting the top five most intense precursor ions and subjecting them for further fragmentation by collision-induced dissociation (CID). The normalized collision energy (NCE) was set to 35 % with an activation time of 30 ms, repeat count of 10 and dynamic exclusion duration of 600 s. The resulting fragmented ions were recorded in the LTQ. For AIMS measurements, the global parent list was enabled, which specifies the proteins of interest, with a peptide mass tolerance of ± 10 ppm. The list of precursor masses was assembled by compiling signature peptides of DES discovery stage studies as well as promising biomarkers of studies involving comparable eye diseases or pathophysiological mechanisms [20, 27, 182, 218, 229]. If parent masses were not identified, other unique peptides were added to the list in order to optimize protein identification before remeasuring the samples. The selection of the experimentally identified peptides list that annotated to specific proteins was carried out manually from the

“msms.txt” file resulting from MaxQuant (version 1.6.0.16) analysis governed by these criterions: contains no missed cleavages, fully tryptic, no modifications and peptide only assumes charge +2. The created peptide inclusion list comprising *m/z* and charge was assigned to the instrument acquisition software before data acquisition. These steps were repeated until protein identification was satisfactory. The resulting parent mass list, which gave off the best overall identification results for all 100 peptides of interest, can be found in **Table 5**. The system was therefore set to separate the samples using several LC steps for them to subsequently be measured in MS mode. If any previously specified *m/z* on the parent list was identified, respective peptides were automatically chosen for MS/MS measurements and fragmented in the LTQ. The resulting records of fragments were then quantified utilizing label-free approaches.

3.2.1.4 Label-free quantification (LFQ) analysis

The LFQ method used in this study has been extensively optimized and successfully used in various studies [20, 27, 182, 218, 229]. To adapt these methods to individual samples, raw protein intensities were used, since normalizing at this stage would eliminate distinctive expressions between samples. Datasets from AIMS measurements were processed by the proteomics software MaxQuant (version 1.6.0.16). This program can identify peptides and proteins by their fragmentation pattern through its search engine Andromeda and quantify them at the same time [235]. Protein recognition was achieved by searching the Uniprot Human database using a customized fasta file based on information tabulated in **Tabel 5** with standard settings, including a peptide mass tolerance of ±10 ppm, a fragment mass tolerance of ±0.5 Da, peptide charge state of +2 and a false discovery rate (FDR) for peptide identification set to 0.01 with ≥ 6 amino acid residues. Proteins were quantified only by unique plus razor peptides. Trypsin was indicated as the digestion enzyme and a maximum number of missed cleavages of 0 was set.

3.2.1.5 Statistical analysis

Statistics were obtained with the software Perseus (version 1.6.5.0), a program designed for MS-based proteomics data [236, 237]. Before analysis, data were $\log_2$-transformed and, for the purpose of quality control, results were filtered to only

include peptides with 70% valid measured values in at least one of the study groups. Missing values were subsequently imputated from a normal distribution in standard settings (width: 0.2, down shift: 1.8). PRR4 is included in the parent mass list with its 4 isoforms (PRR4_N1 to PRR4_N4), but since every individual possesses a distinct combination of 2 – 4 isoforms, they may not be present in all samples [27]. Therefore, the quality control steps described above would eliminate those isoforms from the list of significantly expressed proteins. In an effort to still include PRR4 in further statistics, a sum of all 4 isoform intensities (PRR4_SUM) was added to the list of proteins before quality control steps.

To determine which proteins were significantly expressed between study groups, a multiple-sample ANOVA test with a Benjamini-Hochberg FDR of < 0.05 was carried out. The resulting data sets were used to perform a Pearson correlation of each subgroup, to evaluate method reproducibility and a principle component analysis (PCA) to visualize relationships between samples (category enrichment in components disables). Additionally, the $\log_2$ ratios of peptide intensities were depicted in an unsupervised hierarchical clustering with standard settings (rows and columns tree – Distance: Euclidean, Linkage: Average, Constraint: None, Preprocess with k-means enabled, Number of clusters: 300, Maximal number of iterations: 10, Number of restarts: 1).

Correlations and box plots for age, gender, TBUT and BST differences were conducted *via* Statistica (version 13) with all peptides after quality control steps. For age and gender related statistics, only healthy individuals from the CTRL group were included, to exclude interfering influences from DES, whereas TBUT and BST statistics included all samples. Age, TBUT and BST were investigated *via* standard setting Pearson correlation, while gender correlations were obtained with a Wilcoxon signed-rank test, also in standard settings. Correlation factors were found to be significant with a p-value < 0.05.

3.2.1.6 Functional annotation and pathways analyses

The list of the identified proteins was tabulated in Excel and their gene names were used for subsequent functional annotation and pathways analyses employing Ingenuity Pathway Analysis (IPA) [238]. IPA analyses elucidated the Gene Ontology Cellular Component (GOCC) terms, molecular types, protein-protein interaction (PPI)

networks, and top disease functions associated with the proteins identified to be differentially expressed. Top canonical pathways, diseases & biological functions and upstream regulators of the differentially expressed proteins were presented with p-value calculated using Benjamini-Hochberg (B-H) multiple testing correction (–log B-H values were found to be significant > 1.3). In PPI networks, proteins molecules are represented by their corresponding gene names and only PPIs that were experimentally observed and had direct/indirect interactions were used. The IPA software represents proteins as nodes and connects them through direct or indirect interactions (lines, see figure legends). Nodes are depicted using different shapes to represent the protein's general function (e.g. enzyme or peptidase). Additionally, the nodes visualize an increase or decrease of abundance through color intensity (red = increment, green = decrement).

3.2.2 Establishing a MALDI-TOF-MS method for individual tear samples and characterization of PRR4

3.2.2.1 Method optimization

3.2.2.1.1 Study samples

For method optimization tears of 10 healthy volunteers (5 males, 5 females, median age: 28.1±6.0) were obtained *via* Schirmer strip. No anesthetic was used on the eye prior to sampling. Volunteers were recruited by the Department of Ophthalmology at the University Medical Center of the Johannes Gutenberg-University, Mainz in concordance to the Declaration of Helsinki. Samples were excluded if the volunteer has a diagnosed eye disease, was underage or pregnant.

3.2.2.1.2 Sample preparation

Samples were eluted in PBS and digested *via* Trypsin, as described in detail in **3.2.1.2**. Afterward, they were evaporated to dryness in a SpeedVac Concentrator, before being stored at -20 °C. Before measuring, they were resuspended in 6 µl of 0.1 % TFA solution using sonification. Samples were placed on a MALDI target plate in varying concentrations (see below). 2 µl spots of calibration standard were also added to the plate. 2 µl of a matrix consisting of 2 mg/ml α-cyano-4-hydroxycinnamic acid (CHCA), 60% ACN and 0.1% TFA was added to each spot, followed, depending on optimization step, by varying amounts of reserpine (see below), which functions as an internal standard. The internal standard was introduced to the sample because of two reasons. Since all samples contain a standardized amount of reserpine, it was possible to evaluate a measurements' quality and suppression effect on the one hand, as well as calculating estimated absolute intensities on the other. In between each pipetting step and before measurements, all liquids were evaporated to dryness at room temperature. All optimization steps were conducted with 3 technical replicates per sample to assess reproducibility and variation of peak identification and relative abundance. The following parameters were evaluated to adapt the method for individual tear samples:

a) Complex sample amount without internal standards: 0.5 to 3 µg sample per spot

b) Reserpine amount (internal standard)
c) Separate pipetting and air drying of all spot components successively (sample, reserpine, and matrix) *vs*. spotting of a mixture of them

3.2.2.1.3 MALDI-TOF measurements

Measurements were conducted using an Ultraflex 2 MALDI TOF system with FlexControl (version 2.4), which has been previously optimized by Perumal *et al.* [27]. Following these optimizations, basic settings were as follows: peak selection: 450 – 3700Da, reflector polarity: positive, laser frequency: 100 Hz, peak detection algorithm: SNAP (Sophisticated Numerical Annotation Procedure), building block: Averagine, smoothing algorithm: Savitzky Golay, baseline subtraction: off, S/N threshold: 6, peak width: 0.5 *m/z,* percent heigh: 80%, peak must be higher than: resolution min. 500, signal intensity: high, measuring raster: hexagon, quit sample after: 25 subsequently failed judgments, accumulation: sum of 500 from 50 shot steps, calibration: CalibratePeptideStandards.FAMSMethod

The following parameters underwent optimization steps to achieve improved measurements for individual complex samples:

a) Laser–fuzzy: off vs. on
b) Accumulation: off vs. on
c) Peak detection range: 450 – 3700 m/z
d) Number of shots per spot: 500, 1000, 2000 and 10000

3.2.2.1.4 MALDI-TOF data analysis

Mass spectra conducted *via* Ultraflex 2 MALDI TOF/TOF were subsequently analyzed with FlexAnalysis (version 2.4), which allows for spectra visualization as well as peak identification (including their signal to noise ratio) and relative quantification. Subsequent analyses of protein intensity levels and reproducibility were performed with Statistica 13 through the calculation of medians, Pearson correlations and box plots. PRR4 isoform peptide masses were checked for overlapping with other protein products with Proteome Discoverer (Version 1.1.0.263).

3.2.2.2 Characterization of individual tear sample's PRR4 in MALDI-TOF-MS

3.2.2.2.1 Study samples

Tears were collected from 42 healthy volunteers (28 males, 14 females, median age: 29.9±9.4) *via* Schirmer strips, without the use of anesthetics. Volunteers were recruited by the Department of Ophthalmology at the University Medical Center of the Johannes Gutenberg-University, Mainz in concordance to the Declaration of Helsinki. Samples were excluded if one of the following applied: previous diagnosis of eye-related diseases, age under 18 years, pregnancy.

In a first step, tears from both the left and right eye of 24 volunteers were extracted to evaluate differences in PRR4 intensities and isoform distribution between eyes of the same individual (group A). When they were found to be constant, 18 additional volunteer's tears were sampled from the left eye only (group B).

3.2.2.2.2 Sample preparation

As described in chapter **3.2.1.2**, DES patients' Schirmer strips were put into PBS and shaken to extract tear proteins, followed by overnight in-solution trypsin digestion. Subsequently, 3 µg of each sample was separated into PCR tubes and evaporated to dryness *via* a SpeedVac Concentrator to be stored at – 20 °C.

To conduct measurements, samples were resuspended in 6 µl of 0.1 % TFA solution using sonification. Samples were placed on a MALDI target plate in spots of 2 µl, resulting in 3 technical replicates per patient that were dried at room temperature. Furthermore, 1 µl of reserpine was added to each spot as an internal standard and dried before applying 2 µl of a matrix consisting of 2 mg/ml α-cyano-4-hydroxycinnamic acid (CHCA), 60% ACN and 0.1% TFA. Afterwards, all liquids were evaporated at room temperature once more. Additionally, 2 µl spots of calibration standards were prepared.

3.2.2.2.3 MALDI-TOF measurements

The same previously optimized Ultraflex 2 MALDI TOF system from chapter **3.2.2.1.3** was used, utilizing FlexControl (version 2.4). The optimized settings were as follows - mass range: 450-3700 Da; laser-fuzzy: off; accumulation: on, 2500 shots per spot.

3.2.2.2.4 MALDI-TOF data analysis

As described in **3.2.2.1.4**, mass spectra were analyzed with FlexAnalysis and Statistica. To reduce measurement inconsistencies, intensities of Reserpine and PRR4 isoforms were averaged from three technical replicates per individual. Next, to normalize PRR4 isoform peaks, the median intensity of the internal standard Reserpine of all measurements was calculated and found to be around 5000. Setting this as the value, that reserpine should be at in all samples, the factor in which each sample's internal standard deviates from 5000 was calculated and used to adjust PRR4 intensities. If any of the intensities were below 500 after normalization, the sample was excluded from further analyses. Afterwards, all samples were manually sorted into 6 groups by their isoform expression according to a study by Perumal *et al*. [27].

4. RESULTS

4.1 DES clinical biomarker discovery employing AIMS in a targeted proteomics strategy

Utilizing an extensively optimized AIMS method, all 100 unique peptides of interest could be identified in individual tear samples with excellent scores and sum intensities (see **Table 5**), enabling high quality subsequent analyses. Firstly, after thorough quality control of the LFQ values obtained by MaxQuant, the reproducibility of the experimental workflow was tested by applying Pearson correlations to all groups. Even though there is an unknown number of influences that alter protein content in patients, as has been described in previous chapters, the mean protein content of individual samples measured with this method highly correlate within their groups with median correlation factors of 0.76 ±0.08 for CTRL, 0.71 ±0.07 for DRYlip, 0.69 ±0.1 for DRYaq and 0.66 ±0.05 for DRYaqlip, demonstrating the method's excellent reproducibility and consistency. Hence this study has successfully measured a large number of individual tear samples employing a targeted proteomics method with a high level of reproducibility, which permits further comparison of subgroups and individual patients *via* statistical analysis.

The data was subsequently analyzed *via* PCA (**Figure 8**), which visualizes relationships between samples. The Perseus software achieves this by plotting each individual's LFQ values, resulting in a multidimensional coordinate system due to the involvement of all significantly expressed proteins. It is then simplified to only two dimensions that best distinguish all spots. Therefore, samples containing similar protein expressions are plotted in proximity to each other. What can be inferred from the PCA is that while there are overlapping areas where samples of multiple study groups show similar protein expressions, there are also regions that are more distinctly formed by only one of the groups. Also, there are larger overlapping areas between CTRL & DRYlip and DRYaq & DRYaqlip samples, suggesting that those groups have comparable protein profiles. Especially DRYaqlip, as a combination of lipid and aqueous dysfunction, shows overlapping with both of the other DES subgroups. These results are therefore in concordance to discovery stage results and current hypotheses concerning DES pathophysiology.

Table 5: List of all 100 peptides identified *via* AIMS.

	Gene names	Protein names	Sequence	*m/z*(2+)	*m/z*(+)	Length	Score	Intensity
1	A2M	Alpha-2-macroglobulin	AIGYLNTGYQR	628.3	1254.64	11	222	3.7E+07
2	ACTN4	Alpha-actinin-4	LSGSNPYTTVTPQIINSK	960.5	1919.00	18	290	2.7E+07
3	AGR2	Anterior gradient protein 2 homolog	GWGDQLIWTQTYEEALYK	1101.0	2200.05	18	385	2.2E+07
4	AGT	Angiotensinogen	VLSALQAVQGLLVAQGR	862.0	1722.02	17	86	4.8E+05
5	AKR1A1	Alcohol dehydrogenase [NADP(+)]	GLVQALGLSNFNSR	738.4	1474.79	14	312	1.7E+07
6	ALB	Serum albumin	VPQVSTPTLVEVSR	756.4	1510.84	14	247	6.8E+08
7	ALDH1A1	Retinal dehydrogenase 1	IFVEESIYDEFVR	823.4	1644.80	13	330	1.0E+08
8	ALDH3A1	Aldehyde dehydrogenase, dimeric NADP-preferring	SLEEAIQFINQR	724.4	1446.75	12	358	1.8E+08
9	ANXA1	Annexin A1	GLGTDEDTLIEILASR	851.9	1701.88	16	348	2.5E+08
10	ANXA2	Annexin A2	AEDGSVIDYELIDQDAR	954.9	1907.87	17	349	2.0E+08
11	ANXA3	Annexin A3	GAGTNEDALIEILTTR	837.4	1672.86	16	290	2.1E+07
12	APOA1	Apolipoprotein A-I	VSFLSALEEYTK	693.9	1385.71	12	266	1.6E+07
13	APOBEC3A	DNA dC->dU-editing enzyme APOBEC-3A	IYDYDPLYK	595.3	1188.57	9	125	2.2E+07
14	APOD	Apolipoprotein D	NILTSNNIDVK	615.8	1229.66	11	73	1.6E+08
15	AZGP1	Zinc-alpha-2-glycoprotein	YSLTYIYTGLSK	704.9	1407.73	12	329	1.3E+09
16	C3	Complement C3	IPIEDGSGEVVLSR	735.9	1469.77	14	299	1.4E+08
17	CALR	Calreticulin	FYALSASFEPFSNK	804.4	1606.77	14	142	7.2E+06
18	CASP14	Caspase-14	LENLFEALNNK	652.8	1303.68	11	229	1.8E+08
19	CLU	Clusterin	LFDSDPITVTVPVEVSR	937.5	1872.98	17	316	2.7E+08
20	CMPK1	UMP-CMP kinase	SVDEVFDEVVQIFDK	884.9	1767.86	15	300	1.6E+07
21	CNDP2	Cytosolic non-specific dipeptidase	LPDGSEIPLPPILLGR	844.0	1685.97	16	146	8.4E+06
22	CP	Ceruloplasmin	GAYPLSIEPIGVR	686.4	1370.76	13	176	1.1E+08
23	CST1	Cystatin-SN	QQTVGGVNYFFDVEVGR	958.0	1913.93	17	338	1.6E+08
24	CST3	Cystatin-C	ALDFAVGEYNK	613.8	1225.60	11	216	3.1E+09
25	CST4	Cystatin-S	EQTFGGVNYFFDVEVGR	982.5	1962.91	17	371	6.6E+08
26	CSTB	Cystatin-B	SQVVAGTNYFIK	663.8	1325.70	12	338	1.0E+08
27	CTSB	Cathepsin B	NGPVEGAFSVYSDFLLYK	1003.5	2004.98	18	243	1.2E+06
28	CTSD	Cathepsin D	YSQAVPAVTEGPIPEVLK	949.5	1897.02	18	86	1.5E+08
29	DMBT1	Deleted in malignant brain tumors 1 protein	FGQGSGPIVLDDVR	730.4	1458.75	14	295	2.2E+09
30	ENO1	Alpha-enolase	GNPTVEVDLFTSK	703.9	1405.71	13	323	6.5E+08
31	EZR	Ezrin	IGFPWSEIR	552.8	1103.58	9	150	6.3E+07
32	FBP1	Fructose-1,6-bisphosphatase 1	APVILGSPDDVLEFLK	857.0	1711.94	16	267	2.4E+07

Table 5: (continued)

	Gene names	Protein names	Sequence	*m/z*(2+)	*m/z*(+)	Length	Score	Intensity
33	GDI2	Rab GDP dissociation inhibitor beta	DLGTESQIFISR	683.3	1364.69	12	195	1.2E+07
34	GPI	Glucose-6-phosphate isomerase	TLAQLNPESSLFIIASK	916.5	1831.01	17	332	8.4E+07
35	GSN	Gelsolin	QTQVSVLPEGGETPLFK	915.5	1828.96	17	335	1.3E+08
36	GSTP1	Glutathione S-transferase P	FQDGDLTLYQSNTILR	942.5	1882.94	16	567	7.9E+08
37	HEBP2	Heme-binding protein 2	NQEQLLTLASILR	749.9	1497.85	13	376	4.0E+07
38	HP	Haptoglobin	VTSIQDWVQK	602.3	1202.63	10	255	4.5E+08
39	HPX	Hemopexin	NFPSPVDAAFR	610.8	1219.60	11	153	3.1E+08
40	HSPA8	Heat shock cognate 71 kDa protein	SINPDEAVAYGAAVQAAILSGDK	1130.6	2259.14	23	307	3.1E+07
41	HSPB1	Heat shock protein beta-1	LFDQAFGLPR	582.3	1162.61	10	265	2.4E+08
42	HSPG2	Basement membrane-specific heparan sulfate proteoglycan core protein	LEGDTLIIPR	563.8	1125.64	10	169	2.2E+07
43	IGHA1	Ig alpha-1 chain C region	DASGVTFTWTPSSGK	770.9	1539.72	15	374	9.3E+08
44	IGHM	Ig mu chain C region	QVGSGVTTDQVQAEAK	809.4	1616.80	16	223	1.9E+07
45	IGJ	Immunoglobulin J chain	SSEDPNEDIVER	695.3	1388.61	12	192	2.4E+08
46	IGKC	Ig kappa chain C region	DSTYSLSSTLTLSK	751.9	1501.75	14	323	1.2E+09
47	IGLC3	Ig lambda-3 chain C regions	YAASSYLSLTPEQWK	872.4	1742.85	15	423	1.7E+09
48	ITIH2	Inter-alpha-trypsin inhibitor heavy chain H2	IQPSGGTNINEALLR	791.9	1581.85	15	110	6.2E+06
49	LACRT	Extracellular glycoprotein lacritin	SILLTEQALAK	593.8	1185.70	11	312	1.4E+10
50	LCN1	Lipocalin-1	NNLEALEDFEK	661.3	1320.62	11	330	2.3E+10
51	LCN2	Neutrophil gelatinase-associated lipocalin	VPLQQNFQDNQFQGK	895.9	1789.87	15	304	1.1E+08
52	LDHA	L-lactate dehydrogenase A chain	DLADELALVDVIEDK	829.4	1656.85	15	298	1.1E+08
53	LGALS3	Galectin-3	GNDVAFHFNPR	637.3	1272.60	11	195	1.5E+08
54	LTF	Lactotransferrin	DVTVLQNTDGNNNEAWAK	995.0	1987.92	18	561	2.4E+09
55	LYZ	Lysozyme C	STDYGIFQINSR	700.8	1399.67	12	389	2.1E+10
56	MSLN	Mesothelin	GLLPVLGQPIIR	638.4	1274.81	12	184	4.6E+07
57	NUCB1	Nucleobindin-1	LPEVEVPQHL	580.8	1159.62	10	143	1.4E+07
58	NUCB2	Nucleobindin-2	LVTLEEFLK	546.3	1090.63	9	83	1.2E+07
59	P4HB	Protein disulfide-isomerase	ILEFFGLK	483.8	965.56	8	160	1.2E+07
60	PEBP1	Phosphatidylethanolamine-binding protein 1	GNDISSGTVLSDYVGSGPPK	975.5	1948.94	20	429	3.2E+08
61	PFN1	Profilin-1	TFVNITPAEVGVLVGK	822.5	1642.93	16	281	1.4E+08
62	PIGR	Polymeric immunoglobulin receptor	DGSFSVVITGLR	625.8	1249.67	12	258	4.8E+08
63	PIP	Prolactin-inducible protein	TVQIAAVVDVIR	642.4	1282.76	12	289	7.6E+09
64	PKM	Pyruvate kinase PKM	DPVQEAWAEDVDLR	821.9	1641.76	14	224	2.9E+07

Table 5: (continued)

	Gene names	Protein names	Sequence	*m/z*(2+)	*m/z*(+)	Length	Score	Intensity
65	PPIA	Peptidyl-prolyl cis-trans isomerase A	FEDENFILK	577.8	1153.57	9	264	6.2E+08
66	PRDX1	Peroxiredoxin-1	TIAQDYGVLK	554.3	1106.60	10	226	3.2E+08
67	PRDX5	Peroxiredoxin-5, mitochondrial	THLPGFVEQAEALK	770.4	1538.81	14	175	1.4E+08
68	PRDX6	Peroxiredoxin-6	LPFPIIDDR	543.3	1084.59	9	149	7.8E+07
69	PROL1	Proline-rich protein 1	FSQAVILSQLFPLESIR	974.5	1947.08	17	302	2.7E+08
70	PRR4_N1	Proline-rich protein 4	FPSVSLQEASSFFQR	865.4	1728.85	15	423	4.9E+09
	PRR4_N2	Proline-rich protein 4	FPSVSLQEASSFFR	801.4	1600.79	14	405	1.9E+10
	PRR4_N3	Proline-rich protein 4	HPPPPPFQNQQRPPR	897.0	1791.93	15	166	5.0E+09
	PRR4_N4	Proline-rich protein 4	HPPPPPFQNQQRPPQR	961.0	1919.99	16	128	6.4E+09
71	RBP4	Retinol-binding protein 4	YWGVASFLQK	599.8	1197.62	10	176	9.0E+06
72	RNASE4	Ribonuclease 4	FNTFIHEDIWNIR	852.9	1703.84	13	217	1.4E+07
73	S100A11	Protein S100-A11	DGYNYTLSK	530.7	1059.49	9	220	1.4E+08
74	S100A4	Protein S100-A4	ELPSFLGK	445.7	889.49	8	154	3.3E+08
75	S100A8	Protein S100-A8	ALNSIIDVYHK	636.8	1271.69	11	312	9.1E+08
76	S100A9	Protein S100-A9	NIETIINTFHQYSVK	904.0	1805.93	15	424	5.8E+08
77	S100P	Protein S100-P	ELPGFLQSGK	538.3	1074.57	10	166	2.0E+08
78	SCGB1D1	Secretoglobin family 1D member 1	APLEAVAAK	435.3	868.50	9	194	2.4E+09
79	SCGB2A1	Mammaglobin-B	ELLQEFIDSDAAAEAMGK	969.5	1936.91	18	506	6.8E+09
80	SCUBE2	Signal peptide, CUB and EGF-like domain-containing protein 2	NAELFPEGLR	573.3	1144.59	10	96	1.1E+08
81	SELENBP1	Selenium-binding protein 1	NTGTEAPDYLATVDVDPK	953.5	1904.90	18	274	8.4E+07
82	SERPINA1	Alpha-1-antitrypsin	ITPNLAEFAFSLYR	821.4	1640.86	14	203	1.3E+07
83	SERPINA3	Alpha-1-antichymotrypsin	AVLDVFEEGTEASAATAVK	954.5	1906.95	19	402	3.8E+07
84	SERPINB1	Leukocyte elastase inhibitor	LGVQDLFNSSK	604.3	1206.62	11	261	7.4E+07
85	SERPINC1	Antithrombin-III	VAEGTQVLELPFK	715.9	1429.78	13	187	6.4E+06
86	SFN	14-3-3 protein sigma	YLAEVATGDDK	591.3	1180.56	11	199	1.3E+07
87	TAGLN2	Transgelin-2	DDGLFSGDPNWFPK	797.9	1593.71	14	235	3.3E+07
88	TCN1	Transcobalamin-1	GTSAVNVVLSLK	594.3	1186.69	12	215	1.7E+08
89	TGM2	Protein-glutamine gamma-glutamyltransferase 2	TVEIPDPVEAGEEVK	806.4	1610.80	15	238	1.9E+08
90	TKT	Transketolase	ILATPPQEDAPSVDIANIR	1010.5	2019.06	19	315	5.9E+07
91	TPM4	Tropomyosin alpha-4 chain	IQALQQQADEAEDR	807.9	1613.76	14	136	3.4E+06
92	TTR	Transthyretin	YTIAALLSPYSYSTTAVVTNPK	1180.6	2359.23	22	192	1.5E+07
93	TXN	Thioredoxin	TAFQEALDAAGDK	668.8	1335.63	13	295	3.2E+08

Table 5: (continued)

	Gene names	Protein names	Sequence	*m/z*(2+)	*m/z*(+)	Length	Score	Intensity
94	UBA52	Ubiquitin-60S ribosomal protein L40	TITLEVEPSDTIENVK	894.5	1786.92	16	204	7.3E+07
95	YWHAB	14-3-3 protein beta/alpha	YLIPNATQPESK	680.9	1359.70	12	145	3.8E+07
96	YWHAZ	14-3-3 protein zeta/delta	GIVDQSQQAYQEAFEISK	1021.0	2039.98	18	584	2.3E+08
97	ZG16B	Zymogen granule protein 16 homolog B	YFSTTEDYDHEITGLR	973.9	1945.87	16	380	3.9E+08

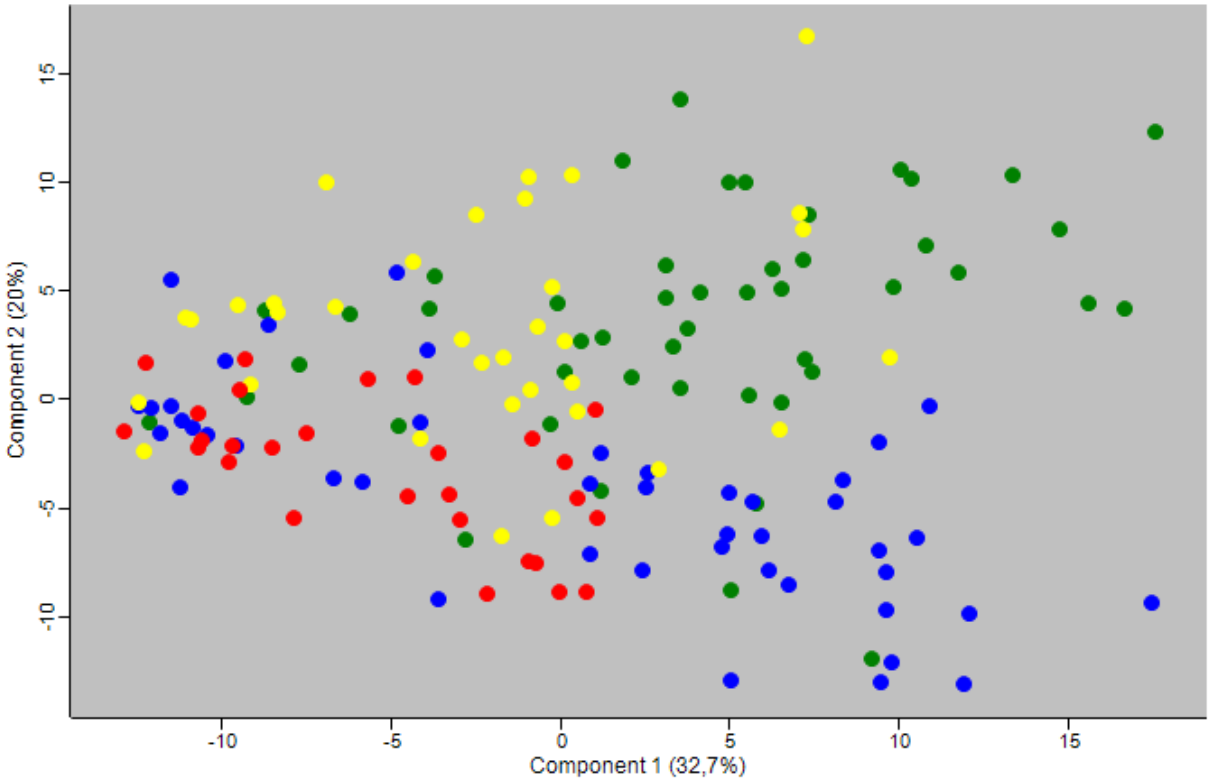

Figure 8: Principle Component Analysis (PCA) of individual samples visualizing their protein content in comparison to each other. Each spot represents one individual's sample. CTRL = green spots, DRYlip = yellow spots, DRYaq = blue spots, DRYaqlip = red spots.

The LFQ data set was then additionally utilized to assess which proteins were significantly expressed between study groups. By applying statistical measures described in chapter **3.2.1.5**, 59 out of 100 peptides that were included in the AIMS measurements of individual samples were found to be differentially expressed with a Benjamini-Hochberg FDR of < 0.05, as shown in **Table 6**. When comparing groups, the numbers of differentially expressed proteins were as follows: DRYlip *vs*. CTRL – 25 proteins, DRYaq *vs*. CTRL – 37 proteins, DRYaqlip *vs*. CTRL – 43 proteins, DRYlip *vs*. DRYaq – 27 proteins, DRYlip *vs*. DRYaqlip – 19 proteins, DRYaq *vs*. DRYaqlip – 18 proteins. To visualize and systematize these alterations, an unsupervised hierarchical clustering of the 59 significant proteins' fold changes was conducted, which can be found in **Figure 9**. A clustering of fold changes was chosen over protein intensities, since absolute change visualizations using color gradients are harder to interpret, especially for low abundant proteins. Relative change depictions like fold changes, therefore, simplify data interpretation, particularly for

those proteins of interest. Two major protein clusters can be observed in **Figure 9**: one that indicates increased intensities in all or most DES subgroups and the other, which visualizes decrements in DRYaq and DRYaqlip. Therefore, the protein fold changes point to a shared mechanism of DES subgroups that are represented by the first cluster, as well as a difference in disease pathway for DRYlip and DRYaq illustrated by the second cluster. DRYaqlip, as a combination of both etiologies, shows both characteristics.

Table 6: Summary of all significantly expressed proteins in comparison to CTRL and between DES subgroups.

Gene name	DRYlip *vs.* CTRL		DRYaq *vs.* CTRL		DRYaqlip *vs.* CTRL		DRYaq *vs.* DRYlip		DRYaqlip *vs.* DRYlip		DRYaqlip *vs.* DRYaq	
	p-value	Log_2 ratio	p-value	Log_2 ratio	p-value	Log_2 ratio	p-value	Log_2 ratio	p-value	Log_2 ratio	p-value	Log_2 ratio
A2M	n.s.	n.s.	1.57E-03	1.26	2.41E-08	2.50	n.s.	n.s.	6.00E-04	1.83	1.37E-02	1.24
ALB	2.01E-03	1.89	9.39E-03	1.48	5.37E-07	2.95	n.s.	n.s.	n.s.	n.s.	1.04E-02	1.48
ALDH3A1	1.41E-03	1.54	4.66E-10	2.70	9.52E-08	2.75	1.78E-03	1.16	4.92E-03	1.21	n.s.	n.s.
ANXA2	8.51E-03	0.94	6,95E-09	1.71	1.96E-05	1.63	4.40E-03	0.77	n.s.	n.s.	n.s.	n.s.
ANXA3	2.55E-03	1.08	8.77E-06	1.37	2.05E-07	1.89	n.s.	n.s.	1.34E-02	0.81	n.s.	n.s.
AZGP1	n.s.	n.s.	5.99E-03	-1.61	n.s.	n.s.	n.s.	n.s.	n.s.	n.s.	n.s.	n.s.
C3	n.s.	n.s.	n.s.	n.s.	8.22E-04	1.64	n.s.	n.s.	n.s.	n.s.	n.s.	n.s.
CASP14	n.s.	n.s.	n.s.	n.s.	1.38E-04	1.33	n.s.	n.s.	1.09E-02	1.00	8.60E-03	1.01
CLU	n.s.	n.s.	8.81E-05	-0.81	2.35E-07	-1.20	2.05E-02	-0.59	6.10E-04	-0.97	n.s.	n.s.
CP	n.s.	n.s.	n.s.	n.s.	2.47E-04	0.87	n.s.	n.s.	n.s.	n.s.	4.87E-03	1.09
CST1	n.s.	n.s.	3.44E-04	-1.39	n.s.	n.s.	8.89E-08	-2.13	1.54E-02	-1.00	6.09E-03	1.12
CST3	6.56E-04	1.53	n.s.	n.s.	8.27E-06	2.47	n.s.	n.s.	n.s.	n.s.	7.64E-03	1.98
CST4	3.67E-03	1.16	7.62E-03	-1.17	n.s.	n.s.	4.96E-07	-2.34	n.s.	n.s.	3.09E-04	1.70
CSTB	n.s.	n.s.	1.22E-02	1.12	8.07E-03	1.55	3.39E-03	1.23	3.14E-03	1.66	n.s.	n.s.
CTSD	4.13E-04	0.82	n.s.	n.s.	n.s.	n.s.	1.99E-03	-1.01	n.s.	n.s.	n.s.	n.s.
DMBT1	n.s.	n.s.	2.24E-05	-1.74	5.72E-06	-1.92	6.21E-07	-2.17	1.52E-08	-2.35	n.s.	n.s.
ENO1	1.03E-02	0.99	3.82E-10	2.02	2.36E-05	1.71	3.05E-04	1.03	n.s.	n.s.	n.s.	n.s.
EZR	2.49E-03	1.20	n.s.	n.s.	1.21E-03	1.52	n.s.	n.s.	n.s.	n.s.	n.s.	n.s.
GPI	8.53E-05	1.84	1.57E-09	2.29	1.14E-10	3.16	n.s.	n.s.	2.68E-04	1.32	4.06E-06	0.88
GSTP1	n.s.	n.s.	8.03E-05	1.53	n.s.	n.s.	n.s.	n.s.	n.s.	n.s.	4.00E-03	-1.41
HEBP2	n.s.	n.s.	1.21E-03	1.18	2.52E-04	1.35	n.s.	n.s.	n.s.	n.s.	n.s.	n.s.

Table 7: (continued)

Gene name	DRYlip *vs.* CTRL		DRYaq *vs.* CTRL		DRYaqlip *vs.* CTRL		DRYaq *vs.* DRYlip		DRYaqlip *vs.* DRYlip		DRYaqlip *vs.* DRYaq	
	p-value	Fold change	p-value	Fold change	p-value	Fold change	p-value	Fold change	p-value	Fold change	p-value	Fold change
HPX	n.s.	n.s.	1.40E-04	1.27	2.43E-04	1.72	n.s.	n.s.	n.s.	n.s.	n.s.	n.s.
HSPA8	2.01E-02	0.83	n.s.	n.s.	9.82E-06	1.73	n.s.	n.s.	n.s.	n.s.	4.40E-03	1.15
HSPB1	n.s.	n.s.	2.95E-02	-1.32	n.s.	n.s.	n.s.	n.s.	n.s.	n.s.	n.s.	n.s.
IGHA1	n.s.	n.s.	n.s.	n.s.	9.88E-04	-1.91	n.s.	n.s.	n.s.	n.s.	n.s.	n.s.
IGKC	5.07E-05	1.29	n.s.	n.s.	5.82E-03	0.95	5.83E-04	-1.50	n.s.	n.s.	1.48E-02	1.15
IGLC3	4.68E-06	1.82	n.s.	n.s.	4.77E-04	1.42	4.72E-05	-2.53	n.s.	n.s.	1.25E-03	2.13
LCN1	n.s.	n.s.	5.12E-03	-1.97	n.s.	n.s.	n.s.	n.s.	n.s.	n.s.	n.s.	n.s.
LCN2	1.79E-03	1.52	n.s.	n.s.	n.s.	n.s.	n.s.	n.s.	1.56E-02	-1.18	n.s.	n.s.
MSLN	n.s.	n.s.	1.72E-06	-1.66	1.13E-05	-1.66	1.55E-04	-1.38	3.01E-04	-1.38	n.s.	n.s.
OPRPN	n.s.	n.s.	7.24E-07	-2.96	3.09E-05	-2.66	8.19E-05	-2.34	5.61E-04	-2.05	n.s.	n.s.
P4HB	8.44E-03	0.67	n.s.	n.s.	5.50E-06	1.32	n.s.	n.s.	1.54E-02	0.64	1.93E-03	0.91
PEBP1	n.s.	n.s.	7.38E-05	1.47	1.62E-06	2.08	n.s.	n.s.	5.00E-03	1.33	n.s.	n.s.
PFN1	n.s.	n.s.	2.36E-02	0.64	4.06E-04	1.24	n.s.	n.s.	n.s.	n.s.	n.s.	n.s.
PIGR	5.66E-03	0.94	1.21E-02	-0.98	n.s.	n.s.	2.17E-05	-1.91	n.s.	n.s.	n.s.	n.s.
PIP	n.s.	n.s.	1.57E-02	-0.74	n.s.	n.s.	1.34E-02	-0.94	n.s.	n.s.	n.s.	n.s.
PKM	n.s.	n.s.	n.s.	n.s.	2.77E-03	1.01	n.s.	n.s.	n.s.	n.s.	6.27E-03	0.83
PPIA	4.80E-03	0.81	4.26E-05	1.00	4.99E-05	1.19	n.s.	n.s.	n.s.	n.s.	n.s.	n.s.
PRDX1	1.87E-03	1.16	2.94E-02	0.77	8.96E-03	1.13	n.s.	n.s.	n.s.	n.s.	n.s.	n.s.
PRDX5	n.s.	n.s.	1.83E-02	0.80	7.42E-03	1.15	n.s.	n.s.	n.s.	n.s.	n.s.	n.s.
PRDX6	n.s.	n.s.	4.51E-03	0.78	1.74E-02	0.78	n.s.	n.s.	n.s.	n.s.	n.s.	n.s.
PRR4_N2	n.s.	n.s.	1,47E-04	-1,89	4.33E-05	-2.37	n.s.	n.s.	n.s.	n.s.	n.s.	n.s.

Table 8: (continued)

Gene name	DRYlip *vs.* CTRL		DRYaq *vs.* CTRL		DRYaqlip *vs.* CTRL		DRYaq *vs.* DRYlip		DRYaqlip *vs.* DRYlip		DRYaqlip *vs.* DRYaq	
	p-value	Fold change	p-value	Fold change	p-value	Fold change	p-value	Fold change	p-value	Fold change	p-value	Fold change
PRR4_SUM	n.s.	n.s.	2.32E-04	-1.17	4.82E-05	-1.48	4.09E-04	-1.17	5.19E-05	-1.48	n.s.	n.s.
RNASE4	2.40E-03	0.80	n.s.	n.s.	n.s.	n.s.	3.11E-05	-1.36	n.s.	n.s.	n.s.	n.s.
S100A11	4.04E-03	1.26	n.s.	n.s.	8.22E-03	1.23	2.08E-02	-0.99	n.s.	n.s.	n.s.	n.s.
S100A8	1.28E-03	1.86	n.s.	n.s.	3.99E-05	2.44	1.71E-02	-1.76	n.s.	n.s.	2.62E-03	2.35
S100A9	5.47E-04	1.98	n.s.	n.s.	2.58E-06	2.70	n.s.	n.s.	n.s.	n.s.	1.18E-03	1.64
SCGB1D1	n.s.	n.s.	2.58E-02	-1.23	n.s.	n.s.	2.57E-03	-2.21	n.s.	n.s.	n.s.	n.s.
SCGB2A1	n.s.	n.s.	n.s.	n.s.	1.24E-03	-2.06	3.38E-03	-1.65	2.73E-05	-2.80	n.s.	n.s.
SCUBE2	1.28E-04	1.77	n.s.	n.s.	n.s.	n.s.	n.s.	n.s.	n.s.	n.s.	n.s.	n.s.
SELENBP1	n.s.	n.s.	3.12E-03	1.14	n.s.	n.s.	5.12E-03	1.16	n.s.	n.s.	n.s.	n.s.
SERPINA3	n.s.	n.s.	5.78E-03	0.71	n.s.	n.s.	n.s.	n.s.	n.s.	n.s.	3.81E-03	-0.74
TCN1	n.s.	n.s.	n.s.	n.s.	1.71E-02	-0.91	1.61E-02	-0.91	2.99E-03	-1.23	n.s.	n.s.
TGM2	n.s.	n.s.	1.22E-03	1.45	n.s.	n.s.	2.73E-03	1.54	n.s.	n.s.	n.s.	n.s.
TKT	1.73E-02	0.94	8.47E-09	2.16	5.71E-07	2.05	1.08E-03	1.22	4.62E-03	1.10	n.s.	n.s.
TXN	n.s.	n.s.	n.s.	n.s.	3.43E-04	1.51	2.11E-02	-1.08	n.s.	n.s.	5.74E-04	1.73
UBA52	2.04E-02	1.04	n.s.	n.s.	2.74E-04	1.61	n.s.	n.s.	n.s.	n.s.	n.s.	n.s.
YWHAB	n.s.	n.s.	1.83E-02	0.92	2.22E-02	1.00	n.s.	n.s.	n.s.	n.s.	n.s.	n.s.
ZG16B	n.s.	n.s.	1.23E-08	-2.50	7.78E-11	-3.26	8.28E-07	-2.33	4.20E-09	-3.10	n.s.	n.s.

Benjamini-Hochberg p-values were found to be significant <0.05. Fold changes are displayed by $\log_2$ ratios. Therefore all values >0 indicate an upregulation (red) and all values <0 indicate a downregulation (blue); **n.s.** = not significant

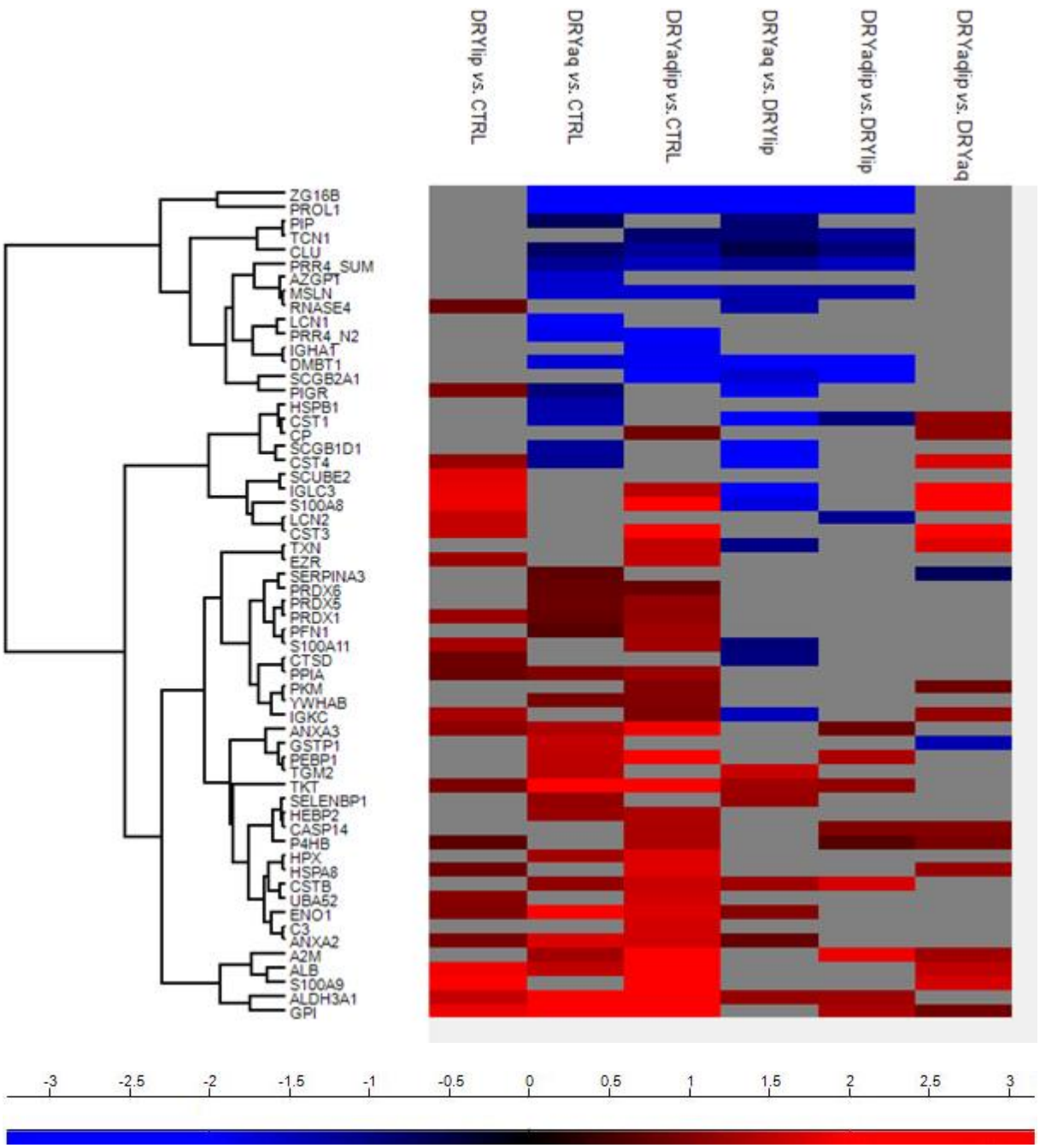

Figure 9: Hierarchical clustering of LFQ fold changes of all significantly expressed proteins (Benjamini-Hochberg FDR < 0.05). Log_2 ratio differences are visualized from low (blue) to high (red). Non-significant expressions are depicted in grey.

After initial quality control steps, LFQ intensities were also used for correlation analyses concerning current diagnostic tests (TBUT, Schirmer strip length), age, and gender with means described in chapter **3.2.1.5**. Statistics for TBUT and Schirmer strip length included all samples in order to evaluate their currently established cut off

values for DES diagnostics, whereas analyses for age and gender correlations included only healthy individuals from CTRL to rule out influences of DES and therefore gain a better understanding of non-disease related alterations. **Table 7** shows the top 20 proteins correlating with those factors. In total, 54 proteins were correlated with Schirmer strip length, 41 to TBUT, 11 to age, and 4 to gender – a list of all of them can be found in **Appendix 1**. When investigating significant correlations for the diagnostic tests of TBUT and Schirmer strip length with specific proteins, they were found to be linear regressions (exemplary graphs in **Figure 10**).

Table 9: Top 20 protein correlations with Schirmer strip length, TBUT, age, and gender.

	Schirmer lenght [mm]		TBUT [s]		Age		Gender	
	r(X,Y)	P	r(X,Y)	P	r(X,Y)	P	T	P
ALDH3A1	-0.60	9.81E-17	-0.23	3.83E-03	n.s.	n.s.	n.s.	n.s.
CST4	0.18	2,.31E-02	-0.31	8.83E-05	n.s.	n.s.	n.s.	n.s.
GPI	-0.69	3.00E-23	-0.41	1.02E-07	n.s.	n.s.	n.s.	n.s.
HSPA8	-0.35	7.74E-06	-0.34	1.09E-05	n.s.	n.s.	-2.23	3.05E-02
IGHA1	0.21	8.28E-03	0.17	3.54E-02	-0.34	1,73E-02	n.s.	n.s.
LACRT	0.25	1.76E-03	0.24	2.49E-03	n.s.	n.s.	2.46	1.76E-02
LCN2	n.s.	n.s.	-0.17	3.22E-02	0.37	1,06E-02	n.s.	n.s.
LGALS3	-0.16	4.69E-02	n.s.	n.s.	-0.30	4,01E-02	n.s.	n.s.
MSLN	0.39	3.41E-07	n.s.	n.s.	-0.30	3,57E-02	n.s.	n.s.
PIGR	0.18	2.50E-02	-0.23	4.33E-03	n.s.	n.s.	n.s.	n.s.
PIP	0.32	4.34E-05	n.s.	n.s.	-0.42	2,63E-03	n.s.	n.s.
PRR4_N1	n.s.	n.s.	n.s.	n.s.	-0.25	1,79E-03	n.s.	n.s.
PRR4_N4	n.s.	n.s.	n.s.	n.s.	-0.38	7,77E-03	n.s.	n.s.
PRR4_SUM	0.35	4.90E-06	n.s.	n.s.	n.s.	n.s.	2.45	1.82E-02
RNASE4	0.24	1.93E-03	-0.20	1.07E-02	n.s.	n.s.	n.s.	n.s.
SCGB1D1	0.22	4.66E-03	n.s.	n.s.	-0.39	5,57E-03	n.s.	n.s.
SCGB2A1	0.35	4.76E-06	n.s.	n.s.	-0.33	2,18E-02	n.s.	n.s.
SCUBE2	-0.17	2.98E-02	-0.27	5.78E-04	n.s.	n.s.	-2.15	3.72E-02
SERPINA3	n.s.	n.s.	n.s.	n.s.	0.29	4,31E-02	n.s.	n.s.
ZG16B	0.64	3.23E-19	n.s.	n.s.	-0.36	1,27E-02	n.s.	n.s.

Results were declared significant with a p-value ≤ 0.05. Positive regression factors are marked in red, negative ones in blue. Gender correlations were calculated as male *vs*. female, therefore positive values indicate an increased abundance and negative ones a decreased expression in males. A list of all correlations and statistical parameters can be found in **Appendix 1**. **n.s.** = not significant

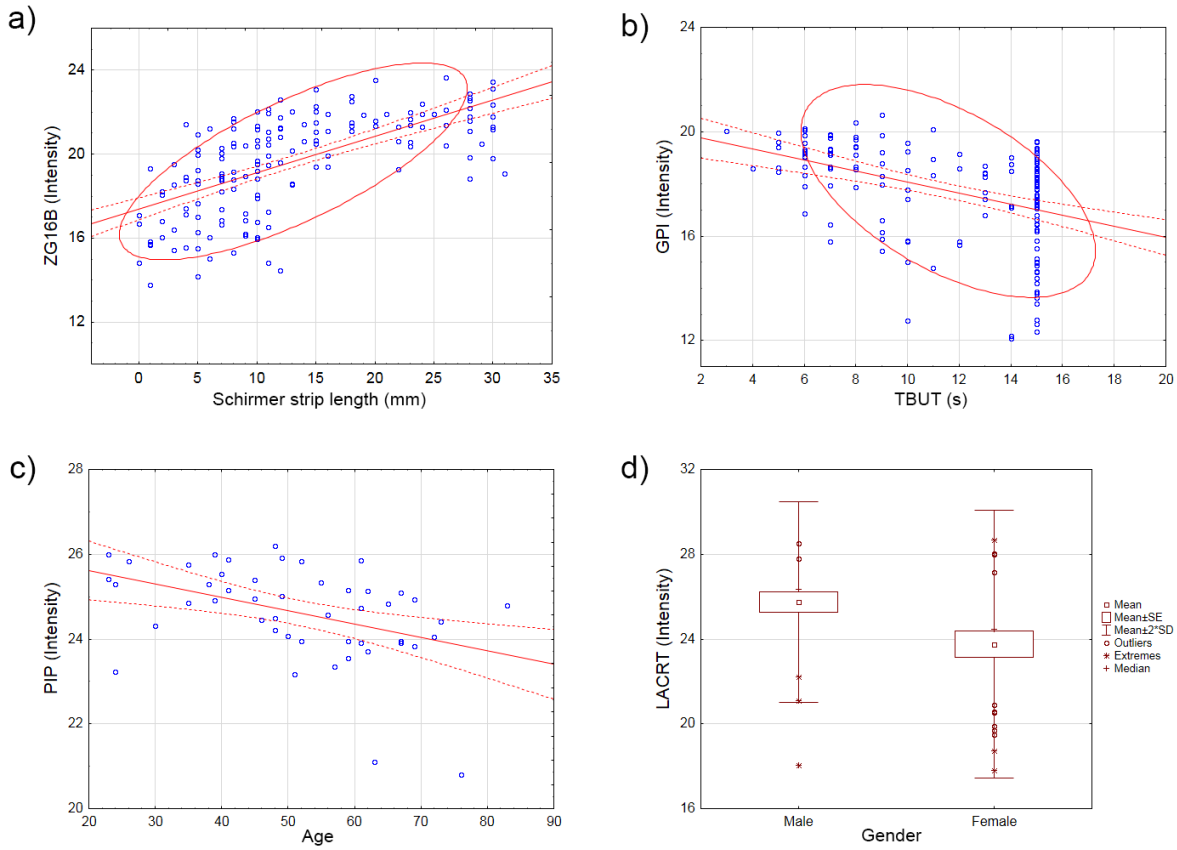

Figure 10: Exemplary correlation graphs from all 4 investigated factors. a) Intensity of ZG16B in regard to Schirmer strip length, **b)** GPI intensity in relation to TBUT, **c)** Age correlation with PIP, **d)** LACRT intensities depending on gender. As can be observed, protein intensities in **a)-c)** are linear regressions.

These results suggest a gradual disease development or loss of compensation leeway, which is in concordance with our current understanding of DES pathophysiology [51]. Age and gender influences on tear film homeostasis also showed linear relationships with protein intensities, namely an increase over time for LCN2 and SERPINA3 and a decrease of crucially downregulated proteins in DES such as PIP, PRR4 and ZG16B. Gender differences in proteins were not very distinct in this study, which may be due to the limited number of samples in CTRL. However, LACRT and PRR4 were found to be higher abundant in males than females, whereas HSPA8 and SCUBE2 were decreased in the former group.

To translate protein intensities to functional analyses, the Ingenuity Pathways Analysis (IPA) software was used. Firstly, in an effort to better understand the molecular and biochemical alterations in DES subgroups, the known protein-protein

interactions between significantly expressed proteins were visualized for each subgroup compared to CTRL (**Figure 11**) and in between subgroups (**Figure 12**). The statistical analyses (see chapter **3.2.1.6**) identify the majority of proteins in DES to be extra- and intracellular ones. Plasma membrane proteins, therefore, play smaller roles in the disease. Moreover, DRYlip shows a substantial amount of increased extracellular proteins, with DRYaq, on the contrary, having more downregulated substances outside of the cell. DRYaqlip, as the combination of both etiologies, represents both aspects, with the total amount of increased proteins being higher than decreased ones. The number of cytoplasmatic substances involved however increases from DRYlip to DRYaqlip. Additionally, a small amount of cytoplasmatic proteins are downregulated in both DRYaq and DRYaqlip. Functional analysis of IPA networks indicates the proteins associated with DRYlip to be almost half split between enzymes and proteins marked as 'others'. Additionally, there are a few transporters and one peptidase included in this subgroup. DRYaq, on the other hand, shows just as many enzymes, but a substantial number of proteins classified as 'others', with most of them being downregulated. Furthermore, there are few transporter, peptidases and transmembrane receptors afflicted by the disease. DRYaqlip involves the highest number of differentially expressed proteins, including a vast number of enzymes, but an even greater amount of 'others', with approximately one-third of them being downregulated. Moreover, the combination subgroup is also associated with the most peptidases, transmembrane receptors, transporters and peptidases.

Furthermore, differentially abundant proteins underwent a stringent Benjamini-Hochberg multiple testing correction in order to identify significantly involved disease mechanisms and upstream regulators of DES. A full list of all p-values can be found in **Appendix 2**. Analysis of the biological and disease functions associated protein expressions to the top networks involved in DES (**Figure 13**). All subgroups showed significant associations to cell movement, apoptosis (see **Figure 13** for more details on the involved proteins), and necrosis. DRYlip e.g. showed particular connections to cell movement ($p = -\log 7.67$), allergy ($p = -\log 8.39$), and eosinophilic inflammation ($p = -\log 7.33$), whereas DRYaq was highly related to apoptosis ($p = -\log 5.52$) and quantitiy of reactive oxygen species ($p = -\log 4.93$). DRYaqlip combines both of the other subgroups' characteristics with e.g. significant changes in cell movement ($p = -\log 9.5$), apoptosis ($p = -\log 8.4$), eosinophilic inflammation ($p = -\log 7.16$), and quantity of reactive oxygen species ($p = -\log 5.74$, see detailed protein involvements in **Figure**

13). Furthermore, analysis of the canonical pathways involved in DES (**Figure 14**) revealed glycolysis to be increased in all subgroups (DRYlip p = -log2.2, DRYaq p = -log1.9, DRYaqlip p = -log3.1, see **Figure 14** for more details). Additionally, clathrin-mediated endocytosis signaling was found to be significantly involved in DRYlip and DRYaqlip (p = -log2.5 and p = -log3.1 respectively). DRYaq and DRYaqlip on the other hand shared associations with LXR/RXR activation (p = -log1.9 and p = -log3.5 respectively), FXR/RXR activation (p = -log1.9 and p = -log2.7 respectively), and acute phase signaling (p = -log2.1 and p = -log3.1, see **Figure 14** for more details). These changes were subsequently connected to upstream regulators (**Figure 15**). For example, lipopolysaccharides were found to be highly related to DRYlip and DRYaqlip (p = -log8.37 and p = -log7.74 respectively, more detailed information in **Figure 15**) as well as TNF (p = -log3.72 and p = -log5.08), while e.g. the sex steroids beta-estradiol was revealed to be connected to DRYaq (p = -log4.23, more details in **Figure 15**).

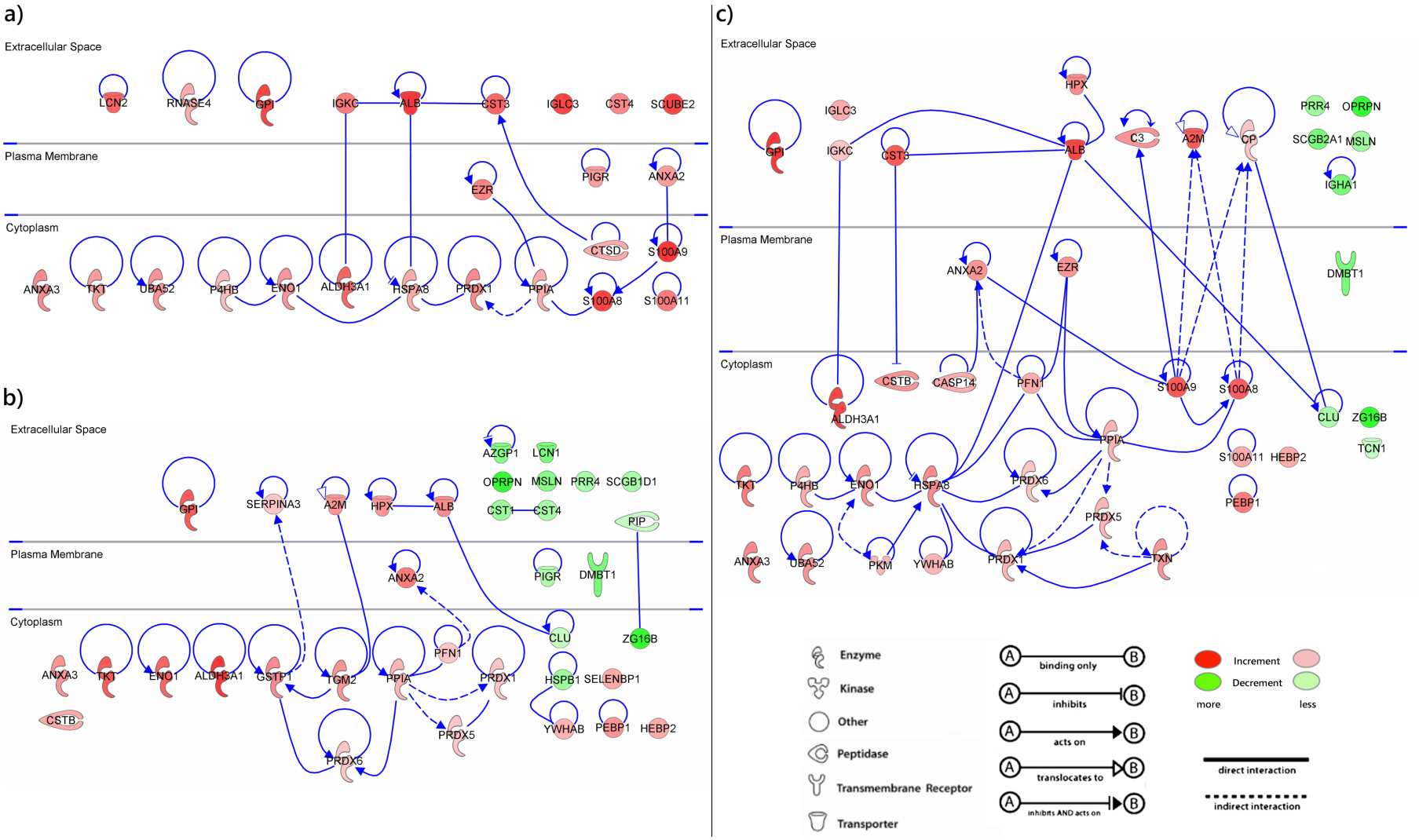

Figure 11: Networks of significantly expressed proteins analyzed with the Ingenuity Pathway Analysis software. a) DRYlip *vs*. CTRL, **b)** DRYaq *vs*. CTRL, **c)** DRYaqlip *vs*. CTRL.

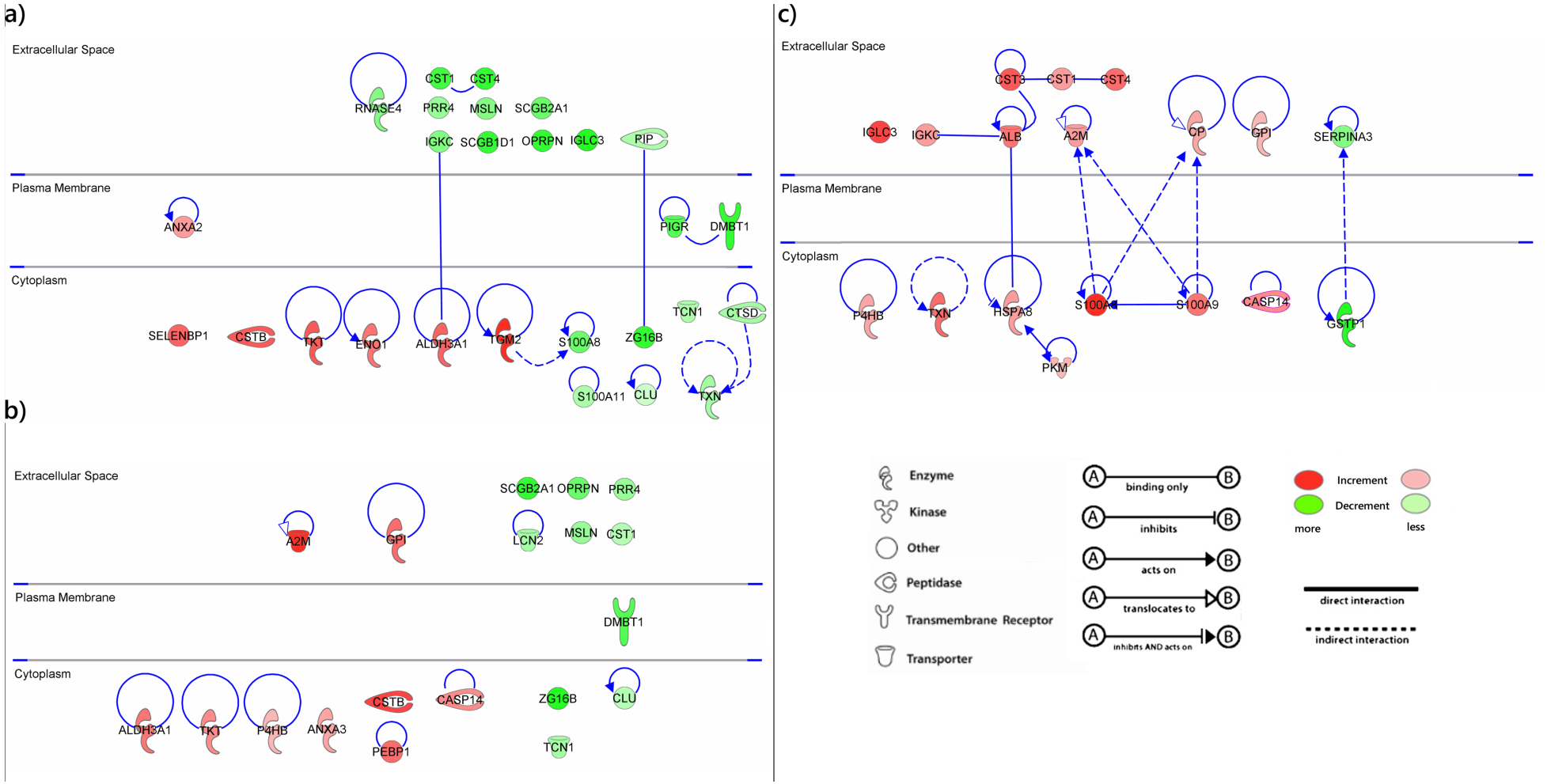

Figure 12: Protein-protein interactions between DES subgroups analyzed with the Ingenuity Pathway Analysis software. a) DRYaq *vs*. DRYlip, **b)** DRYaqlip *vs*. DRYlip, **c)** DRYaqlip *vs*. DRYaq.

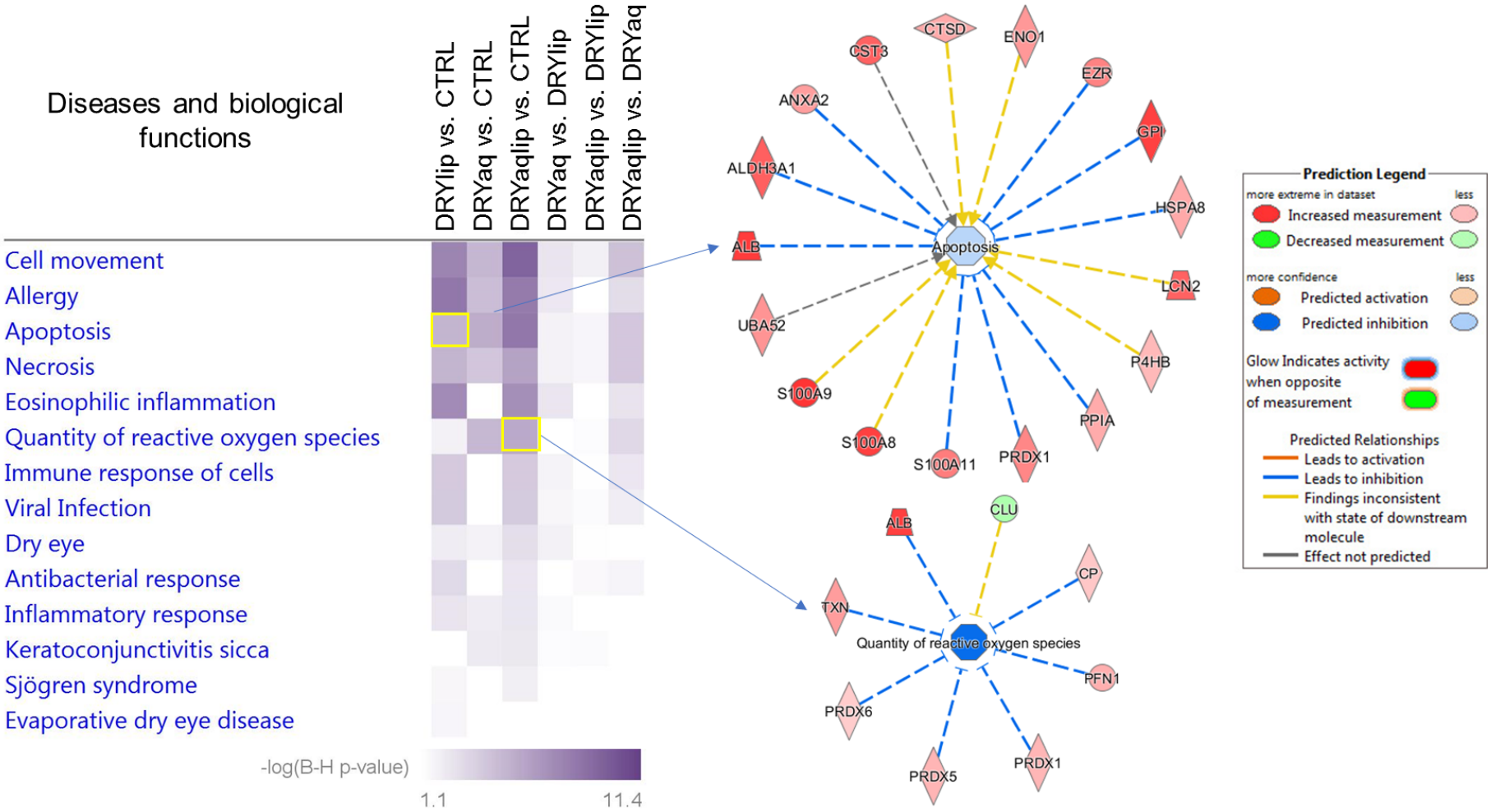

Figure 13: Comparison analysis of the significant diseases and biological functions between the differentially expressed proteins in DES subgroups obtained by IPA. Shown are all involved proteins and their effects on the specific pathways.

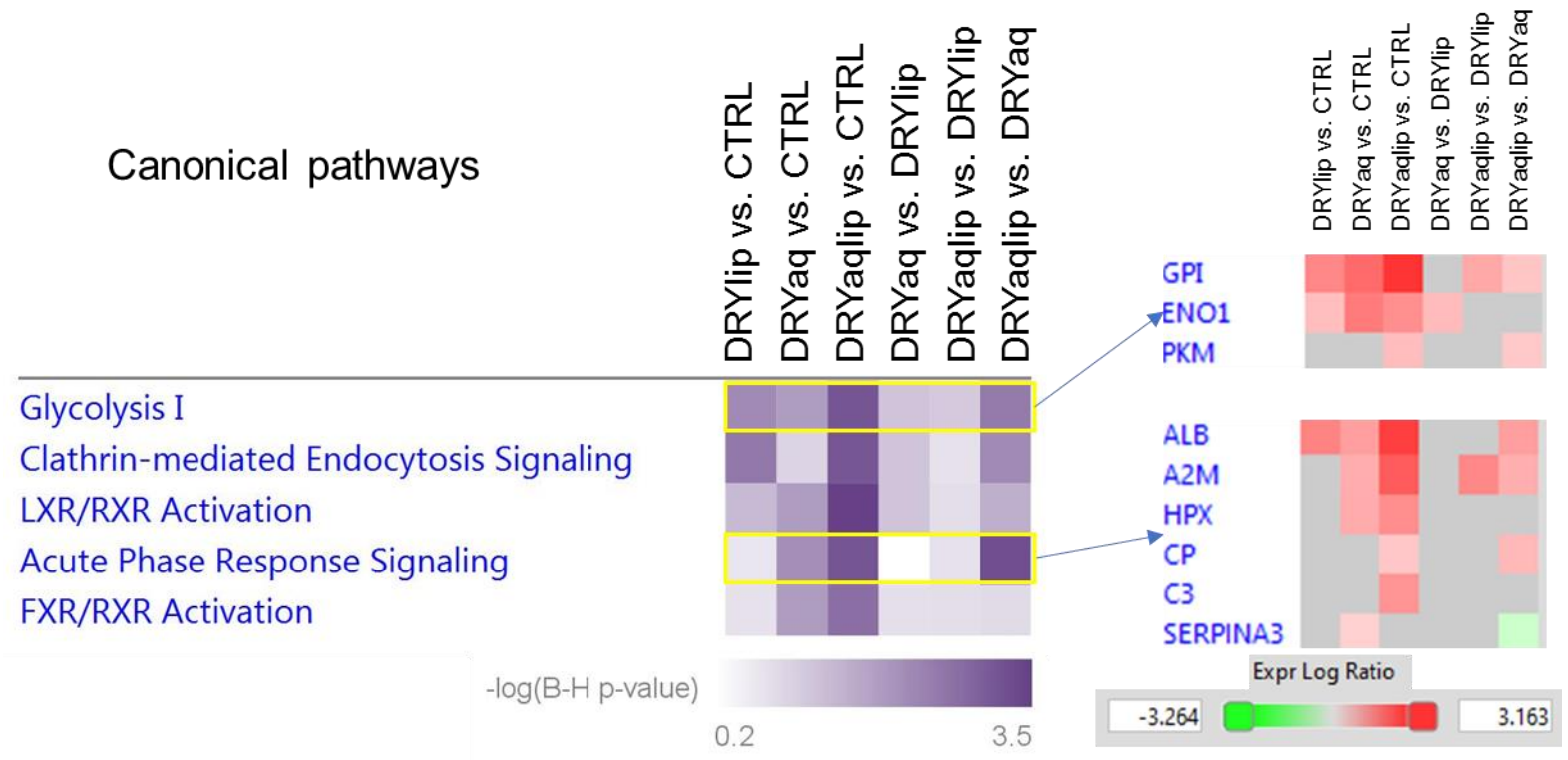

Figure 14: Comparison analysis of the significant canonical pathways between the differentially expressed proteins in DES subgroups obtained by IPA. Shown are all involved proteins and their effects on the specific pathways.

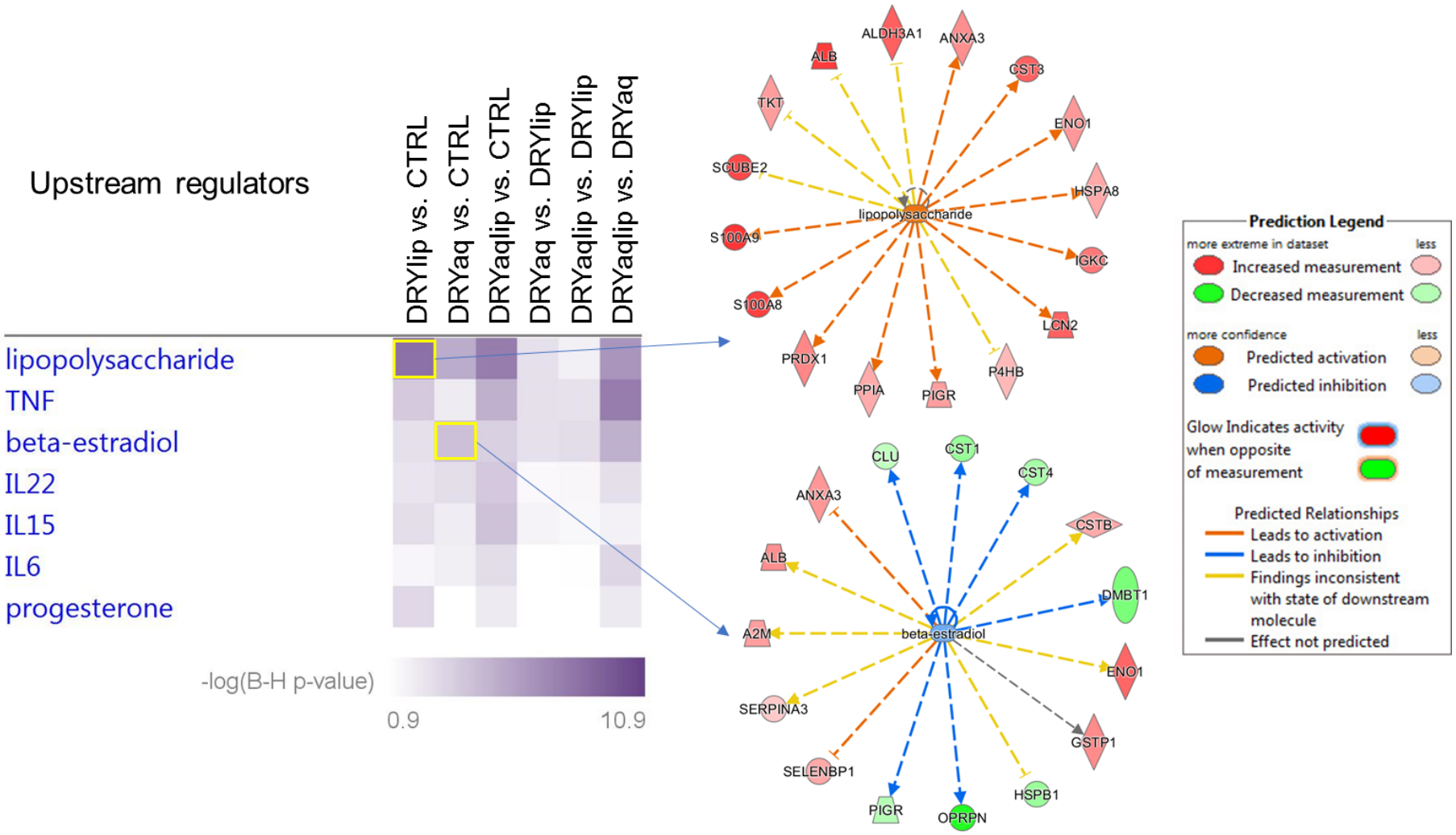

Figure 15: Comparison analysis of the significant upstream regulators between the differentially expressed proteins in DES subgroups obtained by IPA. Shown are all involved proteins and their effects on the specific pathways.

4.2 Establishing a MALDI-TOF-MS method for individual tear samples and characterization of PRR4

4.2.1 Method optimization

MALDI-TOF hard- and software settings were optimized first to ensure the best spectra quality for individual tear samples and improve the evaluation of sample preparation adjustments. For this purpose, an estimated amount of 1 µg of tear protein was used based on comparable previously conducted MS studies [203, 239].

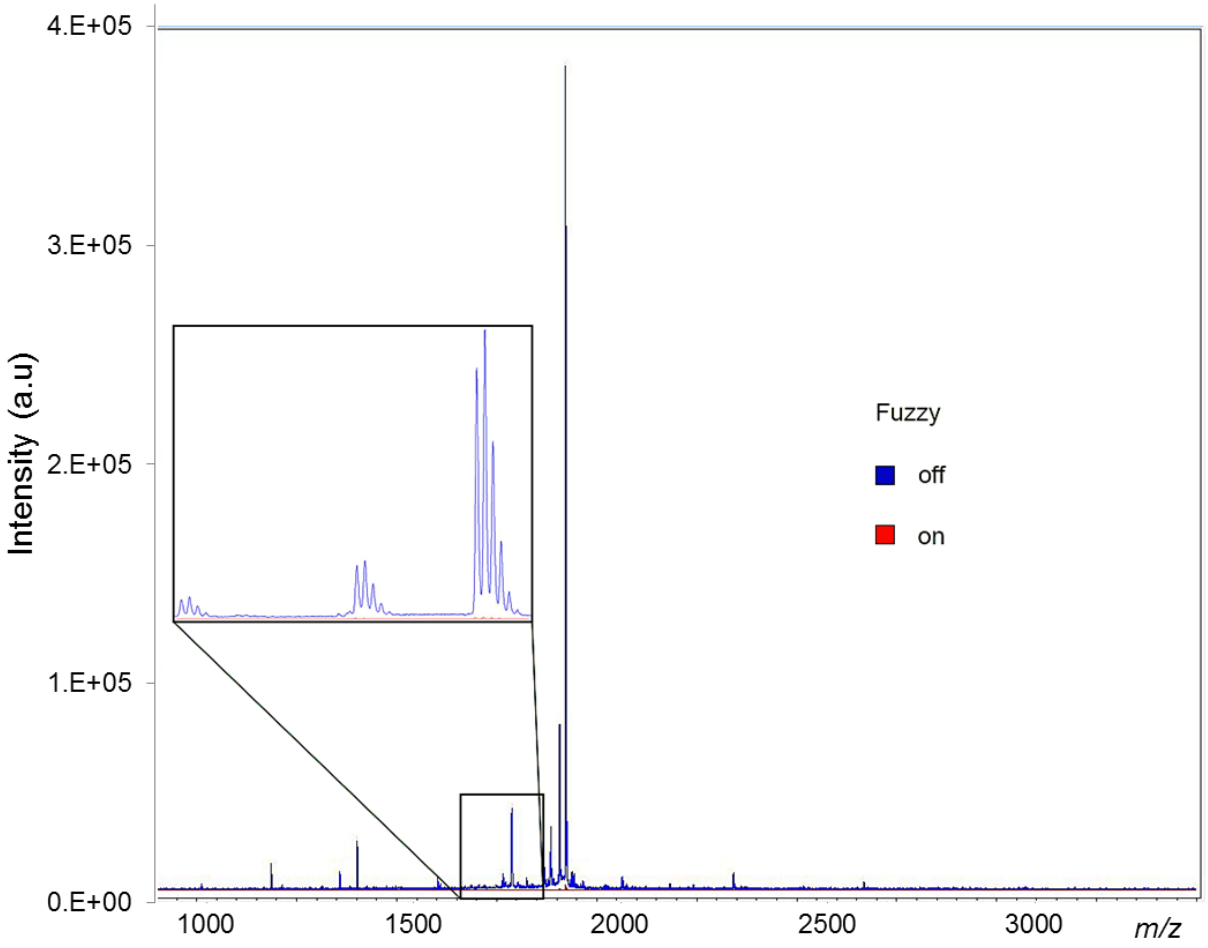

Figure 16: MS spectra with enabled and disabled laser fuzzy

Firstly, the laser fuzzy was turned on or off for measurements. When activated, the fuzzy logic control algorithm evaluates signal intensity and mass resolution of the MS peaks to then adjust laser properties for ion signal intensities to stay in an adequate range [240]. In case of individual tear samples, enabling the laser fuzzy option leads to no peptide peak identification, resulting in an empty spectrum, whereas disabling

this function generated a valid one (see **Figure 16**). However, the spectrum derived without the fuzzy algorithm showed significant noise levels, which decreased the number of identified peptides, especially low abundant ones. Based on these observations, the laser fuzzy was turned off, to be optimized in subsequent steps.

Next, the accumulation function was tested by turning it on and off for measurements. Enabling the accumulation of peak intensities will lead to decreased signal to noise ratios and an increased number of identified peptides. As can be observed in **Figure 17**, a turned-off accumulation function will lead to high levels of noise and therefore makes identification of low abundant peptides difficult. Enabling accumulation, on the other hand, leads to very high signal to noise ratios, resulting in easily distinguishable peptide peaks, also in case of low abundant ones. Therefore, accumulation was turned on in subsequent optimization steps.

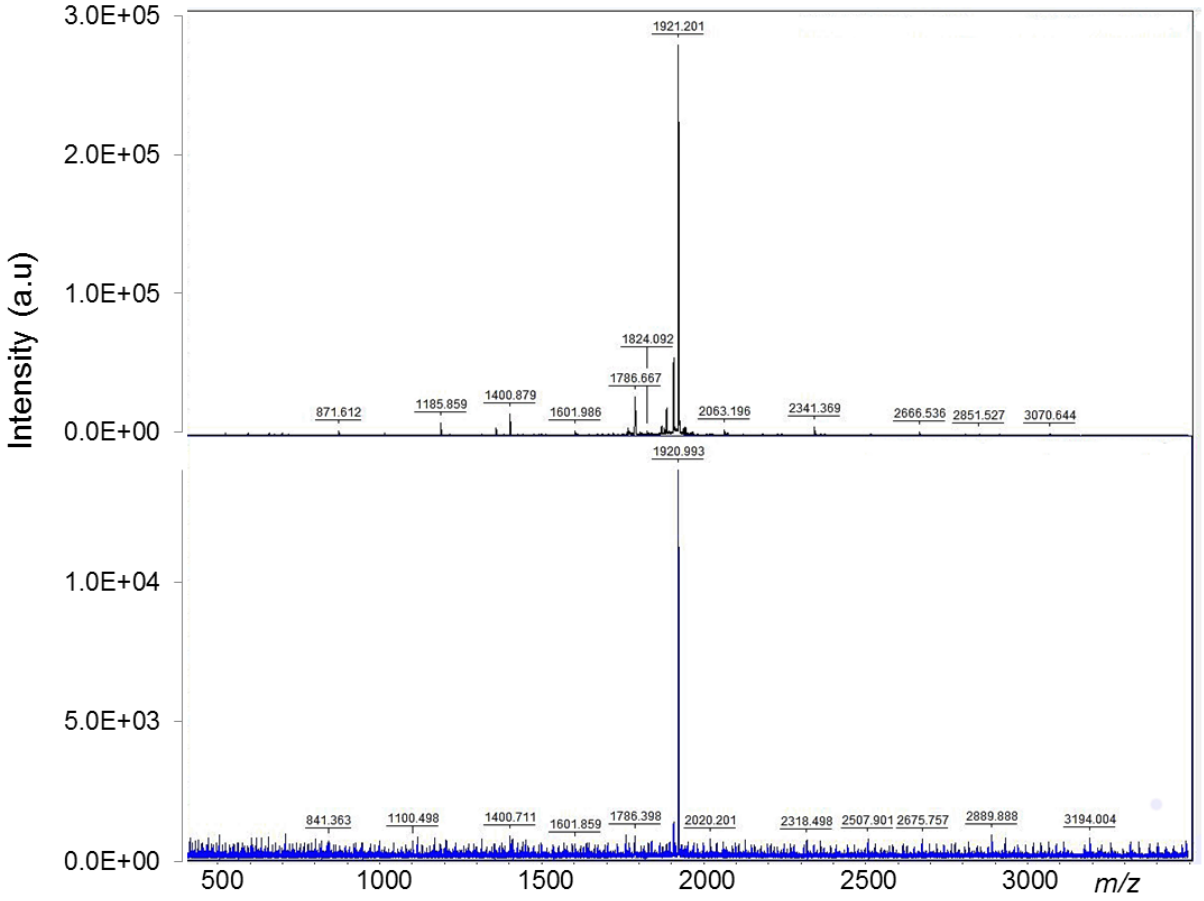

Figure 17: MS spectra with accumulation enabled (black) and disabled (blue)

A peak detection range of 400 – 3700 *m/z* was tested to identify all peptides contained in individual samples. This range was deducted from discovery stage tear

studies and included all peptides previously found in tears (see **Table 3**). Prior and following optimization steps showed no peptide identification below 500 or over 3500 *m/z*, which validated the chosen detection range. Consequently, it was maintained in all adaptation steps.

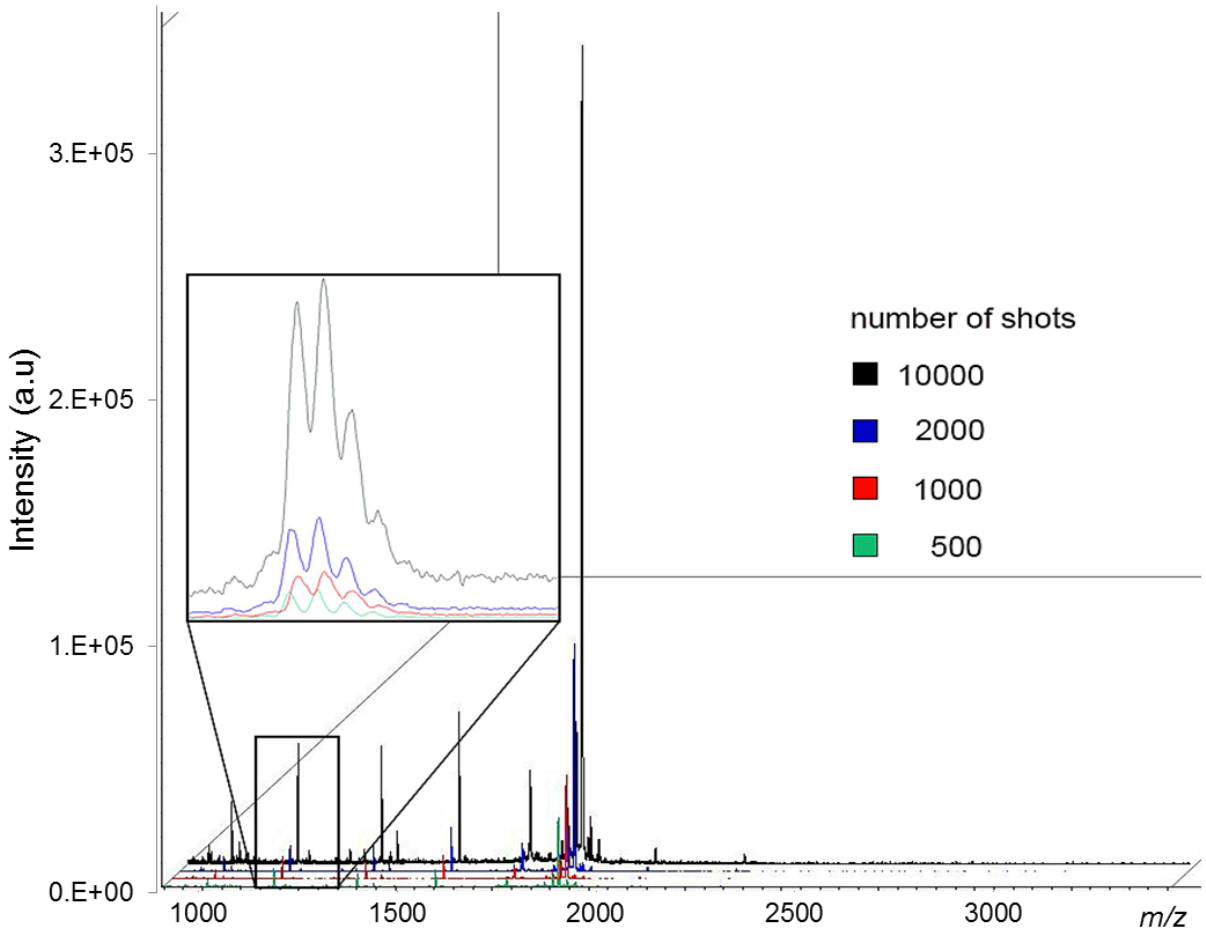

Figure 18: MS spectrum visualizing the different peak intensities acquired with an altering number of laser shots per spot

Furthermore, the number of laser shots per sample spot needed to obtain good peak intensity levels was evaluated. For this purpose, several technical replicates of the same sample were measured with an increasing number of laser shots ranging from 500 to 10000, as represented in **Figure 18**. With rising shot amounts, the intensities of MS peaks are increasing as well, especially of highly abundant peptides. But since MALDI-TOF spectra represent relative abundances, an increase of abundant peptides results in a suppression of rarer ones. Some of these low abundant peptides are not identifiable in spectra obtained with high shot numbers because of

this so-called suppression effect [241]. Therefore, to ensure adequate overall intensity levels on the one hand and as little loss of information due to suppression on the other, the number of identified peptides and their intensities was evaluated for each laser setting. 2500 shots per spot resulted in the best compromise between both aspects, which is why the measurement method was adjusted to this amount.

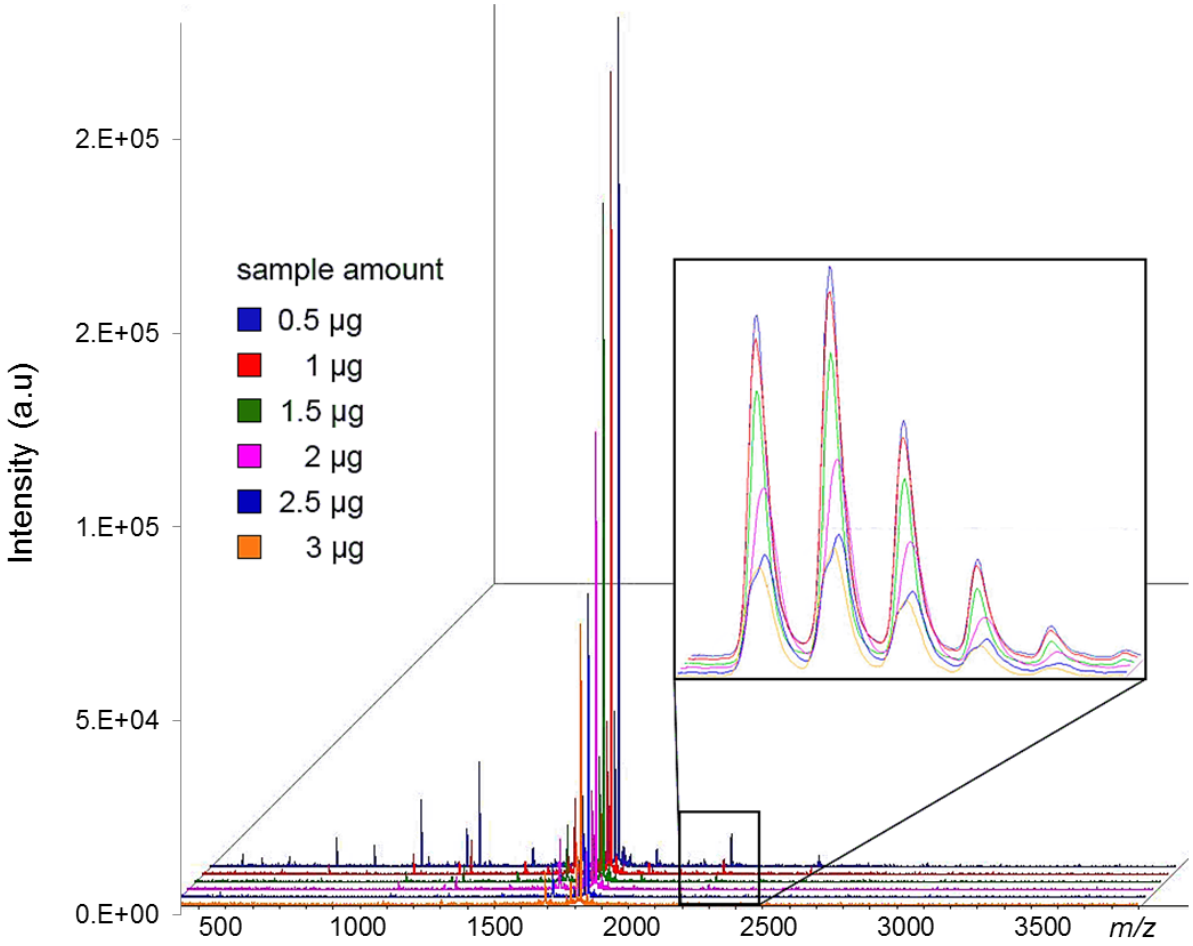

Figure 19: Comparison of different sample amounts measured with otherwise identical parameters

After hard- and software settings were adjusted successfully, optimization of sample and internal standard handling ensured. Firstly, the sample amount was evaluated by measuring and comparing tear protein amounts from 0.5 to 3 µg. As can be observed in **Figure 19**, the overall peak intensities decrease with increasing sample amounts. Assumably this is either because of better ionization conditions or enhanced detections levels in lower sample amounts since higher amounts could overburden the detector [242-244]. Also, low abundant peptides are identified better in smaller

sample amounts due to lessened suppression effects. Therefore, smaller protein amounts are more applicable for MS measurements of individual samples utilizing this method. When comparing peak intensities and variations between technical replicates, 0.5 µg of sample gave off the most constant results. Optimization was therefore continued with 0.5 µg of tear protein, to be reevaluated in measurements containing both sample and internal standard.

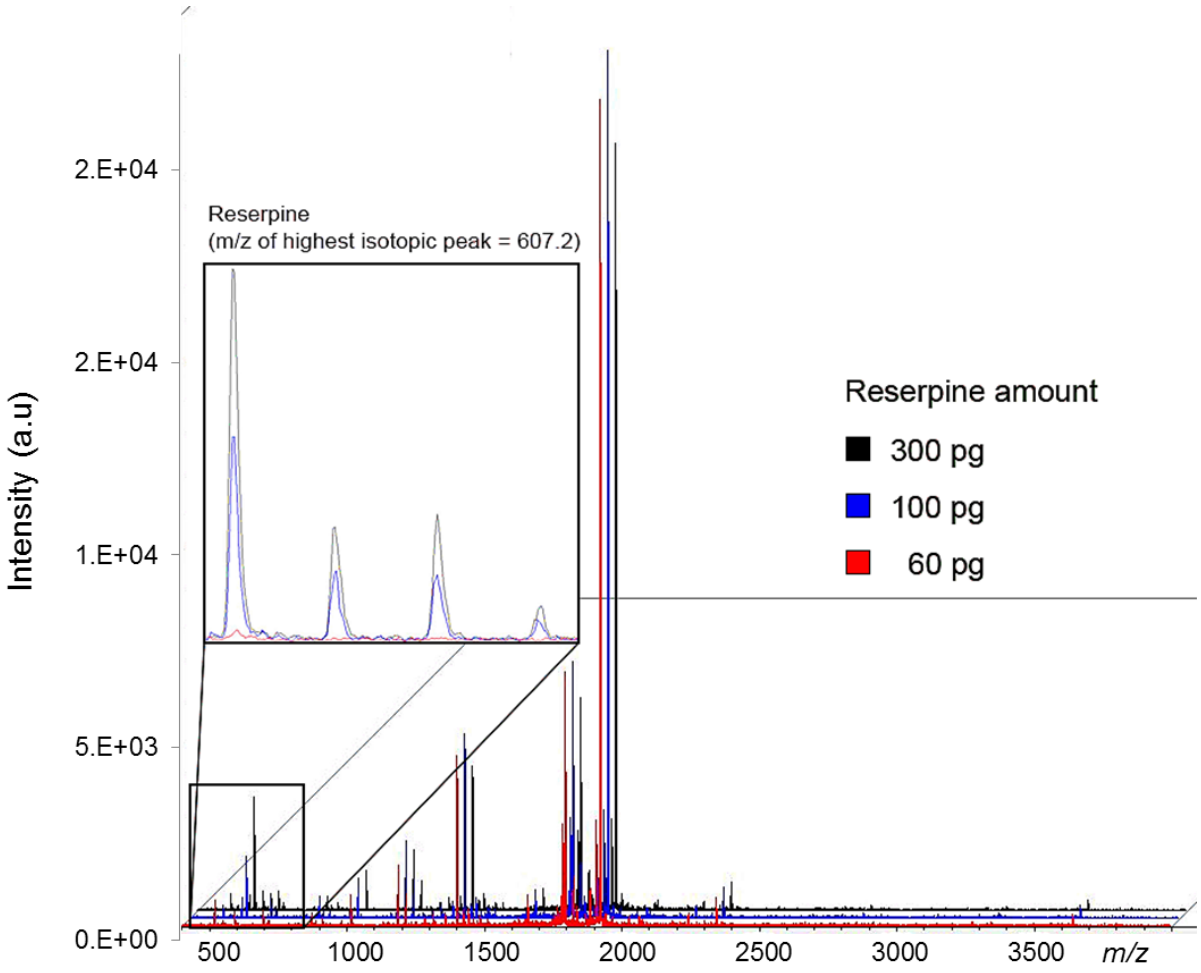

Figure 20: Comparison of 0.5 µg of sample with differing amounts of reserpine

Next, quantification and comparability problems of MALDI-TOF measurements were addressed. Since those measurements only deliver relative abundances, evaluating spectrum quality and comparing results prove to be difficult. Therefore, one needs to either add labeled isotopes to samples to gain absolute abundances or apply label-free strategies, as described in previous chapters. However, applying labeling techniques for all PRR4 isoforms would imply a massive financial burden and take up immense time periods. To reduce both aspects, this study, therefore, utilizes a label-free technique of introducing a set amount of internal standard to each sample. While

this will not allow for accurate absolute quantification, in combination with technical replicates, it will grant evaluation of measurement reproducibility and estimation of fold changes in a fast working method, which is the goal of this study [244, 245]. A molecule that has been repeatedly used in comparable studies because of its high stability in MALDI MS and the lack of mass peak overlay with known peptides in tears is reserpine [246-248]. Based on the amount of reserpine used in previously mentioned studies, 0.5 µg of tear proteins were measured with differing quantities of reserpine in order to obtain adequate peak identifications for both. As can be observed in **Figure 20**, sample peaks show comparable intensities, while representative reserpine amounts are depicted resulting in different intensities for the *m/z* of 607.2. Since reserpine should be able to be identified easily, including high reproducibility, but without adding to the suppression effect, the intermediate peak intensity was chosen for the measurement method after data evaluation, represented by 100 pg of reserpine. This amount, obtained by dilution steps, was subsequently reevaluated by using a standard reserpine solution and 0.5 µg of tear protein, which resulted in reproducible spectra.

Lastly, all previously established parameters were tested for interactions with the matrix during crystallization, since MALDI matrix solutions are known to influence the sample and therefore results as well [242, 243]. In this study, a matrix containing CHCA was used, due to its successful application in several proteomics studies [171, 229, 249]. To assess the best application and crystallization technique for individual tear samples and CHCA matrix, identical samples were spotted both as a mixture of sample, reserpine, and matrix, as well as individually with each component being allowed to dry at room temperature before adding the next. Up until this step, all optimizations were conducted with individual spotting, in concordance to previously published studies [11, 27, 171]. As depicted in **Figure 21**, spotting the three components individually results in higher overall peak intensities for all peptides. Through peak intensity analysis, the variation was found to be smaller in individually spotted samples too, which led to this parameter being retained in sample preparation.

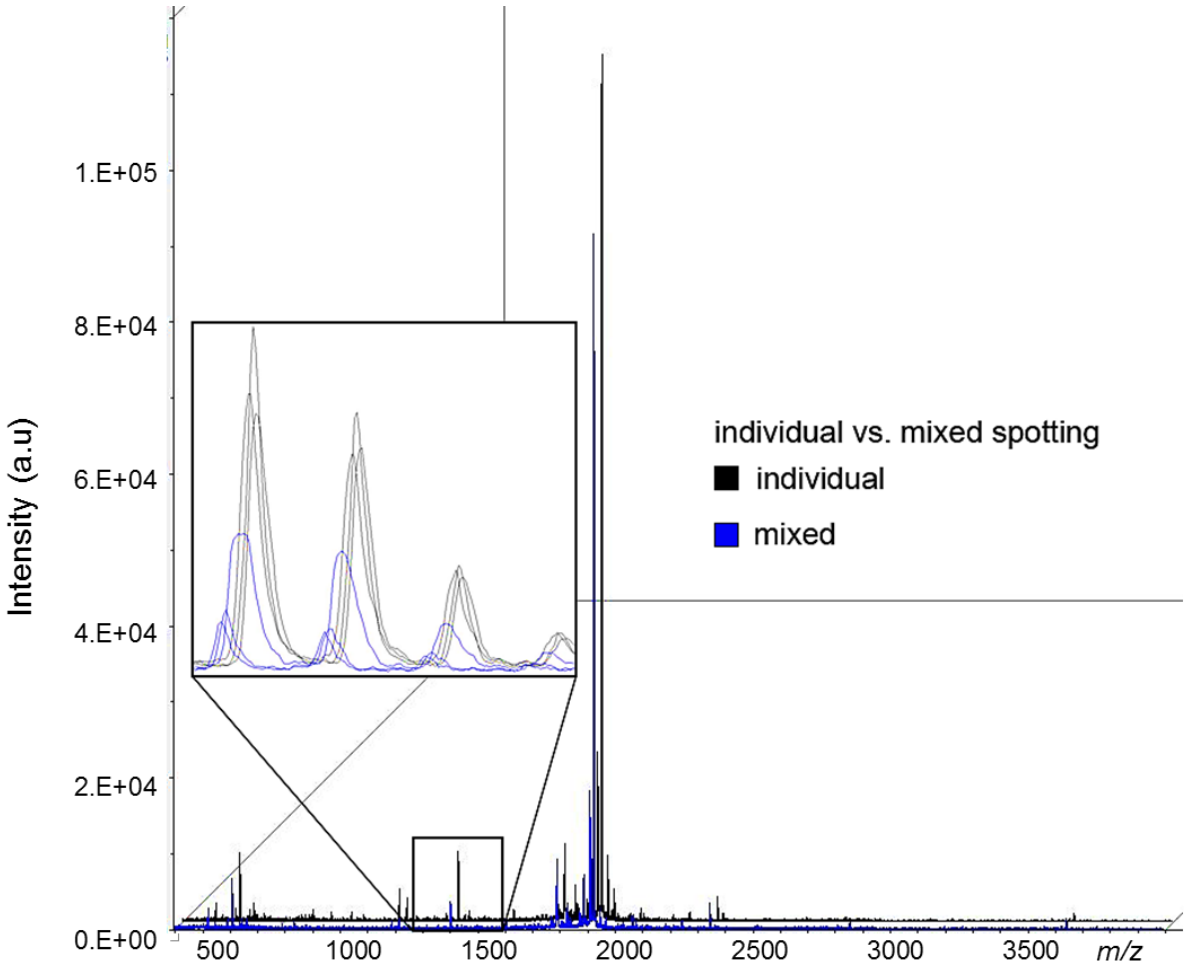

Figure 21: Comparison of peak intensities obtained by individual pipetting of spot components versus pipetting of a mixture of them. The magnification illustrates three technical replicates per parameter, which stresses the increased peak variance in mixed versus individual spotting.

4.2.2 Characterization of individual sample's PRR4 in MALDI-TOF-MS

Using the previously optimized method established in this study, individual tear samples of 42 healthy volunteers were successfully measured to evaluate their PRR4 expression with excellent peak separation and signal to noise ratios of peptides of interest. In order to work around the known limitations of MALDI-TOF measurements concerning measurement inconsistencies and quantification obstacles, multiple quality control and normalization steps were undertaken [244, 245]. The intensities of 3 technical replicates were averaged, intensities under 500 were excluded and PRR4 isoform peaks were normalized by the internal standard reserpine, resulting in 42 high quality spectra, which were used for further analyses.

A list of their normalized intensities for PRR4 isoforms can be found in **Table 8**. The ability to produce these MS spectra of complex individual tear samples marks a novel approach in this field and opens up new possibilities for proteomics research and clinical use.

As can be observed in **Figure 22**, all 4 isoforms of PRR4 were successfully identified in this study [27]. Isoform peaks were checked for any overlapping peptide fragments from other proteins, which there were found to be none. Hence one can conclude that the *m/z* 1601, 1729, 1792 and 1921 solely belong to the protein PRR4. These isoforms therefore represent some of the most distinct peaks of the entire tear proteome, with their combined intensity being the highest one by far in all measured samples.

Individuals were manually sorted into one of the 6 distribution groups previously established by Perumal *et al*. [27]. All of them could be identified in this study, as is represented in **Table 8**. Since previous publications concerning PRR4 isoforms do not address intrapersonal expressions between one individual's eyes, tear samples were extracted and analyzed from both eyes for a first group of healthy volunteers (group A) [20, 27, 182]. However, all individuals showed to express the same PRR4 isoforms in their left and right eye, which is why additional samples were only taken from the left one (group B). The distribution of PRR4 isoform groups of this study (see **Figure 23**) shows group 5 to be the most common one, followed by groups 6 and 1. At the same time, groups 2, 3, and 4 were only represented by a small number of individuals. These results are in concordance with previous results from MALDI-TOF tear sample studies employing additional separation steps by Perumal et al. [27]. The combined expression of *m/z* 1601 and 1921 was found to be even more frequent than group 5's in a study conducted by Perumal *et al.*, which may be due to methodical differences or the coincidental occurrence of isoform distribution in this particular study population [27]. Therefore, discovery stage results concerning the distribution of PRR4 isoforms are largely validated in complex tears samples with the novel method established in this study.

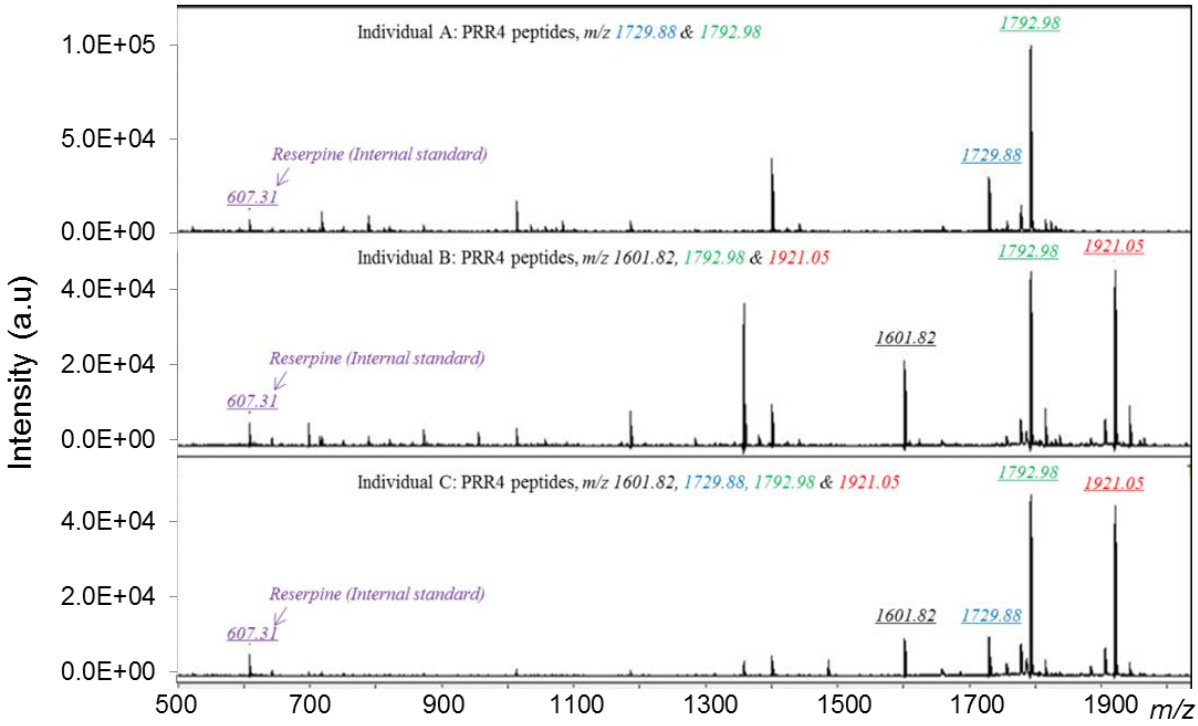

Figure 22: Representative spectra from three healthy individuals (A-C), visualizing the successful identification of all PRR4 isoforms and Reserpine in complex tear samples. Depicted are exemplary combinations of 2–4 isoforms.

Table 10: PRR4 isoform intensities obtained *via* MALDI-TOF and normalized by an internal standard.

	left eye (*m/z*)				right eye (*m/z*)				
Group A	**1601**	**1729**	**1792**	**1920**	**1601**	**1729**	**1792**	**1920**	**PRR4 group**
A01	1558	1086	73417	62390	2008	1655	27629	22431	P6
A02	23517		66243	57729	17593		58206	47625	P5
A03	33301		129172	110471	25381		82074	66672	P5
A04	41921		62907	52312	33483		52867	43280	P5
A05	12594		94610		2777		59522		P3
A06	8326		51714	41997	2354		18713	17196	P5
A07	33204		32339	25541	20675		23670	19266	P5
A08	11752		53763	39139	12656		24355	17939	P5
A09	2283			45776	2417			102188	P1
A10		48791	187095			10787	71640		P2
A11	10619		21660	15230	4334		37432	25426	P5
A12	5630		29381	20881	888		11690	7370	P5
A13	17771		71048	52449	20603		113442	87194	P5
A14	8895		50512	36907	3111		27204	20376	P5
A15	8391		1079	130054	7688		1383	195998	P5
A16	1142	818	45147	33260	2430	1532	35950	27692	P6
A17	50604		87545	68439	41499		51241	41598	P5
A18	71875		87387	65517	47448		46673	35994	P5
A19	18199			101617	4385			103435	P1
A20	5054		42269	32877	7172		57150	44759	P5
A21	15422		31817	23826	28916		70088	51189	P5
A22	21768		71810	48735	10656		59871	40453	P5
A23	11528	8597	178807		4424	4198	105815		P4
A24	688	754	28373	22984	11449	7917	102829	82150	P6
Group B									
B01	2415		19993	15952					P5
B02	23523		93489	87337					P5
B03	7126	5808	71372	78164					P6
B04	2396	2884	65187	45409					P6
B05		13245	86801						P2
B06	7811			35061					P1
B07	6011	6515	77389	56105					P6
B08	9491		35777	32116					P5
B09	8875			108656					P1
B10	13900		38720	37923					P5
B11	8092	11003	98128						P4
B12	957	729	12486	10132					P6
B13	986	769	19441	13282					P6
B14	23942		48698	46861					P5
B15	10727			94978					P1
B16	19150	9981	46854	40039					P6
B17	20520		41025	38393					P5
B18	12718	10918	55936	51691					P6

In group A, samples were extracted from both eyes and group B were only taken from the left eye in group B.

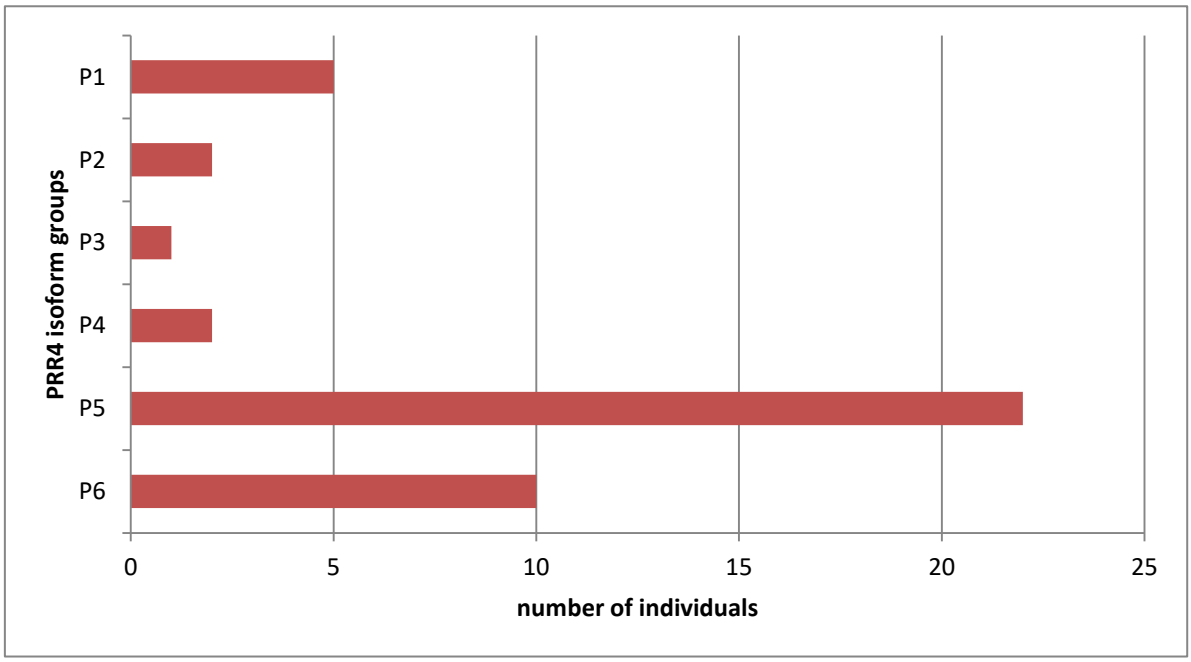

Figure 23: Distribution of PRR4 isoform groups in this study's individual tear samples. Grouping criteria are in concordance with Perumal et al. [27].

5. DISCUSSION

5.1. DES clinical biomarker discovery employing AIMS in a targeted proteomics strategy

Previous studies concerning the pathophysiology of the DES were largely focused on the discovery stage employing pooled tear samples to derive a consensus spectrum for the disease. But in pursuance of additional information about DES mechanisms, its influencing factors, and clinical biomarkers, studies need to explore the interpersonal changes of dry eye patients. Therefore, the previously acquired information has to be verified and expanded in actual complex individual samples to get closer to medical application and improve therapeutic strategies. This study hence aspired to evaluate individual DES samples through AIMS, which is a fast and precise way for quantification of proteins of interest [24]. The parent mass list was based on discovery stage studies that identified the proteins of interest by their unique peptides [20, 27, 182, 218, 229]. Through extensive optimization steps, the list was adapted to successfully measure all 100 peptides of interest with excellent inter-group correlations, which marks the highest number of identified proteins in any targeted-based measurement of tears [16, 17, 20, 27, 182, 207, 213]. Beyond that, this study also includes more samples than any similar predecessors, making the results all the more substantial. This method is therefore fit to identify and quantify an unprecedented amount of tear proteins in complex samples with exceptional reproducibility levels; a feat previously not accomplished by any other study for individual tear samples.

Applying stringent quality control steps and a Benjamini-Hochberg FDR of < 0.05, 59 out of these proteins were found to be significantly differentially expressed. In general, the 59 significantly differentially abundant proteins (DAP) in this study verify many discovery stage results. Firstly, since the parent mass list was based on MS studies of pooled tear samples, the sheer number of significant measurements in this thesis' large study population validates their findings. Secondly, the proteome of the DRYlip patients is closest to healthy volunteers, whereas the DRYaqlip proteome shows the least resemblance to CTRL, as has been hypothesized before [11, 20]. These observations are based on the number of significant changes from CTRL in each subgroup (25 *vs*. 43 for DRYlip and DRYaqlip, respectively), in addition to analyses that factor in all proteins of interest, such as the PCA. Therefore, our

current understanding of DES mechanism and the vicious circle of disease progression is compatible with these outcomes. Additionally, when comparing each protein's intensities to discovery stage results, most fold change trends are in concordance with previous studies. A comprehensive comparison of this study's results to discovery stage ones can be found in **Table 9**. Furthermore, to give an overview of the significant protein's involvement in other diseases, the table contains selected examples of other studies, including MS-based ones, but also consisting of different measurement techniques.

Besides being able to validate previous results, this study also established a substantial amount of new findings that involve proteins found to be not significant in discovery stage studies before or that are essential parts of DES disease mechanism, such as inflammation, but were nevertheless not included in preceding research efforts. In total, 21 out of the 59 DAP of this study include novel revelations for MS-based tear measurements, with most of them being low abundant ones in tears, yet again stressing this group's importance in DES [20]. For instance, considerable proteins such as glucose-6-phosphate isomerase (GPI) and transketolase (TKT) that are significantly upregulated in all DES subgroup or proteins remarkably involved in disease protein interactions such as heat shock protein 8 (HSPA8) were able to be identified as significant substances in human dry eyes in a targeted MS-based study for the first time. In conclusion, these observations once again emphasize the quality of the method used in this study, since it is highly effective in identifying proteins of interest, even in complex samples that mimic circumstances in clinical use. It is especially suitable for DES samples because it calls for lower tear volumes and protein amounts, which works well with the reduced production rate of both in the DES.

Table 11: Summary of this study's protein profiles in comparison to MS-based DES discovery studies and selected protein expressions in literature.

Gene name	Targeted stage (this study)			Discovery stage (based on [11, 12, 17, 20, 22, 229, 230])			GOCC	GOMF& GOBP	Expression profiles in literature	
	DRYlip *vs.* CTRL	DRYaq *vs.* CTRL	DRYaq-lip *vs.* CTRL	DRYlip *vs.* CTRL	DRYaq *vs.* CTRL	DRYaq-lip *vs.* CTRL			Profile	Measured in
A2M	n.s.	UP	UP	UP	UP	UP	ER	Protease inhibitor / Antimicrobial	UP	DM [250]
ALB	UP	UP	UP	UP [230]	UP	UP	ER	Carrier / Binding protein	UP	DRY_CL [13], KC [181], RF [182],
				DOWN [229]					DOWN	BLE [251], Cardiovascular events [252], INF, Malnutrition [253], MK [254]
ALDH3A1	UP	UP	UP	n.s.	UP	UP	C	Oxidoreductase	UP	DM [255], DRY_MDE [14], DRY_SS [18]
ANXA2	UP	UP	UP	DOWN	n.s.	UP	ER	Calcium-dependent phospholipid binding	UP	DRY_SS [18]
ANXA3	UP	UP	UP	n.s.	UP	n.s.	C	Phospholipase A2 inhibitor	UP	Gastric CA [256]
AZGP1	n.s.	DOWN	n.s.	DOWN	n.s.	n.s.	ER	Zinc-binding / Lipid degradation / Cell adhesion / Antigen presentation	UP	Lipolysis, Smokers [257]
									DOWN	DRY_MSD, DRY_MSDE [14], HCC [258], Prostate CA [259]
C3	n.s.	n.s.	UP	n.s.	n.s.	n.s.	ER	Immune & Inflammatory response	UP	DRY_MDE [14], DRY_SS [18], INF [260], Metabolic Syndrome [261]
									DOWN	PNH, RA, SLE, SS [260]
CASP14	n.s.	n.s.	UP	X	X	X	C / N	Endopeptidase / Apoptotic process	UP	chronic SJS [262]
									DOWN	DRY_SS [18]
CLU	n.s.	DOWN	DOWN	n.s.	DOWN	DOWN	C / CM / ER / M / N	Cytoprotective / Misfolded protein binding / Chaperone / Anti-apoptotic / Immunity	UP	DEM [263], DRY_SS [18], HepC [264], high ages, AS, GN, MI [265], OS [266],
									DOWN	RF [182], testicular seminoma [267]

Table 9: (continued)

Gene name	Targeted stage (this study)			Discovery stage (based on [11, 12, 17, 20, 22, 229, 230])			GOCC	GOMF& GOBP	Expression profiles in literature	
	DRYlip *vs.* CTRL	DRYaq *vs.* CTRL	DRYaq-lip *vs.* CTRL	DRYlip *vs.* CTRL	DRYaq *vs.* CTRL	DRYaq-lip *vs.* CTRL			Profile	Measured in
CP	n.s.	n.s.	UP	n.s.	n.s.	UP	ER	Iron ion homeostasis / Post-tanslational protein modification / Acute-phase response	UP	DEM [268], OCD [269], oral contraceptives [270], RA [271], SCH [272],
									DOWN	Wilson's disease [273]
CST1	n.s.	DOWN	n.s.	DOWN	DOWN	n.s.	ER	Endopeptidase inhibitor	UP	Breast CA [274], DRYaq (microarray) [104]
									DOWN	MK [254]
CST3	UP	n.s.	UP	n.s.	n.s.	n.s.	ER	Endopeptidase inhibitor / Neutrophil degranulation / Regulation of tissue remodeling	UP	Ischemic stroke [275]
									DOWN	DEM [276]
CST4	UP	DOWN	n.s.	DOWN	DOWN	DOWN	ER	Cystein protease inhibitor / Antimicrobial	UP	Gastric & Colorectal CA[277]
									DOWN	BLE [251], DRY_MDE, DRY_MSDE [14], DRY_SS [18]
CSTB	n.s.	UP	UP	DOWN	UP	UP	C / N	Cysteine-type endopeptidase inhibitor activity	DOWN	DRY_SS [18]
CTSD	UP	n.s.	n.s.	X	X	X	C / ER	Endopeptidase / Antigen presentation / Neutrophil degranulation	UP	Neuronal INF (NFkB) [278]
DMBT1	n.s.	DOWN	DOWN	n.s.	DOWN	DOWN	C / ER	Protein transport / Scavenger receptor, binds surfactant protein D	UP	DRY_CL [13], Hepatholithiasis [279], IBD [280]
ENO1	UP	UP	UP	UP	UP	UP	C / CM / N	Lyase / Glycolysis / Plasminogen activation / Transcription regulation	UP	Autoimmune diseases [281], Breast CA [282], DRY_SS [283]
EZR	UP	n.s.	UP	n.s.	n.s.	n.s.	C / CM / ER / N	Cell shaping / Cell adhesion	UP	Asthma [284], (chemical) Corneal irritation [285]
GPI	UP	UP	UP	n.s.	n.s.	n.s.	ER	Glycolysis / Gluconeogenesis / Cytokine / Growth factor	UP	RA [286]

Table 9: (continued)

Gene name	Targeted stage (this study)			Discovery stage (based on [11, 12, 17, 20, 22, 229, 230])			GOCC	GOMF& GOBP	Expression profiles in literature	
	DRYlip *vs.* CTRL	DRYaq *vs.* CTRL	DRYaq-lip *vs.* CTRL	DRYlip *vs.* CTRL	DRYaq *vs.* CTRL	DRYaq-lip *vs.* CTRL			Profile	Measured in
GSTP1	n.s.	UP	n.s.	UP	UP	UP	C / M / N	Transferase	UP	CC [287], Liver cell damage [288]
HEBP2	n.s.	UP	UP	X	X	X	C / ER / M	Heme binding / Neutrophil degranulation	UP	Necrosis [289]
HPX	n.s.	UP	UP	n.s.	n.s.	n.s.	ER	Heme binding / Host-virus interaction	UP	INF [290]
HSPA8	UP	n.s.	UP	X	X	X	C / CM / ER / M / N	Acetylation / Methylation / Ubl conjugation	DOWN	SCH [291]
HSPB1	n.s.	DOWN	n.s.	n.s.	n.s.	n.s.	C / N	Thermotolerance / Chaperone / Stress response / Apoptosis inhibition	DOWN	Neurodegenerative diseases [292]
IGHA1	n.s	n.s	DOWN	n.s.	n.s.	n.s.	ER	Antibacterial / Immune response	UP	IOIP [293]
									DOWN	CC [294], DRY_MSDE [14], DRY_SS [18]
IGKC	UP	n.s.	UP	n.s.	n.s.	n.s.	CM / ER	Adaptive immunity / Endopeptidase	DOWN	OCD [295], RF [182]
IGLC3	UP	n.s.	UP	X	X	X	CM / ER	Antigen binding / Complement activation	UP	Mantel cell lymphoma [296]
									DOWN	RF[182]
LCN1	n.s.	DOWN	n.s.	n.s.	DOWN	n.s.	ER	Proteolysis / Long-chain fatty acid transport	UP	CF [297], Cholangio-CA [298], COPD [299], RF [182]
LCN2	UP	n.s.	n.s.	n.s.	DOWN	n.s.	ER	Iron ion binding / Apoptosis / Immune response	UP	acute kidney injury [300], CKD [301], COPD [299], neuron death [302], βTH [303]
MSLN	n.s.	DOWN	DOWN	n.s.	n.s.	n.s.	C / CM / ER	Cell adhesion	UP	MM, pancreatic, ovarian and lung Adeno-CA [304], RF [182]
P4HB	UP	n.s.	UP	n.s.	n.s.	n.s.	C / CM / ER	Chaperone / Protein folding	UP	Renal cell CA [305]

Table 9: (continued)

Gene name	Targeted stage (this study)			Discovery stage (based on [11, 12, 17, 20, 22, 229, 230])			GOCC	GOMF& GOBP	Expression profiles in literature	
	DRYlip *vs.* CTRL	DRYaq *vs.* CTRL	DRYaq-lip *vs.* CTRL	DRYlip *vs.* CTRL	DRYaq *vs.* CTRL	DRYaq-lip *vs.* CTRL			Profile	Measured in
PEBP1	n.s.	UP	UP	n.s.	UP	UP	C	Serine protease inhibitor	UP	DEM, Diabetic nephropathy [306]
									DOWN	DEM, Hypoxia [307]
PFN1	n.s.	UP	UP	n.s.	UP	UP	C / CM / ER	Actin binding / Prolin-rich region binding	UP	Endothelial proliferation [308]
PIGR	UP	DOWN	n.s.	n.s.	UP [229]	UP	CM / ER	Antibacterial / Immunoglobulin transcytosis in epithelial cells	UP	IgA associated immuncomplexes [309]
					DOWN [14]				DOWN	chronic SJS [262], DRY_MDE, DRY_MSDE [14], DRY_SS [18], RF [182]
PIP	n.s.	DOWN	n.s.	DOWN	n.s.	n.s.	ER	Actin binding / AQP5 binding / IgG binding / Immune system regulation	UP	Breast CA [310], MK [254]
									DOWN	KC [311], SS [312]
PKM	n.s.	n.s.	UP	n.s.	n.s.	UP	C / N	Kinase / Transferase / Glycolysis / MHC class II protein complex binding	UP	Most human CAs [313]
PPIA	UP	UP	UP	n.s.	UP	UP	C / ER	Accelerates the folding of protein / Rotamase / Host-virus interaction / Peptide binding	UP	INF, Viral infection, Apoptosis, AS, Arthritis [314, 315]
PRDX1	UP	UP	UP	n.s.	UP	UP	C	Antioxidant / Oxidoreductase / Peroxidase	UP	ARDS [316], DRY_MSDE [14], INF [317]
PRDX5	n.s.	UP	UP	UP	n.s.	n.s.	C / M	Antioxidant / Inflammatory response	UP	MS [318], Sarcoidosis [319]
									DOWN	OS [320], severe Strokes [321]
PRDX6	n.s.	UP	UP	UP	n.s.	n.s.	C	Cadherin binding / Cell redox homeostasis	UP	DEM, Parkinson's disease [322], lung tumor [323]
									DOWN	Cataract [324]
PROL1	n.s.	DOWN	DOWN	n.s.	DOWN	DOWN	ER	Protease inhibitor	DOWN	DRY_MSDE [14], Smokers, TO [19]

Table 9: (continued)

Gene name	Targeted stage (this study)			Discovery stage (based on [11, 12, 17, 20, 22, 229, 230])			GOCC	GOMF& GOBP	Expression profiles in literature	
	DRYlip *vs.* CTRL	DRYaq *vs.* CTRL	DRYaq-lip *vs.* CTRL	DRYlip *vs.* CTRL	DRYaq *vs.* CTRL	DRYaq-lip *vs.* CTRL			Profile	Measured in
PRR4_N2	n.s.	DOWN	DOWN	n.s.	DOWN	DOWN	ER	Unknown	UP	RF [182]
PRR4_SUM	n.s.	DOWN	DOWN	n.s.	DOWN	DOWN			DOWN	DRY_CL [13], DRY_MDE, DRY_MSDE [14], DRY_RA [28], DRY_SJS [325], DRY_SS [18], TO [19]
RNASE4	UP	n.s.	n.s.	X	X	X	ER	Endonuclease / Hydrolase / Nuclease	UP	Angiogenesis, Neurogenesis [326], INF [327]
S100A11	UP	n.s.	UP	n.s.	UP [17] DOWN [229]	UP	C / ER / N	Antimicrobial / Apoptosis / Chemotaxis / Innate immunity / Cell-cell adhesion	UP	INF [328], high ANXA1 [329]
S100A8	UP	n.s.	UP	UP	UP	UP	C / CM / ER	Antimicrobial / Apoptosis / Autophagy / Chemotaxis / Immunity / Inflammatory response / Innate immunity	UP	DRY_SS [18], INF Atherogenesis, CF [330]
S100A9	UP	n.s.	UP	UP	UP	UP	C / CM / ER	Antimicrobial / Apoptosis / Autophagy / Chemotaxis	UP	DRY_SS [18], Myeloid Leukemia [331]
SCGB1D1	n.s.	DOWN	n.s.	UP [229] DOWN [230]	UP [11] DOWN [229]	UP [11] DOWN [229]	ER	Protein heterodimerization activity / Androgen receptor signaling pathway	UP DOWN	DRY_MDE, DRY_MSDE [14] DRY_CL [13]
SCGB2A1	n.s.	n.s.	DOWN	UP	UP [11]	UP [11]	ER	Protein heterodimerization activity / Androgen receptor signaling pathway	DOWN	DRY_MDE, DRY_MSDE [14], RF [182]
SCUBE2	UP	n.s.	n.s.	X	X	X	ER	Organism development / Calcium and lipid binding	UP DOWN	AS [332], Dyslipidemia in Type 2 Diabetes [333] Colorectal CA [334]

Table 9: (continued)

Gene name	Targeted stage (this study)			Discovery stage (based on [11, 12, 17, 20, 22, 229, 230])			GOCC	GOMF& GOBP	Expression profiles in literature	
	DRYlip *vs.* CTRL	DRYaq *vs.* CTRL	DRYaq-lip *vs.* CTRL	DRYlip *vs.* CTRL	DRYaq *vs.* CTRL	DRYaq-lip *vs.* CTRL			Profile	Measured in
SELENBP1	n.s	UP	n.s	UP	n.s	n.s	C / M / N	Selenium binging / Protein transport	UP	major adverse cardiac events [335], SCH, psychosis [336]
									DOWN	COPD [337], Lung CA [338]
SERPINA3	n.s	UP	n.s.	n.s.	n.s.	DOWN	ER	DNA binding / Acute-phase response	UP	DEM [339], Endometrial CA [340], Melanoma [341], prion diseases [342]
TCN1	n.s	n.s	DOWN	DOWN	DOWN	n.s	ER	Cobalamin binding / Neutrophil degranulation	UP	Poor memory performance [343]
									DOWN	cobalamin deficiency [344], DRY_MDE [14]
TGM2	n.s.	UP	n.s.	n.s.	n.s.	UP	C / CM / ER / M	Acyltransferase / Transferase / Protein-glutamine gamma-glutamyltransferase activity	UP	INF [345], SCH (*via* IL-2 increase) [346]
									DOWN	Breast CA [347]
TKT	UP	UP	UP	X	X	X	C / ER / N	Transferase / Metal ion binding	UP	Corneal layers dysfunction [348]
TXN	n.s.	n.s.	UP	n.s.	n.s.	n.s.	C / ER / N	Oxidoreductase / Transcription regulation / Transport	UP	Cardiac hypertrophy [349]
									DOWN	INF [350]
UBA52	UP	n.s.	UP	X	X	X	C / ER / M / N	Protein ubiquitination / Ribosomal protein	UP	INF [351]

Table 9: (continued)

Gene name	Targeted stage (this study)			Discovery stage (based on [11, 12, 17, 20, 22, 229, 230])			GOCC	GOMF& GOBP	Expression profiles in literature	
	DRYlip *vs.* CTRL	DRYaq *vs.* CTRL	DRYaq-lip *vs.* CTRL	DRYlip *vs.* CTRL	DRYaq *vs.* CTRL	DRYaq-lip *vs.* CTRL			Profile	Measured in
YWHAB		UP	UP	n.s.	n.s.	n.s.	C	Host-virus interaction / MAPK cascade	UP	idiopathic pulmonary arterial hypertension [352], Renal cell CA [353]
									DOWN	DEM [354]
ZG16B	n.s.	DOWN	DOWN	DOWN	DOWN	DOWN	ER	Angiogenesis / Endothelial cell migration	UP	RF [182]
									DOWN	Apoptosis, Colorectal CA [355], chronic GvHD, salivary gland damages [356], DRY_MSDE [14], MS [206]

The proteins' occurrences in the cell (GOCC, **C** = cytoplasm, **CM** = cell membrane, **ER** = extracellular region, **M** = Mitochondria, **N**= nucleus), as well as their functions and involvements in biological processes (GOMF & GOBP), are stated. They were manually extracted from the Uniprot database (http://www.uniprot.org). Panels marked with an X have not been part of human sample MS-based discovery stage studies yet. **UP** = upregulated, **DOWN** = downregulated, **n.s.** = not significant. **ALS** = Amyotrophic Lateral Sclerosis, **ARDS** = Acute Respiratory Distress Syndrome, **AS** = atherosclerosis, **BLE** = blepharitis, **CA** = cancer, **CC** = conjunctivochalasis, **CF** = cystic fibrosis, **CKD** = chronic kidney disease, **COPD** = Chronic Obstructive Pulmonary disease, **DEM** = dementia, **DM** = Diabetes mellitus, **DRY_CL** = DES associated with contact lens wear, **DRY_MDE** = mildly symptomatic DES with aqueous deficiency, **DRY_MSDE** = symptomatic aqueous deficiency DES, **DRY_RA** = DES associated with rheumatoid arthritis, **DRY_SJS** = DES associated with Stevens-Johnson Syndrome, **DRY_SS** = DES associated with Sjögren's Syndrome, **GN**= glomerulonephritis, **GvHD** = Graft-versus-Host disease, **HCC** = hepatocellular carcinoma, **HepC** = Hepatitis C, **IBD** = inflammatory bowel disease, **INF** = inflammation, **IOIP** = idiopathic orbital inflammatory pseudotumors, **KC** = Keratoconus, **MC** = mycotic keratitis, **MI**= myocardial infarction, **MM** = malignant mesothelioma, **MS** = multiple sclerosis, **OCD** = Obsessive Compulsive Disorder, **OS** = oxidative stress, **PNH** = Paroxysmal Nocturnal Hemoglobinuria, **RF** = reflex tears, **SCH** = Schizophrenia, **SJS** = Stevens-Johnson Syndrome, **SS** = Sjögren's Syndrome, **TO** = thyroid-associated orbitopathy, **βTH** = β-Thalassemia

Stringent statistical analysis of intensity fold changes, protein networks, and involved disease pathways lead to the affirmation, that the main pathophysiological aspect of DES is in fact inflammation, as is the current hypothesis in research [5, 50, 51]. Since the maintenance and side effects of inflammatory reactions require a great deal of energy and involve many kinds of cells, it is not surprising, that proteins linked to cell movement and metabolic activities are also increased in DES. The result of acute or chronic inflammation is cell damage and therefore necrosis and apoptosis, which are the last major categories, shared in disease study groups. Nevertheless, there are distinct features of each DES subgroup in these pathways that reveal their altering etiologies and effects and therefore expand our knowledge about the disease itself. IPA analysis of diseases and biological functions (see **Figure 13**) found no distinctly significant results for all search terms related to DES (dry eye, evaporative dry eye, keratoconjunctivitis sicca, and Sjögren syndrome). After further investigation, this was found to be based on a lack of information about these subjects in proteomics pathway databases. Yet again this emphasized the importance of this study's results for the unraveling of disease pathophysiology, which is largely unknown at the moment.

5.1.1 Lipid layer dysfunctional DES (DRYlip)

One of the fundamental differences between DRYlip and DRYaq lies in their altering inflammatory mechanisms. DRYlip samples show high associations with bacterial and viral infections, as well as allergies and eosinophilic reactions. Therefore, infectious and allergic entry points to the vicious circle of DES progression are suggested, which is fortified by the significant upstream involvement of lipopolysaccharides, glycolipids found in some gram-negative bacteria, that can induce severe immune responses (**Figure 13** and **15**) [357]. The common endpoint of these aspects, the cellular immune response, was consequently also increased in DRYlip *vs*. CTRL, suggesting, in summary, activation of both the innate and acquired immune system.

On the protein level, this change can, for example, be identified by the upregulation of immunoglobulin kappa constant (IGKC) and immunoglobulin lambda constant 3 (IGLC3) as representatives of antibodies, in addition to polymeric immunoglobulin receptor (PIGR), which aids exocytosis of IgA in mucosal tissues, increasing acquired immune system reactions [309, 358]. The innate immune response is e.g. illustrated

in the increase of lipocalin-2 (LCN2), a protein that not only promotes chemotaxis of leukocytes but also deprives bacteria of iron and therefore inhibits their growth [359]. Other examples include cystatin C and S (CST3 & CST4), inhibitors of lysosomal and cysteine proteases. Through this function, they can prevent the decomposition of extracellular proteins, in turn increasing the aforementioned substances, as well as induce degranulation of neutrophil granulocytes and therefore immune responses [360, 361]. Other highly significantly expressed inflammatory proteins of DRYlip are cytoplasmatic S100A8 and S100A9, which form a complex and act on leukocyte recruitment, neutrophil and macrophage aggregation and cytokine expression [362].

With the upholding of inflammatory reactions also comes the need for an increase in energy provision, cell movement, and transportation. Where the inflammatory aspect of DRYlip mostly involves extracellular proteins identified by IPA as transporters or ‘others’, the ones affected by metabolic and cellular movement pathways are for the most part located in the cytoplasm and perform as enzymes, with the exceptions of albumin (ALB), an extracellular protein heavily involved in substance transportation and metabolic processes, and glucose-6-phosphate isomerase (GPI), which is part of glycolysis, gluconeogenesis and the pentose phosphate pathway in the cell, as well as being a lymphokine inducing immunoglobin secretion in the extracellular region [363-365]. The need for energy in this disease becomes even clearer with the significant results for glycolysis as a canonical pathway in all DES subgroups, as well as an upregulation of enolase 1 (ENO1) and transketolase (TKT) on the protein level, two enzymes of glycolysis and the pentose phosphate pathway. They are also highly abundant in the cornea as so-called crystallins. These structural proteins maintain tissue transparency and the eye’s refractive index [366]. Therefore, these crystallins’ significant increase in all DES subgroups could also presumably be a sign of corneal cell damage. Another protein of the crystalline family is aldehyde dehydrogenase 3 family, member A1 (ALDH3A1), which makes up as much as 40% of the water-soluble protein in the cornea [367]. Its primary function is the maintenance of redox balance since the eye is under constant oxidative stress evoked by ultraviolet radiation [368]. Moreover, it detoxifies acetaldehydes and is part of the metabolism of several crucial substances, such as corticosteroids and neurotransmitters [367]. Other proteins involved in the redox balance of the eye are protein disulfide-isomerase (P4HB) and peroxiredoxin 1 (PRDX1), which are both significantly increased in DRYlip samples and therefore emphasize the amount of oxidative stress induced by this disease. PRDX1 is also known to be elevated in inflammation

through its involvement in T-cell regulation and cytokine induction [317]. Lastly, the aspect of protein metabolism and signaling are also of interest in DRYlip, represented by the notable increase of related pathways in IPA analysis, including clathrin-mediated endocytosis. This becomes apparent on the protein level in the upregulation of peptidylprolyl isomerase A (PPIA) and heat shock 70 kDa protein 8 (HSPA8), chaperones, which are part of cell signaling, cell growth, protein metabolism, protein transport and transcription regulation [315, 369]. Also connected to similar pathways is annexin A3 (ANXA3) through its influences on protein binding and moreover to immune responses by phagocytosis and neutrophil degranulation. Together with the closely related annexin A2 (ANXA2), that aids exocytosis of proteins, ANXA3 is significantly upregulated in all DES subgroups. In summary, lipid deficient DES is based on innate and acquired immune responses, presumably associated to bacterial and viral infections, as well as allergic reactions. That is why most proteins involved in this DES subgroup are connected to either an immune response or its maintenance and cell metabolism. This study's findings therefore introduce important new etiologies of this subgroup, as our current understanding of it is largely based on lipid layer disruptions e.g. through meibomian gland dysfunctions.

5.1.2 Aqueous-deficient DES (DRYaq)

The pathophysiology of aqueous deficient DES certainly shows sign of inflammation and its side effects and mechanism but consists of distinctly different pathways. Overall, based on protein fold changes and IPA pathway analyses, inflammatory reactions are not as pronounced in DRYaq as they are in DRYlip, showing in nonsignificant results for eosinophilic inflammation, viral infection, antibacterial response and immune response of cells. Nevertheless, there are signs of cell stress and damage in DRYaq samples, as can be observed in the involvement of allergic reactions, cell movement, glycolysis, necrosis and apoptosis. Especially noteworthy is the increment of the acute phase response signaling pathway, which tries to limit cell damage invoked by infection, injury, malignancy or immune system malfunctions by an innate immune response of several proteins, as well as farsenoid X receptor and liver X receptor activations as a heterodimer with the retinoid X receptor (FXR/RXR and LXR/RXR), both of which regulate lipid and glucose homeostasis, as

well as immune responses [370-372]. None of these pathways are related to lipid deficient DES.

The difference in inflammatory mechanisms between the two DES entities is observable on the protein level as well. More precisely, none of the extracellular or cytoplasmatic proteins chiefly involved in the immune response of DRYlip patients are significantly expressed in DRYaq. Primary inflammatory proteins of DRYaq are mostly related to the acute phase family and its effect on coagulation, iron-binding and immune regulation. For example, SERPINA3, a protease inhibitor that decreases proteolysis and therefore modulates the immune response in the acute phase, is increased in DRYaq [339]. Furthermore, regulative proteins of coagulation are highly expressed, since they are believed to limit infections by detaining possible pathogens in blood clots [373]. One protein highly associated with said mechanism is alpha 2-macroglobulin (A2M), acute-phase protein and inhibitor of coagulation and fibrinolysis, which also functions as a carrier for many interleukins and ions, therefore affecting the immune response [374, 375]. An additional influence on coagulation is the upregulated phosphatidylethanolamine binding protein 1 (PEBP1), a serine protease inhibitor that not only decreases tissue-type plasminogen and thrombin but is part of several other pathways influencing inflammation, such as the MAP kinase and NF kappa B cascades [376]. The concept of ion binding, especially in case of iron or heme, is based on the fact, that substance deprivation will decrease pathogen growth and therefore limit infectious outbreaks, as well as protect the organism from oxidative stress. DRYaq samples show an increase of several proteins fitting into this category such as hemopexin (HPX), heme-binding protein 2 (HEBP2), and selenium-binding protein 1 (SELENBP1), emphasizing an apparent increase of pathogens, oxidative stress or cell damage and debris. These aspects are moreover supported by the significant increase in the wound healing and apoptosis regulating protein tissue transglutaminase (TGM2), that is also part of cellular motility and the protection of the extracellular matrix [377, 378].

Even though there are apparent differences in DRYaq's inflammatory mechanisms when comparing them to DRYlip, the supporting pathways like metabolic processes and cellular movement are fairly close to each other. For example, DRYaq samples also show increased activities of ALB, ALDH3A1, PPIA, ANXA2, ANXA3 in addition to energy supplying proteins such as GPI, ENO1 and TKT, all of which show an even increased fold change from CTRL samples than DRYlip ones.

A mechanism that has been mentioned several times already, also in the discussion of DRYlip characteristics, is the protection from oxidative stress and reactive oxygen species (ROS). These byproducts of internal or external reaction with oxygen, such as peroxides, superoxide or hydroxyl radicals, harbor both beneficial and damaging potentials, depending on location and ROS concentration. In lower amounts, they are advantageous for several mechanisms, like cellular proliferation or host defense, through regulation of intricate redox systems, but an excessive amount of ROS, e.g. obtained *via* stress, medications or inflammation, are harmful to the organism. Not only do they damage DNA, RNA, lipids, and proteins directly, but they also induce apoptosis through various redox reactions [379, 380]. Therefore, systems disrupted in their redox hemostasis by inflammation, aim to reduce ROS with antioxidative enzymes. While DRYlip mechanisms include some of those, such as P4HB, PRDX1 and ALDH3A1, with the two latter ones also being part of DRYaq, antioxidative reactions are not central parts of its disease pathophysiology. DRYaq, on the other hand, shows a significant increment of ROS reducing enzymes, as can be seen in IPA analyses (**Figures 13**). This category of proteins in aqueous deficient DES consists of glutathione S-transferase P (GSTP1), peroxiredoxin 5 and 6 (PRDX5, PRDX6) and the already mentioned HPX and HEBP2. These aspects indicate that the eye tries to counteract oxidative stress more in DRYaq, leading to the conclusion, that its abundance is greater in this subgroup. It is therefore not surprising, that apoptosis, as a result of oxidative stress and cell damage, is also one of the highly significant pathways of DRYaq (**Figure 13**).

Next to the increased significance of oxidative stress to the disease mechanism of DRYaq, there is another distinct difference to DRYlip that becomes apparent in this study's results. Namely, that is the drastic downregulation of many extra- and intracellular proteins, including the major tear proteins LCN1, PIP, proline-rich protein 1 (PROL1 or OPRPN) and PRR4, that has been demonstrated by several discovery stage studies for DRYaq and DRYaqlip, and is hereby validated in individual samples [11, 20, 27, 229]. It has been hypothesized before that the decrement of those proteins leads to tear film instability and therefore results in inflammation, cell death and apoptosis – the pathways found to be significant in this study [20, 51]. Why this group of proteins is downregulated however remains largely unknown. It is widely hypothesized, that it is due to a lacrimal gland dysfunction because of various reasons (primary damage e.g. in Sjögren Syndrome, or secondary, for example as part of systemic diseases or neuronal malfunctions) [20, 27, 51, 381]. If, however,

this is the case or it comes down to other mechanisms, such as superordinate regulative proteins or individual organism influences (age, gender, hormonal state etc.) needs to be uncovered in future studies and could potentially solve the uncertainties surrounding DES subgroups.

One of the proteins that have a great impact on tear film stability is the highly abundant LCN1. As the principle binding and transport protein of tear lipids, it not only scavenges harmful lipids (e.g. phthalates) and products of inflammation but also prevents evaporation of the aqueous layer [382, 383]. It therefore also greatly reduces surface tension of the tear film and determines tear viscosity and stability. A decrement in LCN1 hence leads to an unstable aqueous layer. Another highly abundant substance in tears, prolactin-inducible protein (PIP), is responsible for the transport of aquaporin 5 to the apical membrane of glands and therefore regulates water secretion. A decrement of this protein, therefore, reduces the aqueous tear layer, as is the case in Sjögren syndrome patients that produce minimal amounts of tears [312]. Additionally, it binds to immunoglobulin G and CD4-T cell receptors, implicating a role in immune reactions [384]. Deleted in malignant brain tumors 1 (DMBT1) is also partaking in inflammatory mechanisms with its ability to bind bacteria and activate the complement system, next to its primary role as a tumor-suppressor protein [385]. Other downregulated substances include Zinc-alpha-2-glycoprotein (AZGP1), a protein involved in lipolysis and transmembrane transport, cystatin-SN (CST1), that, much like CST3 and CST4, inhibits proteolysis, and chaperone proteins of the heat shock family, clusterin (CLU) and heat shock protein beta-1 (HSPB1). Both chaperones also negatively influence apoptosis [265, 386]. Besides those substances that are mostly involved in metabolic, cell movement and inflammatory pathways, the functions of several downregulated proteins are currently unknown, which leads to a lack of information about protein-protein interactions and underlying disease mechanisms. For example, the mesothelial cell antigen mesothelin (MSLN), believed to be part of cell adhesion, and secretoglobin family 1D member 1 (SCGB1D1), associated with the uteroglobulin superfamily, have few scientifically proven functions, especially in tears [304]. Unfortunately, this also applies to three of the majorly significantly DAP in DRYaq - PROL1, PRR4 and zymogen granule protein 16 homolog B (ZG16B). Noteworthy is that several of the proteins found to be downregulated in DRYaq, especially with more or less unknown functions, are increased in reflex tears, such as LCN1, MSLN, PRR4 and ZG16B, which indicates their importance in the acute protective mechanism of the eye [182]. However in case

of chronic diseases based on inflammation, like DES, multiple sclerosis or rheumatoid arthritis, PRR4 and ZG16B were found to be decreased in tears, yet again by mechanism currently unknown [28, 206, 211, 356]. Whether the chronification leads to a lacrimal gland dysfunction, induces regulative mechanism, activates alterations in neurological and hormonal stimulations or follows altogether different pathways is therefore of high interest to the treatment of those diseases.

Judging by ZG16p, a protein closely related to ZG16B that has a presumed role in the sorting and exocytosis of granule content in pancreatic acinar cells and intestinal goblet cells, previous studies have suggested a similar function for ZG16B in tears [20, 229, 387]. This hypothesis would be in concordance to the increment of this protein in reflex tears, suggesting a role in neuronal stimulated exocytosis, but is yet to be verified. Besides its descriptive involvement in several diseases, including chronic Graft-versus-Host-disease and several cancer forms, as well as its decrement in apoptotic tissues, there is currently not much information about this protein's functions [355, 356]. This is also the case with PROL1, a peptidase inhibitor with largely unknown functions in tears. Opiorphin, a product of the PROL1 gene, was found to be secreted by the lacrimal gland and harbor pain-reducing qualities through its ability to reduce enkephalin breakup. Dufour *et al.* suggest the resulting increase of enkephalin to influence tear film homeostasis in some cases of epiphora, in addition to presumed paracrine and autocrine functions of this substance [381].

Lastly, there is PRR4 with its previously discussed challenging identification in MS-based studies. Based on its behavior in DES, reflex tears and other diseases, it is currently believed to be involved in tear film stability, ocular surface defense, and lubrication, with none of them being decisively proven [27, 175, 182, 388]. Due to the statistical methods of this study, which eliminate inconsistently measured proteins due to quality control steps and the fact that each individual expresses a distinct combination of 2 to 4 PRR4 isoforms, not all isoforms were found to be significantly expressed in this study [27]. In order to still compare total PRR4 amounts, the sum of all isoforms was added for statistical analyses and was found to be significantly expressed. Both the sum of all isoforms and isoform 2 by itself were decreased in DRYaq and DRYaqlip, as has been the case in multiple discovery stage studies concerning DES of different etiologies, e.g. contact lens wear, Sjögren syndrome, rheumatoid arthritis and primary dry eye syndrome [13, 14, 18, 20, 27, 28, 325]. Therefore, this study successfully established a method to measure and quantify

PRR4 in individual DES samples with a targeted MS method. Even though this measuring technique does not represent the full potential and intricacy of this protein and its isoform, it is still a vast improvement on current methods, which oftentimes only use precursor masses of isoforms not found to be significant in this study and therefore risk false negatives [11-13, 15, 19, 28, 160, 162, 167, 170, 171, 199-201, 249, 287, 325]. As a result, the method established in this study with its ability to work around the limitations of PRR4 identification and quantification in targeted MS approaches, could greatly improve future research concearning PRR4's functions and role in DES.

In summary, DRYaq does involve inflammatory reactions, but not to the same extent as DRYlip. It mostly involves acute phase proteins, as well as metabolic and cellular movement pathways. Distinct aspects of this subgroup also include the amount of antioxidative enzymes and a substantial number of downregulated proteins, several of which have unknown functions. The decrement of these proteins is mostly attributed to a dysfunction of the lacrimal gland, but the reasons behind it are currently not fully understood. Unraveling this phenomenon could lead to breakthroughs in DES research and treatment.

5.1.3 Lipid and aqueous deficient dry eye syndrome (DRYaqlip)

Finally, the combination of lipid and aqueous DES, DRYaqlip, proves to be a mixture of both DES pathophysiologies in pathway analyses and on the protein level. For example, it shows significance in all diseases, biological mechanisms, and upstream substances previously discussed, especially acute phase response, FXR and LXR/RXR activations, cell movement and apoptosis. Inflammatory reactions include DRYlip characteristics like antibody increment (IGKC, IGLC3), S100-proteins (S100A8, S100A9, S100A11) and CST3, as well as acute phase and DRYaq aspects such as A2M, PEBP1, HEBP2 and HPX. Additionally, it exclusively presents increased abundances for additional acute phase proteins, complement 3 (C3) and ceruloplasmin (CP), which are part of pathogen opsonization and iron-binding. Therefore, the innate immune response of the acute phase is even more increased in DRYaqlip than in DRYaq, implicating the gravest disruption of cell and immune hemostasis in all DES subgroups. Underlying metabolic and cellular movement pathways of DRYlip and DRYaq are also present in DRYaqlip. More precisely this entails the upregulation of ALB, ALDH3A1, ANXA2 & 3, ENO1, GPI, PPIA and TKT.

These proteins, and therefore an upregulation metabolic pathways and cell movement, overlap in all DES subgroup and hence represent the most common mechanism and potential biomarkers. DRYaqlip additionally demonstrates an increase in the glycolytic enzyme pyruvate kinase (PKM), which is probably due to the aggravated need for energy in its disturbed tear film hemostasis. Redox systems and responses to ROS are also highly present in DRYaqlip with increased proteins from both other subgroups, such as P4HB, PRDX1, PRDX5, and PRDX6. Exclusively upregulated in this category also is thioredoxin (TXN), which has proven to be one of the most essential antioxidative enzymes in mammals [350]. Resulting cell damage and apoptosis find their way into DRYaqlip pathways too, with the increase of UBA52 and caspase 14 (CASP14), enzymes of apoptotic reactions, with the latter only being significantly upregulated in DRYaqlip. Seeing that DRYaqlip most significantly involves apoptosis reducing mechanisms out of all subgroups leads to the assumption, that the apoptotic rate in this subgroup and hence also cell damage levels are the highest in all DES, which would be in agreement with the current concept of DRYaqlip pathophysiology; namely, that a complete loss of compensation leeway and combination of lipid and aqueous deficiency would result in the most cell damage and apoptosis. Additionally, the data we gain about apoptotic reactions reinforce previous observations – DRYlip is closest to CTRL and shows the lowest amount of cellular damage, followed by DRYaq and finally DRYaqlip.

The aqueous deficient side of this subgroup furthermore becomes apparent by the downregulation of several proteins including PROL1, PPR4, and ZG16B as well as exclusively diminished ones like transcobalamin-1(TCN1), a transporter for vitamin B12, the IgA related immunoglobulin heavy constant alpha 1 (IGHA1), and mammaglobin B (SCGB2A1). In summary, DRYaqlip shows characteristics of both DES etiologies, in pathway analysis and protein fold changes. It furthermore involves additional proteins revolving around metabolic needs, oxidative stress, acute phase reactions, and apoptosis implying an even intensified disruption of tear film homeostasis compared to the other subgroups. The current hypothesis, considering DRYaqlip as the combination of DRYlip and DRYaq, and seeing it as a possible endpoint of both subgroups, are therefore in concordance with this study's results.

A list of potential biomarker candidates obtained *via* a thorough analysis of protein fold changes, hierarchical clusters, correlations and IPA pathway analyses can be found in **Table 10**. Proteins were divided by their potential to identify all DES

subgroups, individual subgroups or shared aspects of DRYaqlip with DRYlip and DRYaq. Therefore, these proteins also indicate the top molecular and biological functions of each of those categories. Of special importance are HSPA8, which shows the highest amount of protein-protein interactions (PPI) in DRYlip and DRYaqlip, GSTP1 as a regulative protein for DRYaq with 3 PPIs and PPIA, that is highly involved in all DES subgroup regulations, especially for DRYaqlip. Proteins of interest for the differentiation of DRYlip and DRYaq are CST4 and PIGR, which are the only overlapping proteins between those subgroups with significantly altering fold changes, in the sense that they are increased in DRYlip and decreased in DRYaq. Nevertheless, discovery stage results are bivalent for both of these proteins with CST4 showing decreased intensities for DRYlip in a study by Soria *et al.*, whereas PIGR was found to be both increased and decreased in DRYaq before [14, 17, 20]. Further validation in larger populations could, therefore, be useful for re-evaluations. In general, all aforementioned proteins are potential biomarkers and of vital interest to future targeted tear film studies, as well as immunoassay validations. Conclusively, this study brought forth the largest list of verified biomarkers in individual tear samples yet, which represents an immense step towards improved DES diagnosis and treatment strategies.

Table 12: Potential biomarkers for all DES and each subgroup, based on their fold changes and hierarchical clustering of all significant proteins.

Group	HIGH	LOW	Top molecular and biological functions
All DES subgroups	ALB, ALDH3A1, ANXA2, ANXA3, ENO1, GPI, PPIA, PRDX1, TKT	/	Carbohydrate metabolism, protein metabolism, cellular movement, immune response, redox regulation
DRYlip *vs*. CTRL	CST4, PIGR, RNASE4, SCUBE2	/	Immune response, protein metabolism
DRYaq *vs*. CTRL	GSTP1, SELENBP1, SERPINA3, TGM2	AZGP1, CST4, PIGR	Cell movement, immune response, cell adhesion
	/	CST1, HSPB1, LCN1, PIP, SCGB1D1	Protein metabolism, regulation of water transport in apocrine glands
DRYaqlip *vs*. CTRL	C3, CP, PKM	IGHA1, SCGB2A1, TCN1	Immune response, carbohydrate metabolism, protein metabolism
DRYlip & DRYaqlip	CST3, EZR, HSPA8, IGKC, IGLC3, P4HB, S100A11, S100A8, S100A9, UBA52	/	Immune response, cell movement, protein metabolism, cell adhesion
DRYaq & DRYaqlip	A2M, HEBP2, HPX, PRDX5, PRDX6 YWHAB	/	Immune response, redox regulation
	CSTB, PEBP1, PFN1,	CLU, DMBT1, MSLN, PROL1, PRR4_N2, PRR4_SUM, ZG16B	Cell movement, cell adhesion, protein metabolism, unknown

Shared proteins between DRYaqlip and both DRYaq and DRYlip are listed to highlight possible protein biomarkers for underlying disease mechanisms. GOMF and GOBP were manually extracted from the Uniprot database (http://www.uniprot.org) and reorganized into larger categories. **HIGH** = increased abundance, **LOW** = decreased abundance.

5.1.4 Correlation analysis of the clinical attributes

This study not only established biomarkers for DES, but also evaluated the influences of age and gender on the tear proteome of healthy individuals. By evaluating the expression of the verified list of potential DES biomarkers in normal aging processes and different genders, we gain more insight into why women and the elderly are more prone to DES progression. A thorough analysis of both parameters showed that both higher ages and the female sex mimic DES biomarker expression, with age being the bigger influence on normal tears, judging by the amount of significant proteins in the two categories (11 *vs*. 4 respectively). Proteins such as MSLN, PIP, PRR4, and ZG16B were found to be decreased with age. With PIP influencing water transport in glands as well as MSLN, PRR4, and ZG16B being proteins that are secreted by the lacrimal gland, these findings point toward an

insufficiency of the lacrimal gland and a decrease in tear volume. A reason for these symptoms could be gland fibrosis, decreasing hormone levels, and lowered blood flow through the lacrimal gland in higher age groups [79-81]. Additionally, an increase in LCN2 over time indicates inflammatory reactions, as has been proposed by previous studies [127]. However, at the same time, levels of IGHA1, an IgA precursor, were found to be decreasing with age. IgA was both identified to be increased and decreased before with altering measurement techniques, which makes this protein a potential point of further investigations in the future, to clarify the mechanisms of increased inflammation with age [124, 125]. At any rate, age is associated with higher levels of ROS, which cause damage and therefore inflammation and apoptosis to the eye [51]. Older individuals may therefore have potentially more inflamed eyes without any additional pathological factors, which makes them more prone to the development of DES, especially if they are subject of any other aspect that promotes the disease, like bacterial infection.

Gender did not turn out to be highly correlated to DES biomarkers in this study. However, females expressed higher levels of HSPA8 and SCUBE2, as well as lowered abundances of LACRT and PRR4. Interestingly, LACRT was found to be increased in females in a study conducted by Ananthi *et al.*, however, this result was based on subjective evaluations of gel electrophoresis band intensities [156]. It therefore does not fully qualify for comparisons with absolute quantifications obtained in this study. In summary, all of these significant expression levels resemble the ones found in DES, which would explain its increased prevalence in women [25, 134]. As to why these proteins are elevated in women, there is still no definite answer. It is widely assumed, that these gender differences in protein expression are based on altering levels of sex steroids, especially of estrogen, which is believed to have inflammatory properties [132, 140]. These hypotheses are reinforced by this study's results of DES upstream regulators for DRYlip and DRYaqlip, which include beta estradiol and progesterone (**Figure 15**). Since these subgroups' shared pathways mostly revolve around inflammation, a connection to female sex hormones is therefore highly probable and should be subject of further investigation to reduce DES progression in women. Additionally, even though they were not found to be significantly correlated to gender in this study, proteins of future interest in this matter are PIP, SCGB1D1, and SCGB2A1. PIP, which is reduced in DES, is downregulated by estrogens and upregulated by androgens, therefore indicating another entrypoint for females into DES [384]. Moreover, the two mentioned secretoglobulin family

proteins show very bivalent results for DES in discovery stage studies, but were found to be decreased in this work [11, 229, 230]. Since they are involved in androgen receptor signaling pathways, they may be subject to hormonal changes, which would explain the variant results in previous studies due to their altering study populations. Altogether these findings stress the importance of personal medicine in all disease managements, including DES. By providing one of the largest list of age and gender related proteome alterations in tears, this study helped to fortify the notion of increased inflammatory reactions and lacrimal gland dysfunction being the cause of higher DES rates in the elderly and females. Nevertheless, future studies need to expand our knowledge about individual influences on protein expression to optimize diagnostics and treatment to best befit every patient. Additionally, study populations should be recruited and evaluated based on these aspects of personal medicine to secure sufficient results.

Lastly, correlations were also used to assess currently used diagnostic tests like Schirmer tests and TBUT in order to optimize their clinical use. These tests are conducted with a hard cut off of 10 mm / 5 min and 10 s respectively, resulting in established diagnoses of DES and its subgroups. However, due to a poor correlation between these results to actual disease stages, research has tried to move to other ways of identifying DES [107, 108]. But, until today, there is still no gold-standard in this field. One of the reasons for this is the use of non-sensitive biomarkers for inflammation in protein assays without further knowledge about disease pathways, resulting in equally insufficient diagnostic rates [50, 51]. Additionally, this study demonstrates that protein expressions show linear regressions with BST and TBUT values, rather than significant de- or increases below their cut off values. For example, the significant increment of metabolic enzymes such as ALDH3A1, GPI, and HSPA8 in all DES subgroups can be observed in negative regressions for Schirmer strip length and TBUT as well. Due to the linear relationship between these protein’s intensities and established diagnostic test values, one can also conclude significant changes to the tear proteome in values above the cut offs at 10 mm and 10 s respectively, which would clinically lead to false negative DES diagnoses. Additionally, proteins exclusively related to aqueous deficient DES, such as PRR4 and ZG16B show significant linear positive correlations to Schirmer strip values, indicating a broad spectrum of lacrimal gland dysfunction beyond the scope of currently accepted cut off values. Similarly, DAP related to DRYlip, e.g. S100A4 and

S100A8, were found to be negatively correlated to TBUT, proposing a linear increase of those inflammatory mediators in developing tear lipid layer deficiency.

Taking into account our updated understanding of DES progression, these tests, therefore, do not factor in disease manifestations that are currently compensated and show normal tear production and lipid layer stability, but will lead to hyperosmolarity through the DES vicious cycle eventually and may already show signs of it on the protein level. These compensated stages majorly complicate diagnostics, which calls for an optimization of diagnostic tests. Based on this study's results, BST and TBUT need to be used with updated cut off values, that allow for more than just two diagnoses – healthy and DES – since this rules out all compensated stages. Future studies should therefore endeavor to determine healthy, compensated, and disease values for these tests with the use of proteomic biomarkers for definite DES grouping. Of particular interest for clinical determination of DRYaq *vs*. DRYlip DES are proteins like CST4, PIGR, and RNASE4 that, in concordance to previous results in this study, show contrasting linear correlation factors for Schirmer strip length and TBUT. Using this information, BST and TBUT could still be used as rough screening tests to determine clearly healthy or diseased conditions, but also to indicate the grey areas of DES, which would then be subject to further diagnostic tests, such as the greatly improved proteomics approaches used in this study.

5.2 Establishing a MALDI-TOF-MS method for individual tear samples and characterization of PRR4

5.2.1 Method optimization

Results of previous steps in this study once again demonstrated the difficulties of identification and quantification of certain proteins in LC-MS/MS measurements of tears. Especially in case of PRR4, a highly compelling potential biomarker for DES, this is a well-known problem, presumably due to incomplete information about this protein's sequence, which leads to quantification difficulty and errors, and ultimately in a lack of functional analysis [27, 28, 182]. Moreover, the protein's individual expression of 4 isoforms and their unknown behavior or abundance in complex samples further complicates this matter [27]. Therefore, to gain sorely needed basic information on this protein and its behavior in complex samples, measurement techniques and sample preparations needed to be adapted. This study, therefore, aimed to depict PPR4 with as little sample manipulation as possible by stepping back from highly specific targeted proteomics and into a simpler MS technique. This will not only broaden our understanding of PRR4 but tears as a whole since complex individual samples have not been measured this way before.

A simple and fast proteomics method that presents itself for this matter due to several reasons is the so-called matrix-assisted laser desorption time-of-flight (MALDI-TOF) mass spectrometry. Firstly, MALDI is highly suitable for the sample type used, since it is successful in ionizing even large, polar or nonvolatile biomolecules, such as peptides, making it popular in proteomics research. Furthermore, this study endeavors to minimalize sample manipulation and therefore fragmentation during ionization in an effort to represent whole analytes. For this purpose, the soft ionization of MALDI is particularly beneficial [244]. It is based on the concept, that proteomics samples are crystallized with a radiation absorbing matrix for them to be subsequently shot by a laser. The matrix then ingests most of the energy and ionizes the sample by giving off protons, shielding the sample from direct interaction with the energy source and hence making it a soft ionization method. Hard ionization, in contrast, results in high fragmentation levels, as can be observed in electron impact ionization [389]. The use of a soft ionization method, therefore, supports measurements of complex samples due to a reduction of fragment overlay. MALDI is also gentler on samples than other methods using a heated injection chamber and prevents further alterations to temperature-sensitive substances, such as proteins.

Furthermore, MALDI-TOF only requires exceedingly low amounts of proteins, making it very applicable to DES patients with lowered tear and protein production as well as population-based studies [244, 245]. Conclusively this method is well suited for the objective at hand.

Nevertheless, even though MALDI-TOF is widely used in research, individual complex tear samples have not been measured with this method before. This is partly due to this method not yielding absolute, but relative abundances and low abundant proteins not being represented well in complex mixtures, because of suppression effects [244, 245]. Other studies consequently often add separation steps before applying MALDI-TOF; like gel electrophoresis (1DE or 2DE) or chromatography and include labeling techniques, since their objective is to quantify proteins of interest or reduce complexity [27, 170, 182, 202, 229]. On the contrary, this study sets out to represent as many unaltered peptides as possible in a large *m/z* range to depict the complex workings of tears and PRR4. Therefore, quantification is not the main objective, but rather identification of certain proteins of interest, in this case PRR4 isoforms, in samples mimicking the ones in clinical settings. MALDI-TOF therefore still is highly suitable for this study, even though there needed to be extensive optimization steps to ensure high-quality results.

For this purpose, the MS method used by Perumal *et al.* for the fragmentation and validation of PRR4 isoforms has been thoroughly adapted to befit individual tear samples [27]. During the development of this novel methodical approach, the best spectra quality and reproducibility was found to be achieved by disabling the fuzzy logic control, activating the accumulation of shots, keeping the previously established peak detection range and using 2500 shots per sample spot. Additionally, to ensure a high level of reproducibility, three technical replicates per individual were measured and evaluated through statistical analyses of peak intensities and identification levels. This way the occasional outlier was excluded from further analyses, which effectively counteracts inter- and intra-measurement fluctuations.

Furthermore, sample preparation steps were extensively optimized. Firstly, the sample amount was found to be ideal for complex tear samples at 0.5 µg per individual. The observation that the smaller the sample amount, the higher or more consistent peak intensities are might be counterintuitive since other MALDI-TOF proteomics studies use considerably higher protein amounts, but this phenomenon can be explained in multiple ways [202, 210, 229]. First and foremost, the

measurement method and resulting sample preparation need to be considered. As has been mentioned beforehand, other MALDI-TOF proteomics studies employ separation steps which often include purification procedures (e.g. in gel electrophoresis), which modify and dilute samples. Therefore, to be able to measure adequate amounts of peptides in those cases, the sample volume is increased. This study, however, uses unmodified and mostly undiluted samples with the only preparation steps being trypsin digestion, vacuum evaporation for storage and resuspension before sample spotting on the MALDI-TOF measurement plate. Comparable high sample volumes would, therefore, result in drastic suppression effects or detector oversaturation [239-241]. However, even in protein amounts of just over 0.5 µg, suppression inflicted by the few abundant proteins like LTF, LYZ and PRR4, makes identification of low abundant ones difficult. As a result, this study favored the use of 0.5 µg of protein, which works especially well with lowered tear production levels in DES. Furthermore, complex samples harbor unique interactions with the MALDI matrix, therefore influencing crystallization and ionization. Sample crystallization and therefore spotting on the MALDI-TOF measurement plate are highly diverse with techniques ranging from various mixed applications to spotting each component individually in every possible order [390, 391]. Complex samples were found to show more consistent ionization and therefore crystallization in individual spotting and drying of all sample components in between steps, resulting in higher spectra reproducibility levels.

Additionally, the use of the internal standard reserpine was optimized for complex individual tear samples. As has been mentioned before, other studies often introduce labeling techniques if absolute quantification of certain proteins is desired. Since this is a not only time-consuming and expensive method but is also not completely applicable to substances with somewhat unknown amino acid sequences, like PRR4, this study used another approach – the use of an internal standard of known amount to evaluate spectrum quality and estimate peptide fold changes [198, 225, 227]. Reserpine has proven to befit proteomics MALDI-TOF measurements in previous studies due to its *m/z*, which is not shared by peptides of interest, and was therefore chosen for this study as well [246-248]. Using statistical analyses like medians and box plots of reserpine peak intensities in samples, outliers could easily be identified and excluded, therefore increasing spectra quality yet again. Additionally, the use of an internal standard will permit estimated fold changes for PRR4 isoforms, granting

information about their distribution and relative total abundance, in a fast working method.

The last optimization step included the identification of PRR4 isoforms in MALDI-TOF spectra. Oftentimes, peptide sequences are shared or at least similar to some extent in human proteins or even to other substances [392]. Therefore, after digestion of proteins to peptides, those fragments could overlap and make decisive interpretation of results more difficult, especially in complex samples. As a result, this label-free measurement does not qualify for the identification and quantification of all tear proteins. To ensure the correct identification of PPR4, the peptide masses for all 4 isoforms were checked for overlapping products of other proteins by searching peptide databases. Currently, however, digestion products of no other proteins were found to share the same masses, indicating that MS peaks at 1601, 1729, 1792 and 1921 *m/z* can be affiliated to PRR4 only.

Despite the excellent results of this study and its high reproducibility, this method is not without faults and results should be used and interpreted with knowledge about several influencing factors. For one, with inconsistencies in between measurements or even technical replicates due to differing protein crystallization and laser shot patterns, being some of the major disadvantages of MALDI-TOF, quality control is vital in this MS method [244, 245]: However, *via* extensive method optimization, evaluation of multiple technical replicates and normalization steps, those influences were greatly reduced in this study. Still, it is important to note, that normalized intensities are not intended for absolute quantification in this study design. Rather than for absolute quantification purposes, the introduction of reserpine to the sample serves as an additional quality control step to counteract suppression effects and tool for the estimation of fold changes, as has been established in several preceding studies [246-248].

5.2.2 Characterization of individual sample's PRR4 in MALDI-TOF-MS

To date, LTF, LYZ, LCN1, SCGB2A1, ALB, and immunoglobulins were recognized as the main components of the tear proteome, which make up approximately 70% of the tear proteome [15, 160, 162, 163]. PRR4 on the other hand has been measured as making up around 3% of healthy tear proteins [229]. However, in this study's MALDI-TOF spectra, PRR4 isoforms are clearly assignable and in their sum make

PRR4 the most abundant protein by far. Just how abundant it is, varies from individual to individual and between groups, making this subject a case for further investigation in larger study populations employing absolute quantification techniques (e.g. ELISA or multiple reaction monitoring (MRM) MS). Furthermore, the staggering abundance of PRR4 changes our views on its importance in healthy tears substantially, since it may play a bigger role in tear film homeostasis than has been previously anticipated.

PRR4's expression in this study also indicates, that other proteomics methods crucially mismeasure the abundance of this protein. As has been mentioned in previous chapters, this may be due to several reasons. Firstly, the amino acid sequence of PRR4 is not fully known, which makes identification difficult [27, 183]. Additionally, most studies do not use adequate sequences for this protein, therefore making some or all isoforms non-identifiable [12, 15, 28, 160, 162, 200, 325]. Even after the discovery and successful identification of all isoform sequences, statistical analyses of PRR4 in targeted measurements has been made difficult by interpersonal differences in isoform expression. As the significant results for the sum of PRR4 isoforms accentuate, this ultimately leads to a loss of information.

While this study's method allows concise insight into PRR4 expressions in individuals, the isoforms' functions remain unclear. Polymorphisms in this protein have been observed to be based on methylation, acetylation, oxidation and pyroglutamate formation, which may influence their structure or behavior *in vivo* [27]. Whether those modifications restrict or adapt PRR4's function cannot be predicted by their amino acid sequence. Therefore isoforms need to be associated to disease stages in further investigations to unravel their functionality [229, 393]. As to the etiology of those isoforms, this study's results point towards genetic influences. Firstly, both eyes of each healthy individual expressed the same isoforms. Secondly, the relative distribution of isoform groups is mostly similar to previous findings by Perumal *et al.*, except for a decrease in P1 and a corresponding increase in P5 [27]. Whether those differences are due to the study population itself (e.g. population size or the local genetic PRR4 distribution) or altogether different reasons and if those isoforms are influenced by diseases like DES needs to be reevaluated in larger proteomics studies.

All these aspects lead to the conclusion that protein measurements in tears, especially for PRR4, need to be optimized and adapted in order to broaden our

understanding of tear film homeostasis and diseases like DES. Additionally, MS methods with their specific advantages and disadvantages may serve different purposes in further investigations. Much like the use of different imaging techniques in medicine, MS methods should be used for distinct research and diagnostic purposes. For example, a broken arm may be roughly scanned by an X-ray, thoroughly depicted *via* computed tomography (CT) scans, or checked for soft tissue and neurological damage with magnetic resonance imaging (MRI). Each of these methods harbors certain advantages or disadvantages when it comes to diagnostic accuracy, time effort or cost per scan, and is used for a specific view on the same condition. Similarly, MS methods should be applied to research and diagnostic matters depending on the desired outcome and in knowledge about their characteristics. A comparison of different mass spectrometry methods in regard to the time needed for sample preparation and measurements, the sample amount needed, as well as their accuracy and cost can be found in **Table 11**.

Table 13: Comparison of mass spectrometry method characteristics.

Method	Time effort		Sample amount	Cost	Accuracy
	Sample preparation	MS measurement			
MS **(e.g. MALDI-TOF)**	↓ - protein digestion	↓ ~ 10 min per sample	↓ ~ 0.5 to 1 µg	↓ label-free ↑ labeled	↓ - relative quantification (without labeling) - low reproducibility without technical replicates - quantification limited to ~ 20 peptides
Discovery MS/MS **(e.g. LC-MS/MS)**	↑ - protein digestion - separation steps - purification steps	↑ ~ h – days per sample	↑ ~ 50 µg	↔ label-free ↑ Labeled	↔ - absolute quantification of entire proteome (also in label-free samples) - separation step needed to increase accuracy
Targeted MS/MS **(e.g. AIMS)**	↔ - protein digestion - purification steps	↔ ~ 2 h per sample	↔ ~ 10 µg	↔ label-free ↑ Labeled	↑ - absolute quantification of proteins of interest (also in label-free samples)

Arrows indicate a relatively low, medium or high ranking when comparing the three MS methods. Attributes were rated as follows – in the categories **time effort, sample amount and cost**: ↓ **/ green =** lowest amount/shortest time needed, ↔ **/ yellow =** amounts or time needed are situated between highest and lowest ratings, ↑ **/ red =** highest amount/longest time needed; **Accuracy** was rated as follows: ↑ **/ green =** highest level of accuracy, ↔ **/ yellow =** intermediate level of accuracy, ↓ **/ red =** lowest level of accuracy.

For the sake of thorough identification of as many proteins as possible, discovery MS/MS methods may be used. These prove to be time consuming in sample preparation and actual measurement, since separation steps need to be included to reduce suppression effects. As a result, high protein amounts are needed to secure accurate measurements after separation, which may prolong sample collection in clinical or study settings (e.g. in DES due to reduced tear production rates). The hardware used in these studies is expensive and measurements tend to be lengthly, since the objective is to measure a large amount of proteins. Especially when using labeled samples, measurements are therefore comparatively expensive as well. However, discovery MS/MS methods are a powerful tool to gain large amounts of data and can be used for extensive functional analyses. They are therefore especially fit to be used in fundamental research.

Targeted mass spectrometry techniques may be used to identify and quantify certain proteins of interest. Therefore, they do not rely on additional separation steps, which reduce the time effort for sample preparation and MS measurements. Additionally, this results in a decreased amount of needed protein for adequate results. In total, this diminishes the cost per measurement, even though the initial price of mass spectrometers that are able to perform targeted methods is still high. Nevertheless, the results are highly accurate and can be used for extensive biomarker establishment and functional analyses. However, the quality of targeted MS results greatly depends on previously conducted discovery stage studies since they are only depicting selected pieces of information and therefore may even be prone to false positive or negative correlations.

Therefore, to gain a general overview of tear proteins, a MS method that affects sample proteins in the least amount possible is needed. For this purpose, simple MS techniques like MALDI-TOF, that require no extra preparation steps next to digestion, are highly recommended. They enable fast and cost-efficient measurements of the entire proteome, which need as little as 0.5 µg of tear protein, making them especially advantageous to diseases like DES with small sample amounts. Nonetheless, they only result in relative quantification. The use of internal standards or labeling may improve quantification but complicates measurement workflows. Additionally, peptides may not be identified distinctly, due to similar amino acid sequences being shared by multiple proteins. Therefore, this method may not be applicable to accurate identification or quantification of proteins, but should be used

in the sense of a general protein screening with the objective to either identify specific peptides (e.g. pathological expressions) or estimate their abundance in individual's tears. Hence, further optimization and adaptation of this study's method to disease characteristics could lead to the development of fast diagnostic screening methods.

6. CONCLUSION

6.1 Identification of clinical biomarkers in dry eye disease using a targeted proteomics approach

This study unraveled many novel findings in the field of DES research employing proteomics. Firstly, an extensively optimized AIMS method was used to uncover the largest number of biomarker candidates in individual tear samples yet. Thorough functional analysis of those 59 significantly expressed proteins revealed underlying pathophysiological mechanisms for DES subgroups. While all DES patients showed heightened inflammatory reactions and associated metabolic processes, each subgroup also demonstrated unique properties. DRYlip was found to be based on innate and acquired immune responses, presumably associated to bacterial and viral infections, as well as allergic reactions, while inflammation in DRYaq mostly involves acute phase proteins. Additionally, the latter subgroup includes a substantial amount of antioxidative enzymes, indicating a high amount of reactive oxygen species, and a resulting elevation of apoptotic and necrotic cell death. Furthermore, there is a considerable group of extracellular proteins with decreased abundances in DRYaq, several of which have unknown functions, e.g. PRR4 and ZG16B. The decrement of these proteins is mostly attributed to the dysfunction of the lacrimal gland but the reasons behind it are currently not fully understood. The combination of these mechanisms results in DRYaqlip, which shows characteristics of both DES etiologies. It furthermore involves additional proteins involved in metabolic processing, oxidative stress, acute phase reactions, and apoptosis, implying an even intensified disruption of tear film homeostasis compared to the other subgroups. It therefore represents the endpoint of the vicious cycle of DES progression with no remaining compensation leeway. Such an extensive view into the differing pathophysiological mechanisms of DES subgroups has not been achieved with individual samples on such a scale before and greatly improves our understanding of the disease, as well as introducing various opportunities for future research endeavors. Secondly, this study investigated the aspects of personalized medicine in DES. Aging is associated with a progressive lacrimal dysfunction and inflammatory reactions, mimicking protein changes in DES. This study also established gender-specific alterations in tears that indicate healthy females to be closer to DES protein expression than males. These findings are in clear concordance with the observed high prevalence of DES in the elderly and females and stresses the importance of personalized medicine for the recruitment of

study populations, diagnostics and therapy. The data acquired in this study was also used to conclusively identify potential improvements in currently established diagnostic steps, namely the Schirmer test and TBUT. Numerous proteins showed significant linear regressions with BST and TBUT values with gradual de- and increases, rather than drastic intensity changes below their cut off values. Cut offs should therefore be reevaluated and used to screen for clearly healthy or diseased tear films. If BST and TBUT show inconclusive results, further testing should be considered to improve diagnostic sensitivity and specificity, for example proteomics strategies that are able to identify compensated DES states.

Lastly, this study has developed and extensively optimized a novel MALDI-TOF method employing the internal standard reserpine to yield fast results of the highest quality and reproducibility. Not only were all 4 PRR4 isoforms distinctly detectable in one MS spectrum with this method, but PRR4 was also identified as the protein with the highest abundance in tears thus far. In summary, this study has provided a comprehensive mechanistic insight at the clinical aspect in the maintenance of human tear homeostasis and DES research, especially the highly abundant PRR4. The outcomes of this study will be instrumental for future translational efforts for improved clinical management and treatment development for DES in a more personalized manner.

6.2 Identifizierung klinischer Biomarker für das trockene Augen-Syndrom mithilfe eines gezielten proteomischen Ansatzes

Diese Studie enthüllte viele neue Erkenntnisse auf dem Gebiet der DES-Forschung unter Verwendung von Proteomik. Erstens wurde eine umfassend optimierte AIMS-Methode verwendet, um die bisher größte Anzahl von Biomarkerkandidaten in einzelnen Tränenproben aufzudecken. Eine gründliche Funktionsanalyse dieser 59 signifikant exprimierten Proteine ergab zugrunde liegende pathophysiologische Mechanismen für DES-Untergruppen. Während alle DES-Patienten erhöhte Entzündungsreaktionen und damit verbundene Stoffwechselprozesse zeigten, besitzt jede Untergruppe auch einzigartige Eigenschaften. Es wurde festgestellt, dass DRYlip auf angeborenen und erworbenen Immunantworten basiert, die vermutlich mit bakteriellen und viralen Infektionen sowie allergischen Reaktionen verbunden sind, während Entzündungen in DRYaq hauptsächlich Akute-Phase-Proteine betreffen. Zusätzlich involviert diese Untergruppe eine erhebliche Menge an

antioxidativen Enzymen, was auf eine hohe Menge an reaktiven Sauerstoffspezies und eine daraus resultierende Erhöhung des apoptotischen und nekrotischen Zelltods hinweist. Darüber hinaus gibt es eine beträchtliche Gruppe von extrazellulären Proteinen mit verringerter Häufigkeit in DRYaq, von denen einige unbekannte Funktionen haben, z.B. PRR4 und ZG16B. Die Verringerungt dieser Proteine wird hauptsächlich auf die Funktionsstörung der Tränendrüse zurückgeführt, aber die Gründe dafür sind derzeit nicht vollständig geklärt. Die Kombination dieser Mechanismen führt zu DRYaqlip, das Eigenschaften beider DES-Ätiologien zeigt. Darüber hinaus sind hier zusätzliche Proteine beteiligt, die an der Stoffwechselverarbeitung, oxidativem Stress, Akuten-Phase-Reaktion und Apoptose beteiligt sind, was im Vergleich zu den anderen Untergruppen eine noch verstärkte Störung der Tränenfilmhomöostase impliziert. Es stellt daher den Endpunkt des Teufelskreises der DES-Progression ohne verbleibenden Kompensationsspielraum dar. Ein derart umfassender Einblick in die unterschiedlichen pathophysiologischen Mechanismen von DES-Untergruppen wurde bisher mit einzelnen Proben in einem solchen Maßstab nicht erreicht und verbessert unser Verständnis der Krankheit erheblich und bietet verschiedene Möglichkeiten für zukünftige Forschungsbemühungen. Darüber hinaus untersuchte diese Studie die Aspekte der personalisierten Medizin in DES. Altern ist mit einer fortschreitenden Tränenfunktionsstörung und entzündlichen Reaktionen verbunden, die Proteinveränderungen bei DES nachahmen. Diese Studie stellte auch geschlechtsspezifische Veränderungen bei Tränen fest, die darauf hinweisen, dass gesunde Frauen der DES-Proteinexpression näher sind als Männer. Diese Ergebnisse stimmen eindeutig mit der beobachteten hohen Prävalenz von DES bei älteren Menschen und Frauen überein und unterstreichen die Bedeutung der personalisierten Medizin für die Rekrutierung von Studienpopulationen, Diagnostik und Therapie. Die in dieser Studie erfassten Daten wurden auch verwendet, um mögliche Verbesserungen der derzeit etablierten diagnostischen Schritte, nämlich des Schirmer-Tests und des TBUT, zu identifizieren. Zahlreiche Proteine zeigten signifikante lineare Regressionen mit BST- und TBUT-Werten mit allmählicher Abnahme und Zunahme, anstatt drastischer Intensitätsänderungen unterhalb ihrer Grenzwerte. Diese Tests sollten daher neu bewertet und verwendet werden, um nach eindeutig gesunden oder erkrankten Tränenfilmen zu suchen. Wenn BST und TBUT nicht eindeutige Ergebnisse zeigen, sollten weitere Tests in Betracht gezogen werden, um die diagnostische Sensitivität und Spezifität zu verbessern,

beispielsweise Proteomik-Strategien, mit denen kompensierte DES-Zustände identifiziert werden können.

Schließlich hat diese Studie eine neuartige MALDI-TOF-Methode entwickelt und umfassend optimiert, bei der der interne Standard Reserpin verwendet wird, um schnelle Ergebnisse von höchster Qualität und Reproduzierbarkeit zu erzielen. Mit dieser Methode waren nicht nur alle 4 PRR4-Isoformen in einem MS-Spektrum eindeutig nachweisbar, sondern PRR4 wurde auch als das Protein mit der höchsten Häufigkeit in Tränen identifiziert. Zusammenfassend hat diese Studie einen umfassenden mechanistischen Einblick in den klinischen Aspekt bei der Aufrechterhaltung der menschlichen Tränenhomöostase und der DES-Forschung gegeben, insbesondere in das häufig vorkommende PRR4. Die Ergebnisse dieser Studie werden für zukünftige Bemühungen zur Verbesserung des klinischen Managements und der Behandlungsentwicklung für DES auf personalisiertere Weise von entscheidender Bedeutung sein.

7. REFERENCES

1. Bron, A.J., *The Definition and Classification of Dry Eye Disease*, in *Dry Eye: A Practical Approach*, C. Chan, Editor. 2015, Springer Berlin Heidelberg: Berlin, Heidelberg. p. 1-19.
2. Dana, R., et al., *Estimated Prevalence and Incidence of Dry Eye Disease Based on Coding Analysis of a Large, All-age United States Health Care System.* Am J Ophthalmol, 2019.
3. Caffery, B., et al., *Prevalence of dry eye disease in Ontario, Canada: A population-based survey.* Ocul Surf, 2019.
4. Titiyal, J.S., et al., *Prevalence and risk factors of dry eye disease in North India: Ocular surface disease index-based cross-sectional hospital study.* Indian J Ophthalmol, 2018. **66**(2): p. 207-211.
5. Craig, J.P., et al., *TFOS DEWS II Definition and Classification Report.* Ocul Surf, 2017. **15**(3): p. 276-283.
6. Friedman, N.J., *Impact of dry eye disease and treatment on quality of life.* Curr Opin Ophthalmol, 2010. **21**(4): p. 310-6.
7. Nichols, K.K., J.J. Nichols, and G.L. Mitchell, *The lack of association between signs and symptoms in patients with dry eye disease.* Cornea, 2004. **23**(8): p. 762-70.
8. Begley, C.G., et al., *The relationship between habitual patient-reported symptoms and clinical signs among patients with dry eye of varying severity.* Invest Ophthalmol Vis Sci, 2003. **44**(11): p. 4753-61.
9. Zivy, M. and D. de Vienne, *Proteomics: a link between genomics, genetics and physiology.* Plant Mol Biol, 2000. **44**(5): p. 575-80.
10. Aebersold, R. and M. Mann, *Mass spectrometry-based proteomics.* Nature, 2003. **422**(6928): p. 198-207.
11. Boehm, N., et al., *Alterations in the tear proteome of dry eye patients--a matter of the clinical phenotype.* Invest Ophthalmol Vis Sci, 2013. **54**(3): p. 2385-92.
12. Grus, F.H., et al., *SELDI-TOF-MS ProteinChip array profiling of tears from patients with dry eye.* Invest Ophthalmol Vis Sci, 2005. **46**(3): p. 863-76.
13. Nichols, J.J. and K.B. Green-Church, *Mass spectrometry-based proteomic analyses in contact lens-related dry eye.* Cornea, 2009. **28**(10): p. 1109-17.
14. Srinivasan, S., et al., *iTRAQ quantitative proteomics in the analysis of tears in dry eye patients.* Invest Ophthalmol Vis Sci, 2012. **53**(8): p. 5052-9.
15. Zhou, L., et al., *Identification of tear fluid biomarkers in dry eye syndrome using iTRAQ quantitative proteomics.* J Proteome Res, 2009. **8**(11): p. 4889-905.
16. Soria, J., et al., *Tear proteome analysis in ocular surface diseases using label-free LC-MS/MS and multiplexed-microarray biomarker validation.* Sci Rep, 2017. **7**(1): p. 17478.
17. Soria, J., et al., *Tear proteome and protein network analyses reveal a novel pentamarker panel for tear film characterization in dry eye and meibomian gland dysfunction.* J Proteomics, 2013. **78**: p. 94-112.
18. Li, B., et al., *Tear proteomic analysis of Sjogren syndrome patients with dry eye syndrome by two-dimensional-nano-liquid chromatography coupled with tandem mass spectrometry.* Sci Rep, 2014. **4**: p. 5772.
19. Matheis, N., et al., *Proteomics Differentiate Between Thyroid-Associated Orbitopathy and Dry Eye Syndrome.* Invest Ophthalmol Vis Sci, 2015. **56**(4): p. 2649-56.

20. Perumal, N., et al., *Proteomics analysis of human tears from aqueous-deficient and evaporative dry eye patients.* Sci Rep, 2016. **6**: p. 29629.

21. Jung, J.H., et al., *Proteomic analysis of human lacrimal and tear fluid in dry eye disease.* Sci Rep, 2017. **7**(1): p. 13363.

22. Chen, X., et al., *Integrated Tear Proteome and Metabolome Reveal Panels of Inflammatory-Related Molecules via Key Regulatory Pathways in Dry Eye Syndrome.* J Proteome Res, 2019. **18**(5): p. 2321-2330.

23. Kolman, I., et al., *Investigation of tear protein composition in healthy and dry eye subjects using trapped ion mobility spectrometry coupled with quadrupole time of flight.* Acta Ophthalmologica, 2019. **97**(S263).

24. Jaffe, J.D., et al., *Accurate inclusion mass screening: a bridge from unbiased discovery to targeted assay development for biomarker verification.* Mol Cell Proteomics, 2008. **7**(10): p. 1952-62.

25. Stapleton, F., et al., *TFOS DEWS II Epidemiology Report.* Ocul Surf, 2017. **15**(3): p. 334-365.

26. Liotta, L.A., E.C. Kohn, and E.F. Petricoin, *Clinical proteomics: personalized molecular medicine.* JAMA, 2001. **286**(18): p. 2211-4.

27. Perumal, N., et al., *Characterization of lacrimal proline-rich protein 4 (PRR4) in human tear proteome.* Proteomics, 2014. **14**(13-14): p. 1698-709.

28. Aluru, S.V., et al., *Lacrimal proline rich 4 (LPRR4) protein in the tear fluid is a potential biomarker of dry eye syndrome.* PLoS One, 2012. **7**(12): p. e51979.

29. Chao, W., et al., *Report of the Inaugural Meeting of the TFOS i(2) = initiating innovation Series: Targeting the Unmet Need for Dry Eye Treatment.* Ocul Surf, 2016. **14**(2): p. 264-316.

30. Castro, J.S., et al., *Prevalence and Risk Factors of self-reported dry eye in Brazil using a short symptom questionnaire.* Sci Rep, 2018. **8**(1): p. 2076.

31. Farrand, K.F., et al., *Prevalence of Diagnosed Dry Eye Disease in the United States Among Adults Aged 18 Years and Older.* Am J Ophthalmol, 2017. **182**: p. 90-98.

32. Song, P., et al., *Variations of dry eye disease prevalence by age, sex and geographic characteristics in China: a systematic review and meta-analysis.* J Glob Health, 2018. **8**(2): p. 020503.

33. Hashemi, H., et al., *Prevalence of dry eye syndrome in an adult population.* Clin Exp Ophthalmol, 2014. **42**(3): p. 242-8.

34. Uchino, M., et al., *Prevalence of dry eye disease and its risk factors in visual display terminal users: the Osaka study.* Am J Ophthalmol, 2013. **156**(4): p. 759-66.

35. Yokoi, N., et al., *Importance of tear film instability in dry eye disease in office workers using visual display terminals: the Osaka study.* Am J Ophthalmol, 2015. **159**(4): p. 748-54.

36. Lemp, M.A., *Report of the National Eye Institute/Industry workshop on Clinical Trials in Dry Eyes.* CLAO J, 1995. **21**(4): p. 221-32.

37. *The definition and classification of dry eye disease: report of the Definition and Classification Subcommittee of the International Dry Eye WorkShop (2007).* Ocul Surf, 2007. **5**(2): p. 75-92.

38. Li, M., et al., *Assessment of vision-related quality of life in dry eye patients.* Invest Ophthalmol Vis Sci, 2012. **53**(9): p. 5722-7.

39. Schiffman, R.M., et al., *Utility assessment among patients with dry eye disease.* Ophthalmology, 2003. **110**(7): p. 1412-9.

40. Shigeyasu, C., et al., *Quality of life measures and health utility values among dry eye subgroups.* Health Qual Life Outcomes, 2018. **16**(1): p. 170.

41. Uchino, M., et al., *Dry eye disease and work productivity loss in visual display users: the Osaka study.* Am J Ophthalmol, 2014. **157**(2): p. 294-300.

42. Sullivan, R.M., et al., *Economic and quality of life impact of dry eye symptoms in women with Sjogren's syndrome.* Adv Exp Med Biol, 2002. **506**(Pt B): p. 1183-8.

43. Asiedu, K., S.K. Dzasimatu, and S. Kyei, *Impact of Dry Eye on Psychosomatic Symptoms and Quality of Life in a Healthy Youthful Clinical Sample.* Eye Contact Lens, 2018. **44 Suppl 2**: p. S404-S409.

44. Fernandez, C.A., et al., *Dry eye syndrome, posttraumatic stress disorder, and depression in an older male veteran population.* Invest Ophthalmol Vis Sci, 2013. **54**(5): p. 3666-72.

45. Zheng, Y., et al., *The Prevalence of Depression and Depressive Symptoms among Eye Disease Patients: A Systematic Review and Meta-analysis.* Sci Rep, 2017. **7**: p. 46453.

46. Ayaki, M., et al., *Sleep and mood disorders in women with dry eye disease.* Sci Rep, 2016. **6**: p. 35276.

47. Han, K.T., J.H. Nam, and E.C. Park, *Do Sleep Disorders Positively Correlate with Dry Eye Syndrome? Results of National Claim Data.* Int J Environ Res Public Health, 2019. **16**(5).

48. McDonald, M., et al., *Economic and Humanistic Burden of Dry Eye Disease in Europe, North America, and Asia: A Systematic Literature Review.* Ocul Surf, 2016. **14**(2): p. 144-67.

49. Yu, J., C.V. Asche, and C.J. Fairchild, *The economic burden of dry eye disease in the United States: a decision tree analysis.* Cornea, 2011. **30**(4): p. 379-87.

50. Willcox, M.D.P., et al., *TFOS DEWS II Tear Film Report.* Ocul Surf, 2017. **15**(3): p. 366-403.

51. Bron, A.J., et al., *TFOS DEWS II pathophysiology report.* Ocul Surf, 2017. **15**(3): p. 438-510.

52. Stern, M.E., et al., *The role of the lacrimal functional unit in the pathophysiology of dry eye.* Exp Eye Res, 2004. **78**(3): p. 409-16.

53. Willshire, C., R.J. Buckley, and A.J. Bron, *Central Connections of the Lacrimal Functional Unit.* Cornea, 2017. **36**(8): p. 898-907.

54. Kathleen S. Kunert WS, H.B., *Trockenes Auge: Anatomie, Physiologie, Pathophysiologie, Diagnose und Therapie des Sicca-Syndroms.* Heidelberg: Kaden, 2016.

55. Georgiev, G.A., et al., *Surface relaxations as a tool to distinguish the dynamic interfacial properties of films formed by normal and diseased meibomian lipids.* Soft Matter, 2014. **10**(30): p. 5579-88.

56. Holly, F.J., *Formation and rupture of the tear film.* Exp Eye Res, 1973. **15**(5): p. 515-25.

57. Rosenfeld, L. and G.G. Fuller, *Consequences of interfacial viscoelasticity on thin film stability.* Langmuir, 2012. **28**(40): p. 14238-44.

58. Green-Church, K.B., et al., *The international workshop on meibomian gland dysfunction: report of the subcommittee on tear film lipids and lipid-protein interactions in health and disease.* Invest Ophthalmol Vis Sci, 2011. **52**(4): p. 1979-93.

59. Gipson, I.K. and P. Argueso, *Role of mucins in the function of the corneal and conjunctival epithelia.* Int Rev Cytol, 2003. **231**: p. 1-49.

60. Guzman-Aranguez, A., F. Mantelli, and P. Argueso, *Mucin-type O-glycans in tears of normal subjects and patients with non-Sjogren's dry eye.* Invest Ophthalmol Vis Sci, 2009. **50**(10): p. 4581-7.

61. Gipson, I.K., Y. Hori, and P. Argueso, *Character of ocular surface mucins and their alteration in dry eye disease.* Ocul Surf, 2004. **2**(2): p. 131-48.

62. Aknin, M.L., et al., *Normal but not altered mucins activate neutrophils.* Cell Tissue Res, 2004. **318**(3): p. 545-51.

63. Yazdani, M., et al., *Tear Metabolomics in Dry Eye Disease: A Review.* Int J Mol Sci, 2019. **20**(15).

64. Baudouin, C., et al., *Revisiting the vicious circle of dry eye disease: a focus on the pathophysiology of meibomian gland dysfunction.* Br J Ophthalmol, 2016. **100**(3): p. 300-6.

65. Lemp, A., Sullivan, B. D., Crews, L. A., *Biomarkers in dry eye disease.* Eur Ophthal Rev, 2012. **6**: p. 157-163.

66. Lemp, M.A., et al., *Distribution of aqueous-deficient and evaporative dry eye in a clinic-based patient cohort: a retrospective study.* Cornea, 2012. **31**(5): p. 472-8.

67. Asiedu, K., S.K. Dzasimatu, and S. Kyei, *Clinical subtypes of dry eye in youthful clinical sample in Ghana.* Cont Lens Anterior Eye, 2018.

68. Achtsidis, V., et al., *Dry eye syndrome in subjects with diabetes and association with neuropathy.* Diabetes Care, 2014. **37**(10): p. e210-1.

69. Zou, X., et al., *Prevalence and clinical characteristics of dry eye disease in community-based type 2 diabetic patients: the Beixinjing eye study.* BMC Ophthalmol, 2018. **18**(1): p. 117.

70. Cakir, B.K., et al., *Ocular surface changes in patients treated with oral antidiabetic drugs or insulin.* Eur J Ophthalmol, 2016. **26**(4): p. 303-6.

71. Zhang, Y., et al., *Influence of Pilocarpine and Timolol on Human Meibomian Gland Epithelial Cells.* Cornea, 2017. **36**(6): p. 719-724.

72. Ooi, K.G., et al., *Association of dyslipidaemia and oral statin use, and dry eye disease symptoms in the Blue Mountains Eye Study.* Clin Exp Ophthalmol, 2018.

73. Dana, R., et al., *Comorbidities and Prescribed Medications in Patients With or Without Dry Eye Disease: A Population-Based Study.* Am J Ophthalmol, 2019. **198**: p. 181-192.

74. Karaman Erdur, S., et al., *Ocular surface and tear parameters in patients with chronic hepatitis C at initial stages of hepatic fibrosis.* Eye Contact Lens, 2015. **41**(2): p. 117-20.

75. Tiwari, S., et al., *Aqueous Deficient Dry Eye Syndrome Post Orbital Radiotherapy: A 10-Year Retrospective Study.* Transl Vis Sci Technol, 2017. **6**(3): p. 19.

76. Ozek, D., O.E. Kemer, and A. Omma, *Association between systemic activity index and dry eye severity in patients with primary Sjogren syndrome.* Arq Bras Oftalmol, 2019. **82**(1): p. 45-50.

77. Wang, H., et al., *Analysis of Clinical Characteristics of Immune-Related Dry Eye.* J Ophthalmol, 2017. **2017**: p. 8532397.

78. Sullivan, D.A., et al., *Meibomian Gland Dysfunction in Primary and Secondary Sjogren Syndrome.* Ophthalmic Res, 2018. **59**(4): p. 193-205.

79. Bian, F., et al., *Age-associated antigen-presenting cell alterations promote dry-eye inducing Th1 cells.* Mucosal Immunol, 2019.

80. Obata, H., et al., *Histopathologic study of human lacrimal gland. Statistical analysis with special reference to aging.* Ophthalmology, 1995. **102**(4): p. 678-86.

81. Feng, Y., et al., *The effects of hormone replacement therapy on dry eye syndromes evaluated by Schirmer test depend on patient age.* Cont Lens Anterior Eye, 2016. **39**(2): p. 124-7.

82. Sullivan, D.A., et al., *Androgen deficiency, Meibomian gland dysfunction, and evaporative dry eye.* Ann N Y Acad Sci, 2002. **966**: p. 211-22.

83. El Ameen, A., et al., *Influence of cataract surgery on Meibomian gland dysfunction.* J Fr Ophtalmol, 2018. **41**(5): p. e173-e180.

84. Ziemanski, J.F., et al., *Relation Between Dietary Essential Fatty Acid Intake and Dry Eye Disease and Meibomian Gland Dysfunction in Postmenopausal Women.* Am J Ophthalmol, 2018. **189**: p. 29-40.

85. Rathnakumar, K., et al., *Prevalence of dry eye disease and its association with dyslipidemia.* J Basic Clin Physiol Pharmacol, 2018. **29**(2): p. 195-199.

86. Mathers, W.D., et al., *Meibomian gland morphology and tear osmolarity: changes with Accutane therapy.* Cornea, 1991. **10**(4): p. 286-90.

87. Li, D.Q., et al., *Stimulation of matrix metalloproteinases by hyperosmolarity via a JNK pathway in human corneal epithelial cells.* Invest Ophthalmol Vis Sci, 2004. **45**(12): p. 4302-11.

88. Massingale, M.L., et al., *Analysis of inflammatory cytokines in the tears of dry eye patients.* Cornea, 2009. **28**(9): p. 1023-7.

89. Enriquez-de-Salamanca, A., et al., *Tear cytokine and chemokine analysis and clinical correlations in evaporative-type dry eye disease.* Mol Vis, 2010. **16**: p. 862-73.

90. Lee, S.Y., et al., *Analysis of tear cytokines and clinical correlations in Sjogren syndrome dry eye patients and non-Sjogren syndrome dry eye patients.* Am J Ophthalmol, 2013. **156**(2): p. 247-253 e1.

91. Kato, H., et al., *Relationship Between Ocular Surface Epithelial Damage, Tear Abnormalities, and Blink in Patients With Dry Eye.* Cornea, 2019. **38**(3): p. 318-324.

92. De Paiva, C.S. and S.C. Pflugfelder, *Corneal epitheliopathy of dry eye induces hyperesthesia to mechanical air jet stimulation.* Am J Ophthalmol, 2004. **137**(1): p. 109-15.

93. Bourcier, T., et al., *Decreased corneal sensitivity in patients with dry eye.* Invest Ophthalmol Vis Sci, 2005. **46**(7): p. 2341-5.

94. Enriquez-de-Salamanca, A., S. Bonini, and M. Calonge, *Molecular and cellular biomarkers in dry eye disease and ocular allergy.* Curr Opin Allergy Clin Immunol, 2012. **12**(5): p. 523-33.

95. Chalmers, R.L., et al., *The agreement between self-assessment and clinician assessment of dry eye severity.* Cornea, 2005. **24**(7): p. 804-10.

96. Bron, A.J., *Diagnosis of dry eye.* Surv Ophthalmol, 2001. **45 Suppl 2**: p. S221-6.

97. Pflugfelder, S.C., et al., *Evaluation of subjective assessments and objective diagnostic tests for diagnosing tear-film disorders known to cause ocular irritation.* Cornea, 1998. **17**(1): p. 38-56.

98. Abetz, L., et al., *Development and validation of the impact of dry eye on everyday life (IDEEL) questionnaire, a patient-reported outcomes (PRO) measure for the assessment of the burden of dry eye on patients.* Health Qual Life Outcomes, 2011. **9**: p. 111.

99. Lucca, J.A., J.N. Nunez, and R.L. Farris, *A comparison of diagnostic tests for keratoconjunctivitis sicca: lactoplate, Schirmer, and tear osmolarity.* CLAO J, 1990. **16**(2): p. 109-12.

100. Zeev, M.S., D.D. Miller, and R. Latkany, *Diagnosis of dry eye disease and emerging technologies.* Clin Ophthalmol, 2014. **8**: p. 581-90.

101. Khanal, S. and T.J. Millar, *Barriers to clinical uptake of tear osmolarity measurements.* Br J Ophthalmol, 2012. **96**(3): p. 341-4.

102. Keech, A., M. Senchyna, and L. Jones, *Impact of time between collection and collection method on human tear fluid osmolarity.* Curr Eye Res, 2013. **38**(4): p. 428-36.

103. Goren, M.B. and S.B. Goren, *Diagnostic tests in patients with symptoms of keratoconjunctivitis sicca.* Am J Ophthalmol, 1988. **106**(5): p. 570-4.

104. Boehm, N., et al., *Proinflammatory cytokine profiling of tears from dry eye patients by means of antibody microarrays.* Invest Ophthalmol Vis Sci, 2011. **52**(10): p. 7725-30.

105. Messmer, E.M., et al., *Matrix Metalloproteinase 9 Testing in Dry Eye Disease Using a Commercially Available Point-of-Care Immunoassay.* Ophthalmology, 2016. **123**(11): p. 2300-2308.

106. Sambursky, R., et al., *Sensitivity and specificity of a point-of-care matrix metalloproteinase 9 immunoassay for diagnosing inflammation related to dry eye.* JAMA Ophthalmol, 2013. **131**(1): p. 24-8.

107. Schargus, M., et al., *Correlation of Tear Film Osmolarity and 2 Different MMP-9 Tests With Common Dry Eye Tests in a Cohort of Non-Dry Eye Patients.* Cornea, 2015. **34**(7): p. 739-44.

108. Lanza, N.L., et al., *The Matrix Metalloproteinase 9 Point-of-Care Test in Dry Eye.* Ocul Surf, 2016. **14**(2): p. 189-95.

109. Geyer, P.E., et al., *Revisiting biomarker discovery by plasma proteomics.* Mol Syst Biol, 2017. **13**(9): p. 942.

110. Ginsburg, G.S. and J.J. McCarthy, *Personalized medicine: revolutionizing drug discovery and patient care.* Trends Biotechnol, 2001. **19**(12): p. 491-6.

111. Olivier, M., et al., *The Need for Multi-Omics Biomarker Signatures in Precision Medicine.* Int J Mol Sci, 2019. **20**(19).

112. Wu, P.W., et al., *Proteomic analysis of hair shafts from monozygotic twins: Expression profiles and genetically variant peptides.* Proteomics, 2017. **17**(13-14).

113. Gordon, L., et al., *Neonatal DNA methylation profile in human twins is specified by a complex interplay between intrauterine environmental and genetic factors, subject to tissue-specific influence.* Genome Res, 2012. **22**(8): p. 1395-406.

114. Costello, L.C. and R.B. Franklin, *Tumor cell metabolism: the marriage of molecular genetics and proteomics with cellular intermediary metabolism; proceed with caution!* Mol Cancer, 2006. **5**: p. 59.

115. Schaup, H.W., *A paradigm for ribosome fidelity modulation in protein synthesis.* J Theor Biol, 1978. **71**(2): p. 215-24.

116. Zhang, Z., et al., *High-throughput proteomics.* Annu Rev Anal Chem (Palo Alto Calif), 2014. **7**: p. 427-54.

117. Shen, Q., et al., *A targeted proteomics approach reveals a serum protein signature as diagnostic biomarker for resectable gastric cancer.* EBioMedicine, 2019.

118. Bradshaw, R.A., H. Hondermarck, and H. Rodriguez, *Cancer Proteomics and the Elusive Diagnostic Biomarkers.* Proteomics, 2019: p. e1800445.

119. Ricciuti, B., G.C. Leonardi, and M. Brambilla, *Emerging Biomarkers in the Era of Personalized Cancer Medicine.* Dis Markers, 2019. **2019**: p. 5907238.

120. Kim, S., et al., *High tumoral PD-L1 expression and low PD-1(+) or CD8(+) tumor-infiltrating lymphocytes are predictive of a poor prognosis in primary diffuse large B-cell lymphoma of the central nervous system.* Oncoimmunology, 2019. **8**(9): p. e1626653.

121. Andrieu, G.P., et al., *BET protein targeting suppresses the PD-1/PD-L1 pathway in triple-negative breast cancer and elicits anti-tumor immune response.* Cancer Lett, 2019. **465**: p. 45-58.

122. Aguilar, E.J., et al., *Outcomes to first-line pembrolizumab in patients with non-small cell lung cancer and very high PD-L1 expression.* Ann Oncol, 2019.

123. de Paiva, C.S., *Effects of Aging in Dry Eye.* Int Ophthalmol Clin, 2017. **57**(2): p. 47-64.

124. Sen, D.K., et al., *Biological variation of immunoglobulin concentrations in normal human tears related to age and sex.* Acta Ophthalmol (Copenh), 1978. **56**(3): p. 439-44.

125. McGill, J.I., et al., *Normal tear protein profiles and age-related changes.* Br J Ophthalmol, 1984. **68**(5): p. 316-20.

126. Micera, A., et al., *Age-Related Changes to Human Tear Composition.* Invest Ophthalmol Vis Sci, 2018. **59**(5): p. 2024-2031.

127. Nattinen, J., et al., *Age-associated changes in human tear proteome.* Clin Proteomics, 2019. **16**: p. 11.

128. Tummanapalli, S.S., et al., *The Effect of Age, Gender and Body Mass Index on Tear Film Neuromediators and Corneal Nerves.* Curr Eye Res, 2019: p. 1-8.

129. Kollock, C.W., *Diseases and functional disorders of the eye, produced by normal and abnormal conditions of the sexual organs.* Trans S C Med Assoc, 1888: p. 97-102.

130. Khan, D., R. Dai, and S. Ansar Ahmed, *Sex differences and estrogen regulation of miRNAs in lupus, a prototypical autoimmune disease.* Cell Immunol, 2015. **294**(2): p. 70-9.

131. D'Arbonneau, F., et al., *Thyroid dysfunction in primary Sjogren's syndrome: a long-term followup study.* Arthritis Rheum, 2003. **49**(6): p. 804-9.

132. Ostrer, H., *Sex-based differences in gene transmission and gene expression.* Lupus, 1999. **8**(5): p. 365-9.

133. Azzarolo, A.M., et al., *Hypophysectomy-induced regression of female rat lacrimal glands: partial restoration and maintenance by dihydrotestosterone and prolactin.* Invest Ophthalmol Vis Sci, 1995. **36**(1): p. 216-26.

134. Sullivan, D.A., et al., *TFOS DEWS II Sex, Gender, and Hormones Report.* Ocul Surf, 2017. **15**(3): p. 284-333.

135. Imbert, Y., et al., *MUC1 and estrogen receptor alpha gene polymorphisms in dry eye patients.* Exp Eye Res, 2009. **88**(3): p. 334-8.

136. Sullivan, B.D., et al., *Complete androgen insensitivity syndrome: effect on human meibomian gland secretions.* Arch Ophthalmol, 2002. **120**(12): p. 1689-99.

137. Chew, C.K., et al., *The casual level of meibomian lipids in humans.* Curr Eye Res, 1993. **12**(3): p. 255-9.

138. Sullivan, D.A. and L.E. Hann, *Hormonal influence on the secretory immune system of the eye: endocrine impact on the lacrimal gland accumulation and secretion of IgA and IgG.* J Steroid Biochem, 1989. **34**(1-6): p. 253-62.

139. Sullivan, D.A. and M.R. Allansmith, *Hormonal modulation of tear volume in the rat.* Exp Eye Res, 1986. **42**(2): p. 131-9.

140. Zylberberg, C., et al., *Estrogen up-regulation of metalloproteinase-2 and -9 expression in rabbit lacrimal glands.* Exp Eye Res, 2007. **84**(5): p. 960-72.

141. Khandelwal, P., S. Liu, and D.A. Sullivan, *Androgen regulation of gene expression in human meibomian gland and conjunctival epithelial cells.* Mol Vis, 2012. **18**: p. 1055-67.

142. Versura, P., G. Giannaccare, and E.C. Campos, *Sex-steroid imbalance in females and dry eye.* Curr Eye Res, 2015. **40**(2): p. 162-75.

143. Truong, S., et al., *Sex hormones and the dry eye.* Clin Exp Optom, 2014. **97**(4): p. 324-36.

144. Schaumberg, D.A., et al., *Hormone replacement therapy and dry eye syndrome.* JAMA, 2001. **286**(17): p. 2114-9.

145. Krenzer, K.L., et al., *Effect of androgen deficiency on the human meibomian gland and ocular surface.* J Clin Endocrinol Metab, 2000. **85**(12): p. 4874-82.

146. Schein, O.D., et al., *Prevalence of dry eye among the elderly.* Am J Ophthalmol, 1997. **124**(6): p. 723-8.

147. Brandt, J.E., et al., *Sex differences in Sjogren's syndrome: a comprehensive review of immune mechanisms.* Biol Sex Differ, 2015. **6**: p. 19.

148. Cohen, L.S., et al., *Risk for new onset of depression during the menopausal transition: the Harvard study of moods and cycles.* Arch Gen Psychiatry, 2006. **63**(4): p. 385-90.

149. Cyranowski, J.M., et al., *Adolescent onset of the gender difference in lifetime rates of major depression: a theoretical model.* Arch Gen Psychiatry, 2000. **57**(1): p. 21-7.

150. Maciel, G., et al., *Prevalence of Primary Sjogren's Syndrome in a US Population-Based Cohort.* Arthritis Care Res (Hoboken), 2017. **69**(10): p. 1612-1616.

151. Li, W. and M.C. Lin, *Sex Disparity in How Pain Sensitivity Influences Dry Eye Symptoms.* Cornea, 2019. **38**(10): p. 1291-1298.

152. Gibson, E.J., et al., *Local synthesis of sex hormones: are there consequences for the ocular surface and dry eye?* Br J Ophthalmol, 2017. **101**(12): p. 1596-1603.

153. Luu-The, V., *Assessment of steroidogenesis and steroidogenic enzyme functions.* J Steroid Biochem Mol Biol, 2013. **137**: p. 176-82.

154. Luu-The, V. and F. Labrie, *The intracrine sex steroid biosynthesis pathways.* Prog Brain Res, 2010. **181**: p. 177-92.

155. Suzuki, T., et al., *Expression of sex steroid hormone receptors in human cornea.* Curr Eye Res, 2001. **22**(1): p. 28-33.

156. Ananthi, S., et al., *Comparative proteomics of human male and female tears by two-dimensional electrophoresis.* Exp Eye Res, 2011. **92**(6): p. 454-63.

157. Mii, S., et al., *Analysis of human tear proteins by two-dimensional electrophoresis.* Electrophoresis, 1992. **13**(6): p. 379-82.

158. van Setten, G.B., G.S. Schultz, and S. Macauley, *Growth factors in human tear fluid and in lacrimal glands.* Adv Exp Med Biol, 1994. **350**: p. 315-9.

159. Nava, A., et al., *The effects of age, gender, and fluid dynamics on the concentration of tear film epidermal growth factor.* Cornea, 1997. **16**(4): p. 430-8.

160. Zhou, L., et al., *In-depth analysis of the human tear proteome.* J Proteomics, 2012. **75**(13): p. 3877-85.

161. Dor, M., et al., *Investigation of the global protein content from healthy human tears.* Exp Eye Res, 2019. **179**: p. 64-74.

162. Zhou, L. and R.W. Beuerman, *Tear analysis in ocular surface diseases.* Prog Retin Eye Res, 2012. **31**(6): p. 527-50.

163. Kijlstra, A., S.H. Jeurissen, and K.M. Koning, *Lactoferrin levels in normal human tears.* Br J Ophthalmol, 1983. **67**(3): p. 199-202.

164. Ahn, S.M. and R.J. Simpson, *Body fluid proteomics: Prospects for biomarker discovery.* Proteomics Clin Appl, 2007. **1**(9): p. 1004-15.

165. Zhao, M., et al., *A Comparative Proteomics Analysis of Five Body Fluids: Plasma, Urine, Cerebrospinal Fluid, Amniotic Fluid, and Saliva.* Proteomics Clin Appl, 2018. **12**(6): p. e1800008.

166. Hu, S., J.A. Loo, and D.T. Wong, *Human body fluid proteome analysis.* Proteomics, 2006. **6**(23): p. 6326-53.

167. Csosz, E., et al., *Diabetic retinopathy: Proteomic approaches to help the differential diagnosis and to understand the underlying molecular mechanisms.* J Proteomics, 2017. **150**: p. 351-358.

168. Kallo, G., et al., *Changes in the Chemical Barrier Composition of Tears in Alzheimer's Disease Reveal Potential Tear Diagnostic Biomarkers.* PLoS One, 2016. **11**(6): p. e0158000.

169. Versura, P., et al., *Diagnostic performance of a tear protein panel in early dry eye.* Mol Vis, 2013. **19**: p. 1247-57.

170. Li, N., et al., *Characterization of human tear proteome using multiple proteomic analysis techniques.* J Proteome Res, 2005. **4**(6): p. 2052-61.

171. Funke, S., et al., *Longitudinal analysis of taurine induced effects on the tear proteome of contact lens wearers and dry eye patients using a RP-RP-Capillary-HPLC-MALDI TOF/TOF MS approach.* J Proteomics, 2012. **75**(11): p. 3177-90.

172. Karnati, R., D.E. Laurie, and G.W. Laurie, *Lacritin and the tear proteome as natural replacement therapy for dry eye.* Exp Eye Res, 2013. **117**: p. 39-52.

173. McKown, R.L., et al., *Lacritin and other new proteins of the lacrimal functional unit.* Exp Eye Res, 2009. **88**(5): p. 848-58.

174. *Lacripep™ in Subjects With Dry Eye Associated With Primary Sjögren's Syndrome.* ClinicalTrials.gov, 2017. **U.S. National Library of Medicine**(clinicaltrials.gov/ct2/show/study/NCT03226444).

175. Boze, H., et al., *Proline-rich salivary proteins have extended conformations.* Biophys J, 2010. **99**(2): p. 656-65.

176. Csosz, E., et al., *Quantitative analysis of proteins in the tear fluid of patients with diabetic retinopathy.* J Proteomics, 2012. **75**(7): p. 2196-204.

177. Baraniuk, J.N., et al., *Protein networks in induced sputum from smokers and COPD patients.* Int J Chron Obstruct Pulmon Dis, 2015. **10**: p. 1957-75.

178. Casado, B., et al., *Protein expression in sputum of smokers and chronic obstructive pulmonary disease patients: a pilot study by CapLC-ESI-Q-TOF.* J Proteome Res, 2007. **6**(12): p. 4615-23.

179. Ekizoglu, S., et al., *PRR4: A novel downregulated gene in laryngeal cancer.* Oncol Lett, 2018. **15**(4): p. 4669-4675.

180. Zinovyeva, M.V., et al., *Identification of some human genes oppositely regulated during esophageal squamous cell carcinoma formation and human embryonic esophagus development.* Dis Esophagus, 2010. **23**(3): p. 260-70.

181. Acera, A., et al., *Changes in tear protein profile in keratoconus disease.* Eye (Lond), 2011. **25**(9): p. 1225-33.

182. Perumal, N., et al., *Characterization of human reflex tear proteome reveals high expression of lacrimal proline-rich protein 4 (PRR4).* Proteomics, 2015. **15**(19): p. 3370-81.

183. Bennick, A., *Structural and genetic aspects of proline-rich proteins.* J Dent Res, 1987. **66**(2): p. 457-61.

184. Wichmann, C., et al., *MaxQuant.Live Enables Global Targeting of More Than 25,000 Peptides.* Mol Cell Proteomics, 2019. **18**(5): p. 982-994.

185. Cox, J. and M. Mann, *MaxQuant enables high peptide identification rates, individualized p.p.b.-range mass accuracies and proteome-wide protein quantification.* Nat Biotechnol, 2008. **26**(12): p. 1367-72.

186. Carvalho, A.S., D. Penque, and R. Matthiesen, *Bottom up proteomics data analysis strategies to explore protein modifications and genomic variants.* Proteomics, 2015. **15**(11): p. 1789-1792.

187. Catherman, A.D., O.S. Skinner, and N.L. Kelleher, *Top Down proteomics: Facts and perspectives.* Biochemical and Biophysical Research Communications, 2014. **445**(4): p. 683-693.

188. Tang, N., P. Tornatore, and S.R. Weinberger, *Current developments in SELDI affinity technology.* Mass Spectrom Rev, 2004. **23**(1): p. 34-44.

189. Hill, H.H., Jr., et al., *Ion mobility spectrometry.* Anal Chem, 1990. **62**(23): p. 1201A-1209A.

190. Michelmann, K., et al., *Fundamentals of trapped ion mobility spectrometry.* J Am Soc Mass Spectrom, 2015. **26**(1): p. 14-24.

191. Stephens, W.E., *A Pulsed Mass Spectrometer with Time Dispersion.* Physical Review, 1946. **69**(11-1): p. 691-691.

192. Zubarev, R.A. and A. Makarov, *Orbitrap Mass Spectrometry.* Analytical Chemistry, 2013. **85**(11): p. 5288-5296.

193. Scigelova, M., et al., *Fourier Transform Mass Spectrometry.* Molecular & Cellular Proteomics, 2011. **10**(7).

194. Paul, W., *Electromagnetic Traps for Charged and Neutral Particles.* Reviews of Modern Physics, 1990. **62**(3): p. 531-540.

195. Sleno, L. and D.A. Volmer, *Ion activation methods for tandem mass spectrometry.* Journal of Mass Spectrometry, 2004. **39**(10): p. 1091-1112.

196. Morris, H.R., D.H. Williams, and R.D. Ambler, *Determination of Sequences of Protein-Derived Peptides and Peptide Mixtures by Mass Spectrometry.* Biochemical Journal, 1971. **125**(1): p. 189-&.

197. Vasilopoulou, C.G., et al., *Trapped ion mobility spectrometry and PASEF enable in-depth lipidomics from minimal sample amounts.* Nat Commun, 2020. **11**(1): p. 331.

198. Bantscheff, M., et al., *Quantitative mass spectrometry in proteomics: a critical review.* Anal Bioanal Chem, 2007. **389**(4): p. 1017-31.

199. de Souza, G.A., L.M. Godoy, and M. Mann, *Identification of 491 proteins in the tear fluid proteome reveals a large number of proteases and protease inhibitors.* Genome Biol, 2006. **7**(8): p. R72.

200. Green-Church, K.B., et al., *Investigation of the human tear film proteome using multiple proteomic approaches.* Mol Vis, 2008. **14**: p. 456-70.

201. Lema, I., et al., *Proteomic analysis of the tear film in patients with keratoconus.* Mol Vis, 2010. **16**: p. 2055-61.

202. Pong, J.C., et al., *Identification of hemopexin in tear film.* Anal Biochem, 2010. **404**(1): p. 82-5.

203. Pieragostino, D., et al., *Differential protein expression in tears of patients with primary open angle and pseudoexfoliative glaucoma.* Mol Biosyst, 2012. **8**(4): p. 1017-28.

204. Pieragostino, D., et al., *Shotgun proteomics reveals specific modulated protein patterns in tears of patients with primary open angle glaucoma naive to therapy.* Mol Biosyst, 2013. **9**(6): p. 1108-16.

205. Li, B., et al., *Tear proteomic analysis of patients with type 2 diabetes and dry eye syndrome by two-dimensional nano-liquid chromatography coupled with tandem mass spectrometry.* Invest Ophthalmol Vis Sci, 2014. **55**(1): p. 177-86.

206. Salvisberg, C., et al., *Exploring the human tear fluid: discovery of new biomarkers in multiple sclerosis.* Proteomics Clin Appl, 2014. **8**(3-4): p. 185-94.

207. Masoudi, S., et al., *Method development for quantification of five tear proteins using selected reaction monitoring (SRM) mass spectrometry.* Invest Ophthalmol Vis Sci, 2014. **55**(2): p. 767-75.

208. Leonardi, A., et al., *Identification of human tear fluid biomarkers in vernal keratoconjunctivitis using iTRAQ quantitative proteomics.* Allergy, 2014. **69**(2): p. 254-60.

209. Tong, L., et al., *Quantitation of 47 human tear proteins using high resolution multiple reaction monitoring (HR-MRM) based-mass spectrometry.* J Proteomics, 2015. **115**: p. 36-48.

210. Funke, S., et al., *Analysis of the effects of preservative-free tafluprost on the tear proteome.* Am J Transl Res, 2016. **8**(10): p. 4025-4039.

211. Aluru, S.V., et al., *Tear Fluid Protein Changes in Dry Eye Syndrome Associated with Rheumatoid Arthritis: A Proteomic Approach.* Ocul Surf, 2017. **15**(1): p. 112-129.

212. Aass, C., et al., *Comparative proteomic analysis of tear fluid in Graves' disease with and without orbitopathy.* Clin Endocrinol (Oxf), 2016. **85**(5): p. 805-812.

213. Scieranski, *Identifizierung von Biomarkern aus Tränen von Sicca- und Glaukompatienten mit einer Targeted Proteomikstrategie.* 2017.

214. Aqrawi, L.A., et al., *Identification of potential saliva and tear biomarkers in primary Sjogren's syndrome, utilising the extraction of extracellular vesicles and proteomics analysis.* Arthritis Res Ther, 2017. **19**(1): p. 14.

215. Yenihayat, F., et al., *Comparative proteome analysis of the tear samples in patients with low-grade keratoconus.* Int Ophthalmol, 2018. **38**(5): p. 1895-1905.

216. Gerber-Hollbach, N., et al., *Tear Film Proteomics Reveal Important Differences Between Patients With and Without Ocular GvHD After Allogeneic Hematopoietic Cell Transplantation.* Invest Ophthalmol Vis Sci, 2018. **59**(8): p. 3521-3530.

217. Nattinen, J., et al., *Patient stratification in clinical glaucoma trials using the individual tear proteome.* Sci Rep, 2018. **8**(1): p. 12038.

218. Manicam, C., et al., *Proteomics Unravels the Regulatory Mechanisms in Human Tears Following Acute Renouncement of Contact Lens Use: A Comparison between Hard and Soft Lenses.* Sci Rep, 2018. **8**(1): p. 11526.

219. Boerger, M., et al., *Proteomic analysis of tear fluid reveals disease-specific patterns in patients with Parkinson's disease - A pilot study.* Parkinsonism Relat Disord, 2019.

220. Roger Eidet, J., *Tear proteome in uveitis.* Acta Ophthalmologica, 2019. **97**(S263).

221. Ji, Y.W., et al., *Changes in Human Tear Proteome Following Topical Treatment of Dry Eye Disease: Cyclosporine A Versus Diquafosol Tetrasodium.* Invest Ophthalmol Vis Sci, 2019. **60**(15): p. 5035-5044.

222. Kenny, A., et al., *Proteins and microRNAs are differentially expressed in tear fluid from patients with Alzheimer's disease.* Sci Rep, 2019. **9**(1): p. 15437.

223. Ong, S.E., et al., *Stable isotope labeling by amino acids in cell culture, SILAC, as a simple and accurate approach to expression proteomics.* Mol Cell Proteomics, 2002. **1**(5): p. 376-86.

224. Gygi, S.P., et al., *Quantitative analysis of complex protein mixtures using isotope-coded affinity tags.* Nat Biotechnol, 1999. **17**(10): p. 994-9.

225. Ross, P.L., et al., *Multiplexed protein quantitation in Saccharomyces cerevisiae using amine-reactive isobaric tagging reagents.* Mol Cell Proteomics, 2004. **3**(12): p. 1154-69.

226. Gerber, S.A., et al., *Absolute quantification of proteins and phosphoproteins from cell lysates by tandem MS.* Proc Natl Acad Sci U S A, 2003. **100**(12): p. 6940-5.

227. Bantscheff, M., et al., *Quantitative mass spectrometry in proteomics: critical review update from 2007 to the present.* Anal Bioanal Chem, 2012. **404**(4): p. 939-65.

228. Cox, J., et al., *Accurate proteome-wide label-free quantification by delayed normalization and maximal peptide ratio extraction, termed MaxLFQ.* Mol Cell Proteomics, 2014. **13**(9): p. 2513-26.

229. Perumal, N., *Characterization of Human Tear Proteome in Dry Eye Syndrome.* Doctoral Thesis, 2015.

230. Versura, P., et al., *Tear proteomics in evaporative dry eye disease.* Eye (Lond), 2010. **24**(8): p. 1396-402.

231. Grus, F.H. and A.J. Augustin, *High performance liquid chromatography analysis of tear protein patterns in diabetic and non-diabetic dry-eye patients.* Eur J Ophthalmol, 2001. **11**(1): p. 19-24.

232. Maissa, C. and M. Guillon, *Tear film dynamics and lipid layer characteristics--effect of age and gender.* Cont Lens Anterior Eye, 2010. **33**(4): p. 176-82.

233. Craig, J.P. and A. Tomlinson, *Importance of the lipid layer in human tear film stability and evaporation.* Optom Vis Sci, 1997. **74**(1): p. 8-13.

234. Wright, J.C. and G.E. Meger, *A Review of the Schirmer Test for Tear Production.* JAMA Ophthalmology, 1962. **67**(5): p. 564-565.

235. Cox, J., et al., *Andromeda: a peptide search engine integrated into the MaxQuant environment.* J Proteome Res, 2011. **10**(4): p. 1794-805.

236. Tyanova, S. and J. Cox, *Perseus: A Bioinformatics Platform for Integrative Analysis of Proteomics Data in Cancer Research.* Methods Mol Biol, 2018. **1711**: p. 133-148.

237. Tyanova, S., et al., *The Perseus computational platform for comprehensive analysis of (prote)omics data.* Nat Methods, 2016. **13**(9): p. 731-40.

238. Krämer, A., et al., *Causal analysis approaches in ingenuity pathway analysis.* Bioinformatics, 2013. **30**(4): p. 523-530.

239. Gonzalez, N., et al., *Evaluation of inter-day and inter-individual variability of tear peptide/protein profiles by MALDI-TOF MS analyses.* Mol Vis, 2012. **18**: p. 1572-82.

240. Jensen, O.N., et al., *Automation of matrix-assisted laser desorption/ionization mass spectrometry using fuzzy logic feedback control.* Anal Chem, 1997. **69**(9): p. 1706-14.

241. Annesley, T.M., *Ion suppression in mass spectrometry.* Clin Chem, 2003. **49**(7): p. 1041-4.

242. Karas, M., U. Bahr, and U. Gießmann, *Matrix-assisted laser desorption ionization mass spectrometry.* Mass Spectrometry Reviews, 1991. **10**(5): p. 335-357.

243. Lehmann, W.D., M. Kessler, and W.A. König, *Investigations on basic aspects of fast atom bombardment mass spectrometry: Matrix effects, sample effects, sensitivity and quantification.* Biomedical Mass Spectrometry, 1984. **11**(5): p. 217-222.

244. Bucknall, M., Fung, K.Y.C. & Duncan, M.W., *Practical quantitative biomedical applications of MALDI-TOF mass spectrometry.* J. Am. Soc. Spectrom, 2002. **13**: p. 1015–1027.

245. Szajli, E., T. Feher, and K.F. Medzihradszky, *Investigating the quantitative nature of MALDI-TOF MS.* Mol Cell Proteomics, 2008. **7**(12): p. 2410-8.

246. Oviano, M., et al., *Universal protocol for the rapid automated detection of carbapenem-resistant Gram-negative bacilli directly from blood cultures by matrix-assisted laser*

desorption/ionisation time-of-flight mass spectrometry (MALDI-TOF/MS). Int J Antimicrob Agents, 2016. **48**(6): p. 655-660.

247. Fu, Q., et al., *Application of porous metal enrichment probe sampling to single cell analysis using matrix-assisted laser desorption ionization time of flight mass spectrometry (MALDI-TOF-MS).* J Mass Spectrom, 2016. **51**(1): p. 62-8.

248. Pabst, M., et al., *Quantification of saquinavir from lysates of peripheral blood mononuclear cells using microarrays and standard MALDI-TOF-MS.* J Am Soc Mass Spectrom, 2014. **25**(6): p. 1083-6.

249. Fung, K.Y., et al., *Characterization of the in vivo forms of lacrimal-specific proline-rich proteins in human tear fluid.* Proteomics, 2004. **4**(12): p. 3953-9.

250. Rastogi, V., P. Kalra, and M. Vanitha Gowda, *Relationship between Salivary Alpha-2 Macroglobulin and HbA1c among Patients with Type-2 Diabetes Mellitus: A Cross-sectional Study.* Indian Journal of Endocrinology and Metabolism, 2019. **23**(2): p. 184-187.

251. Koo, B.S., et al., *Comparative analysis of the tear protein expression in blepharitis patients using two-dimensional electrophoresis.* J Proteome Res, 2005. **4**(3): p. 719-24.

252. Pignatelli, P., et al., *Serum albumin and risk of cardiovascular events in primary and secondary prevention: a systematic review of observational studies and Bayesian meta-regression analysis.* Intern Emerg Med, 2019.

253. Cabrerizo, S., et al., *Serum albumin and health in older people: Review and meta analysis.* Maturitas, 2015. **81**(1): p. 17-27.

254. Ananthi, S., et al., *Comparative analysis of the tear protein profile in mycotic keratitis patients.* Mol Vis, 2008. **14**: p. 500-7.

255. Younus, H., S. Ahmad, and M.F. Alam, *Correlation between the activity of aldehyde dehydrogenase and oxidative stress markers in the saliva of diabetic patients.* Protein Pept Lett, 2019.

256. Wang, K. and J. Li, *Overexpression of ANXA3 is an independent prognostic indicator in gastric cancer and its depletion suppresses cell proliferation and tumor growth.* Oncotarget, 2016. **7**(52): p. 86972-86984.

257. Vanni, H., et al., *Cigarette smoking induces overexpression of a fat-depleting gene AZGP1 in the human.* Chest, 2009. **135**(5): p. 1197-1208.

258. Tian, H., et al., *Downregulation of AZGP1 by Ikaros and histone deacetylase promotes tumor progression through the PTEN/Akt and CD44s pathways in hepatocellular carcinoma.* Carcinogenesis, 2017. **38**(2): p. 207-217.

259. Kristensen, G., et al., *Predictive value of AZGP1 following radical prostatectomy for prostate cancer: a cohort study and meta-analysis.* J Clin Pathol, 2019. **72**(10): p. 696-704.

260. Shih, A.R. and M.R. Murali, *Laboratory tests for disorders of complement and complement regulatory proteins.* Am J Hematol, 2015. **90**(12): p. 1180-6.

261. van Oostrom, A.J., et al., *The metabolic syndrome in relation to complement component 3 and postprandial lipemia in patients from an outpatient lipid clinic and healthy volunteers.* Atherosclerosis, 2007. **190**(1): p. 167-73.

262. Ueta, M., et al., *Gene expression analysis of conjunctival epithelium of patients with Stevens-Johnson syndrome in the chronic stage.* BMJ Open Ophthalmol, 2019. **4**(1): p. e000254.

263. Yang, C., et al., *Association between clusterin concentration and dementia: a systematic review and meta-analysis.* Metab Brain Dis, 2019. **34**(1): p. 129-140.

264. Lin, C.C., et al., *Apolipoprotein J, a glucose-upregulated molecular chaperone, stabilizes core and NS5A to promote infectious hepatitis C virus virion production.* J Hepatol, 2014. **61**(5): p. 984-93.

265. Sansanwal, P., L. Li, and M.M. Sarwal, *Inhibition of intracellular clusterin attenuates cell death in nephropathic cystinosis.* J Am Soc Nephrol, 2015. **26**(3): p. 612-25.

266. Trougakos, I.P., *The molecular chaperone apolipoprotein J/clusterin as a sensor of oxidative stress: implications in therapeutic approaches - a mini-review.* Gerontology, 2013. **59**(6): p. 514-23.

267. Liu, B., et al., *Downregulation of clusterin expression in human testicular seminoma.* Cell Physiol Biochem, 2013. **32**(4): p. 1117-23.

268. Lutsenko, S., et al., *Cellular multitasking: the dual role of human Cu-ATPases in cofactor delivery and intracellular copper balance.* Arch Biochem Biophys, 2008. **476**(1): p. 22-32.

269. Virit, O., et al., *High ceruloplasmin levels are associated with obsessive compulsive disorder: a case control study.* Behav Brain Funct, 2008. **4**: p. 52.

270. Elkassabany, N.M., et al., *Green plasma-revisited.* Anesthesiology, 2008. **108**(4): p. 764-5.

271. Koskelo, P., et al., *Serum ceruloplasmin concentration in rheumatoid arthritis, ankylosing spondylitis, psoriasis and sarcoidosis.* Acta Rheumatol Scand, 1966. **12**(4): p. 261-6.

272. Wolf, T.L., J. Kotun, and J.H. Meador-Woodruff, *Plasma copper, iron, ceruloplasmin and ferroxidase activity in schizophrenia.* Schizophr Res, 2006. **86**(1-3): p. 167-71.

273. Scheinberg, I.H. and D. Gitlin, *Deficiency of ceruloplasmin in patients with hepatolenticular degeneration (Wilson's disease).* Science, 1952. **116**(3018): p. 484-5.

274. Dai, D.N., et al., *Elevated expression of CST1 promotes breast cancer progression and predicts a poor prognosis.* J Mol Med (Berl), 2017. **95**(8): p. 873-886.

275. Wang, Y., et al., *Determination of Clinical Cut-Off Values for Serum Cystatin C Levels to Predict Ischemic Stroke Risk.* J Stroke Cerebrovasc Dis, 2019. **28**(11): p. 104345.

276. Maetzler, W., et al., *The CST3 BB genotype and low cystatin C cerebrospinal fluid levels are associated with dementia in Lewy body disease.* J Alzheimers Dis, 2010. **19**(3): p. 937-42.

277. Dou, Y., et al., *Antibody-sandwich ELISA analysis of a novel blood biomarker of CST4 in gastrointestinal cancers.* Onco Targets Ther, 2018. **11**: p. 1743-1756.

278. Gan, P., et al., *Knockdown of cathepsin D protects dopaminergic neurons against neuroinflammation-mediated neurotoxicity through inhibition of NF-kappaB signalling pathway in Parkinson's disease model.* Clin Exp Pharmacol Physiol, 2018.

279. Sasaki, M., et al., *Expression of deleted in malignant brain tumor-1 (DMBT1) molecule in biliary epithelium is augmented in hepatolithiasis: possible participation in lithogenesis.* Dig Dis Sci, 2003. **48**(7): p. 1234-40.

280. Madsen, J., et al., *A variant form of the human deleted in malignant brain tumor 1 (DMBT1) gene shows increased expression in inflammatory bowel diseases and interacts with dimeric trefoil factor 3 (TFF3).* PLoS One, 2013. **8**(5): p. e64441.

281. Prado, L.L., et al., *Anti-alpha-enolase antibodies in Behcet's disease: a marker of mucocutaneous and articular disease activity?* Clin Exp Rheumatol, 2018. **36**(6 Suppl 115): p. 28-32.

282. Cancemi, P., et al., *Expression of Alpha-Enolase (ENO1), Myc Promoter-Binding Protein-1 (MBP-1) and Matrix Metalloproteinases (MMP-2 and MMP-9) Reflect the Nature and Aggressiveness of Breast Tumors.* Int J Mol Sci, 2019. **20**(16).

283. Olivares-Martinez, E., et al., *alpha-enolase is an antigenic target in primary Sjogren's syndrome.* Clin Exp Rheumatol, 2019. **37 Suppl 118**(3): p. 29-35.

284. Wu, Q. and O. Eickelberg, *Ezrin in Asthma: A First Step to Early Biomarkers of Airway Epithelial Dysfunction.* Am J Respir Crit Care Med, 2019. **199**(4): p. 408-410.

285. Ye, D.J., et al., *Discovery of Ezrin Expression as a Potential Biomarker for Chemically Induced Ocular Irritation Using Human Corneal Epithelium Cell Line and a Reconstructed Human Cornea-like Epithelium Model.* Toxicol Sci, 2018. **165**(2): p. 335-346.

286. Matsumoto, I., et al., *Revisit of autoimmunity to glucose-6-phosphate isomerase in experimental and rheumatoid arthritis.* Mod Rheumatol, 2019: p. 1-7.

287. Acera, A., et al., *Changes in tear protein profile in patients with conjunctivochalasis.* Cornea, 2011. **30**(1): p. 42-9.

288. Beckett, G.J., et al., *Plasma glutathione S-transferase measurements after paracetamol overdose: evidence for early hepatocellular damage.* Gut, 1985. **26**(1): p. 26-31.

289. Szigeti, A., et al., *Induction of necrotic cell death and mitochondrial permeabilization by heme binding protein 2/SOUL.* FEBS Lett, 2006. **580**(27): p. 6447-54.

290. Tolosano, E. and F. Altruda, *Hemopexin: structure, function, and regulation.* DNA Cell Biol, 2002. **21**(4): p. 297-306.

291. Bozidis, P., et al., *HSP70 polymorphisms in first psychotic episode drug-naive schizophrenic patients.* Life Sci, 2014. **100**(2): p. 133-7.

292. Arrigo, A.P., et al., *Hsp27 (HspB1) and alphaB-crystallin (HspB5) as therapeutic targets.* FEBS Lett, 2007. **581**(19): p. 3665-74.

293. Jin, R., et al., *Quantification of Epstein-Barr virus DNA in patients with idiopathic orbital inflammatory pseudotumor.* PLoS One, 2013. **8**(1): p. e50812.

294. Zhang, X.R., et al., *[The tear proteomics analysis of conjunctivochalasis].* Zhonghua Yan Ke Za Zhi, 2009. **45**(2): p. 135-40.

295. Zamanian Azodi, M., et al., *Fluoxetine Regulates Ig Kappa Chain C Region Expression Levels in the Serum of Obsessive-Compulsive Disorder Patients: A proteomic Approach.* Iran J Pharm Res, 2017. **16**(3): p. 1264-1271.

296. Ghorbian, S., et al., *Evaluation diagnostic usefulness of immunoglobulin light chains (Igkappa, Iglambda) and incomplete IGH D-J clonal gene rearrangements in patients with B-cell non-Hodgkin lymphomas using BIOMED-2 protocol.* Clin Transl Oncol, 2014. **16**(11): p. 1006-11.

297. Redl, B., et al., *Identification of a lipocalin in mucosal glands of the human tracheobronchial tree and its enhanced secretion in cystic fibrosis.* Lab Invest, 1998. **78**(9): p. 1121-9.

298. Tian, Y., *LCN 1 is highly expressed in cholangiocarcinoma patients and indicates poor prognosis.* Int J Clin Exp Med, 2018. **11**(10).

299. Wang, X.R., et al., *Increased serum levels of lipocalin-1 and -2 in patients with stable chronic obstructive pulmonary disease.* Int J Chron Obstruct Pulmon Dis, 2014. **9**: p. 543-9.

300. Goldstein, S.L., *Acute kidney injury biomarkers: renal angina and the need for a renal troponin I.* BMC Med, 2011. **9**: p. 135.

301. Nickolas, T.L., et al., *NGAL (Lcn2) monomer is associated with tubulointerstitial damage in chronic kidney disease.* Kidney Int, 2012. **82**(6): p. 718-22.

302. Bi, F., et al., *Reactive astrocytes secrete lcn2 to promote neuron death.* Proc Natl Acad Sci U S A, 2013. **110**(10): p. 4069-74.

303. Roudkenar, M.H., et al., *Upregulation of neutrophil gelatinase-associated lipocalin, NGAL/Lcn2, in beta-thalassemia patients.* Arch Med Res, 2008. **39**(4): p. 402-7.

304. Hassan, R. and M. Ho, *Mesothelin targeted cancer immunotherapy.* Eur J Cancer, 2008. **44**(1): p. 46-53.

305. Zhu, Z., et al., *Overexpression of P4HB is correlated with poor prognosis in human clear cell renal cell carcinoma.* Cancer Biomark, 2019.

306. Rajkumar, K., et al., *Understanding perspectives of signalling mechanisms regulating PEBP1 function.* Cell Biochem Funct, 2016. **34**(6): p. 394-403.

307. Burgula, S., et al., *Downregulation of PEBP1 in rat brain cortex in hypoxia.* J Mol Neurosci, 2010. **41**(1): p. 36-47.

308. Ding, Z., et al., *Silencing profilin-1 inhibits endothelial cell proliferation, migration and cord morphogenesis.* J Cell Sci, 2006. **119**(Pt 19): p. 4127-37.

309. Kaetzel, C.S., et al., *The polymeric immunoglobulin receptor (secretory component) mediates transport of immune complexes across epithelial cells: a local defense function for IgA.* Proc Natl Acad Sci U S A, 1991. **88**(19): p. 8796-800.

310. Honma, N., et al., *Comparative study of monoclonal antibody B72.3 and gross cystic disease fluid protein-15 as markers of apocrine carcinoma of the breast.* APMIS, 2006. **114**(10): p. 712-9.

311. Priyadarsini, S., et al., *Gross cystic disease fluid protein-15/prolactin-inducible protein as a biomarker for keratoconus disease.* PLoS One, 2014. **9**(11): p. e113310.

312. Gallo, A., et al., *Gross Cystic Disease Fluid Protein-15(GCDFP-15)/Prolactin-Inducible Protein (PIP) as Functional Salivary Biomarker for Primary Sjogren's Syndrome.* J Genet Syndr Gene Ther, 2013. **4**.

313. Desai, S., et al., *Tissue-specific isoform switch and DNA hypomethylation of the pyruvate kinase PKM gene in human cancers.* Oncotarget, 2014. **5**(18): p. 8202-10.

314. Wei, Y., et al., *Antiapoptotic and proapoptotic signaling of cyclophilin A in endothelial cells.* Inflammation, 2013. **36**(3): p. 567-72.

315. Hoffmann, H. and C. Schiene-Fischer, *Functional aspects of extracellular cyclophilins.* Biol Chem, 2014. **395**(7-8): p. 721-35.

316. Liu, D., et al., *Proteomic analysis of lung tissue in a rat acute lung injury model: identification of PRDX1 as a promoter of inflammation.* Mediators Inflamm, 2014. **2014**: p. 469358.

317. Mullen, L., et al., *Cysteine Oxidation Targets Peroxiredoxins 1 and 2 for Exosomal Release through a Novel Mechanism of Redox-Dependent Secretion.* Mol Med, 2015. **21**: p. 98-108.

318. Holley, J.E., et al., *Peroxiredoxin V in multiple sclerosis lesions: predominant expression by astrocytes.* Mult Scler, 2007. **13**(8): p. 955-61.

319. Fischer, A., et al., *A novel sarcoidosis risk locus for Europeans on chromosome 11q13.1.* Am J Respir Crit Care Med, 2012. **186**(9): p. 877-85.

320. Avila, P.C., et al., *Peroxiredoxin V contributes to antioxidant defense of lung epithelial cells.* Lung, 2008. **186**(2): p. 103-14.

321. Kunze, A., et al., *Peroxiredoxin 5 (PRX5) is correlated inversely to systemic markers of inflammation in acute stroke.* Stroke, 2014. **45**(2): p. 608-10.

322. Power, J.H., et al., *Nonselenium glutathione peroxidase in human brain : elevated levels in Parkinson's disease and dementia with lewy bodies.* Am J Pathol, 2002. **161**(3): p. 885-94.

323. Yun, H.M., et al., *PRDX6 promotes lung tumor progression via its GPx and iPLA2 activities.* Free Radic Biol Med, 2014. **69**: p. 367-76.

324. Kubo, E., et al., *TAT-mediated PRDX6 protein transduction protects against eye lens epithelial cell death and delays lens opacity.* Am J Physiol Cell Physiol, 2008. **294**(3): p. C842-55.

325. Saijyothi, A.V., et al., *Two dimensional electrophoretic analysis of human tears: collection method in dry eye syndrome.* Electrophoresis, 2010. **31**(20): p. 3420-7.

326. Li, S., et al., *Ribonuclease 4 protects neuron degeneration by promoting angiogenesis, neurogenesis, and neuronal survival under stress.* Angiogenesis, 2013. **16**(2): p. 387-404.

327. Gupta, S.K., B.J. Haigh, and T.T. Wheeler, *Abundance of RNase4 and RNase5 mRNA and protein in host defence related tissues and secretions in cattle.* Biochem Biophys Rep, 2016. **8**: p. 261-267.

328. Cecil, D.L. and R. Terkeltaub, *Transamidation by transglutaminase 2 transforms S100A11 calgranulin into a procatabolic cytokine for chondrocytes.* J Immunol, 2008. **180**(12): p. 8378-85.

329. Rety, S., et al., *Structural basis of the Ca(2+)-dependent association between S100C (S100A11) and its target, the N-terminal part of annexin I.* Structure, 2000. **8**(2): p. 175-84.

330. Passey, R.J., et al., *S100A8: emerging functions and regulation.* J Leukoc Biol, 1999. **66**(4): p. 549-56.

331. Cheng, P., et al., *Inhibition of dendritic cell differentiation and accumulation of myeloid-derived suppressor cells in cancer is regulated by S100A9 protein.* J Exp Med, 2008. **205**(10): p. 2235-49.

332. Ali, H., et al., *Localization and characterization of a novel secreted protein, SCUBE2, in the development and progression of atherosclerosis.* Kobe J Med Sci, 2013. **59**(4): p. E122-31.

333. Ali, H., et al., *Upregulation of SCUBE2 expression in dyslipidemic type 2 diabetes mellitus is associated with endothelin-1.* Diabetes Metab Syndr, 2019. **13**(5): p. 2869-2872.

334. Song, Q., et al., *Decreased expression of SCUBE2 is associated with progression and prognosis in colorectal cancer.* Oncol Rep, 2015. **33**(4): p. 1956-64.

335. Kuhn, E.C., et al., *Circulating levels of selenium-binding protein 1 (SELENBP1) are associated with risk for major adverse cardiac events and death.* J Trace Elem Med Biol, 2019. **52**: p. 247-253.

336. Kanazawa, T., et al., *The utility of SELENBP1 gene expression as a biomarker for major psychotic disorders: replication in schizophrenia and extension to bipolar disorder with psychosis.* Am J Med Genet B Neuropsychiatr Genet, 2008. **147B**(6): p. 686-9.

337. Nakamura, H., et al., *Discovery of candidate proteins, PIGR and SELENBP1, as novel markers of airway diseases in COPD.* European Respiratory Journal, 2013. **42**(Suppl 57): p. P593.

338. Zeng, G.Q., et al., *The function and significance of SELENBP1 downregulation in human bronchial epithelial carcinogenic process.* PLoS One, 2013. **8**(8): p. e71865.

339. Kalsheker, N.A., *Alpha 1-antichymotrypsin.* Int J Biochem Cell Biol, 1996. **28**(9): p. 961-4.

340. Yang, G.D., et al., *SERPINA3 promotes endometrial cancer cells growth by regulating G2/M cell cycle checkpoint and apoptosis.* Int J Clin Exp Pathol, 2014. **7**(4): p. 1348-58.

341. Zhou, J., et al., *Up-regulation of SERPINA3 correlates with high mortality of melanoma patients and increased migration and invasion of cancer cells.* Oncotarget, 2017. **8**(12): p. 18712-18725.

342. Vanni, S., et al., *Differential overexpression of SERPINA3 in human prion diseases.* Sci Rep, 2017. **7**(1): p. 15637.

343. Akkouh, I.A., et al., *Expression of TCN1 in Blood is Negatively Associated with Verbal Declarative Memory Performance.* Sci Rep, 2018. **8**(1): p. 12654.

344. Carmel, R., J. Parker, and Z. Kelman, *Mutations of TCN1 Cause Transcobalamin I Deficiency with Low Serum Cobalamin Levels That Are Indistinguishable From Cobalamin Deficiency.* Blood, 2009. **114**(22): p. 1989-1989.

345. Lai, T.S. and C.S. Greenberg, *Histaminylation of fibrinogen by tissue transglutaminase-2 (TGM-2): potential role in modulating inflammation.* Amino Acids, 2013. **45**(4): p. 857-64.

346. Bradford, M., et al., *The functional significance of the TGM2 gene in schizophrenia: a correlation of SNPs and circulating IL-2 levels.* J Neuroimmunol, 2011. **232**(1-2): p. 5-7.

347. Ai, L., et al., *The transglutaminase 2 gene (TGM2), a potential molecular marker for chemotherapeutic drug sensitivity, is epigenetically silenced in breast cancer.* Carcinogenesis, 2008. **29**(3): p. 510-8.

348. Sax, C.M., et al., *Transketolase gene expression in the cornea is influenced by environmental factors and developmentally controlled events.* Cornea, 2000. **19**(6): p. 833-41.

349. Nagarajan, N., S. Oka, and J. Sadoshima, *Modulation of signaling mechanisms in the heart by thioredoxin 1.* Free Radic Biol Med, 2017. **109**: p. 125-131.

350. Yoshida, T., et al., *The involvement of thioredoxin and thioredoxin binding protein-2 on cellular proliferation and aging process.* Ann N Y Acad Sci, 2005. **1055**: p. 1-12.

351. Miranda, M. and A. Sorkin, *Regulation of receptors and transporters by ubiquitination: new insights into surprisingly similar mechanisms.* Mol Interv, 2007. **7**(3): p. 157-67.

352. Wang, T., et al., *Integrated bioinformatic analysis reveals YWHAB as a novel diagnostic biomarker for idiopathic pulmonary arterial hypertension.* J Cell Physiol, 2019. **234**(5): p. 6449-6462.

353. Minamida, S., et al., *14-3-3 protein beta/alpha as a urinary biomarker for renal cell carcinoma: proteomic analysis of cyst fluid.* Anal Bioanal Chem, 2011. **401**(1): p. 245-52.

354. Zahid, S., et al., *Differential expression of proteins in brain regions of Alzheimer's disease patients.* Neurochem Res, 2014. **39**(1): p. 208-15.

355. Escudero-Paniagua, B., et al., *PAUF/ZG16B promotes colorectal cancer progression through alterations of the mitotic functions and the Wnt/beta-catenin pathway.* Carcinogenesis, 2019.

356. da Silva, A., *Salivary Zymogen Granule Protein 16B Drops at Onset of Chronic Graft-Versus-Host Disease: A Possible Salivary Biomarker for Oral Chronic Graft-Versus-Host Disease.* Biology of Blood and Marrow Transplantation, 2019. **25**(3): p. S26.

357. Moran, A.P., M.M. Prendergast, and B.J. Appelmelk, *Molecular mimicry of host structures by bacterial lipopolysaccharides and its contribution to disease.* FEMS Immunol Med Microbiol, 1996. **16**(2): p. 105-15.

358. Suter, L., et al., *[Rule of antibody structure. The primary structure of a monoclonal immunoglobulin L-chain of kappa-type, subgroup 3 (Bence-Jones protein Ti). IV. The complete amino acid sequence and its significance for the mechanism of antibody production].* Hoppe Seylers Z Physiol Chem, 1972. **353**(2): p. 189-208.

359. Yang, J., et al., *An iron delivery pathway mediated by a lipocalin.* Mol Cell, 2002. **10**(5): p. 1045-56.

360. Takahashi, M., et al., *Immunofluorescence localization of cystatins in human lacrimal gland and in the exorbital lacrimal gland of the rat.* Acta Ophthalmol (Copenh), 1992. **70**(5): p. 625-31.

361. Baron, A., A. DeCarlo, and J. Featherstone, *Functional aspects of the human salivary cystatins in the oral environment.* Oral Diseases, 1999. **5**(3): p. 234-240.

362. Croce, K., et al., *Myeloid-related protein-8/14 is critical for the biological response to vascular injury.* Circulation, 2009. **120**(5): p. 427-36.

363. Cordeiro, A.T., et al., *Crystal structure of human phosphoglucose isomerase and analysis of the initial catalytic steps.* Biochim Biophys Acta, 2003. **1645**(2): p. 117-22.

364. Lichenstein, H.S., et al., *Afamin is a new member of the albumin, alpha-fetoprotein, and vitamin D-binding protein gene family.* J Biol Chem, 1994. **269**(27): p. 18149-54.

365. Gurney, M.E., et al., *Neuroleukin: a lymphokine product of lectin-stimulated T cells.* Science, 1986. **234**(4776): p. 574-81.

366. Jester, J.V., *Corneal crystallins and the development of cellular transparency.* Semin Cell Dev Biol, 2008. **19**(2): p. 82-93.

367. Pappa, A., N.A. Sophos, and V. Vasiliou, *Corneal and stomach expression of aldehyde dehydrogenases: from fish to mammals.* Chem Biol Interact, 2001. **130-132**(1-3): p. 181-91.

368. Pappa, A., et al., *Aldh3a1 protects human corneal epithelial cells from ultraviolet- and 4-hydroxy-2-nonenal-induced oxidative damage.* Free Radic Biol Med, 2003. **34**(9): p. 1178-89.

369. Mayer, M.P. and B. Bukau, *Hsp70 chaperones: cellular functions and molecular mechanism.* Cell Mol Life Sci, 2005. **62**(6): p. 670-84.

370. Heinrich, P.C., J.V. Castell, and T. Andus, *Interleukin-6 and the acute phase response.* Biochem J, 1990. **265**(3): p. 621-36.

371. Jiao, Y., Y. Lu, and X.Y. Li, *Farnesoid X receptor: a master regulator of hepatic triglyceride and glucose homeostasis.* Acta Pharmacol Sin, 2015. **36**(1): p. 44-50.

372. Joseph, S.B., et al., *Reciprocal regulation of inflammation and lipid metabolism by liver X receptors.* Nat Med, 2003. **9**(2): p. 213-9.

373. Jain, S., V. Gautam, and S. Naseem, *Acute-phase proteins: As diagnostic tool.* J Pharm Bioallied Sci, 2011. **3**(1): p. 118-27.

374. Liu, N., et al., *Transcuprein is a macroglobulin regulated by copper and iron availability.* J Nutr Biochem, 2007. **18**(9): p. 597-608.

375. Sottrup-Jensen, L., *Alpha-macroglobulins: structure, shape, and mechanism of proteinase complex formation.* J Biol Chem, 1989. **264**(20): p. 11539-42.

376. Yeung, K., et al., *Mechanism of suppression of the Raf/MEK/extracellular signal-regulated kinase pathway by the raf kinase inhibitor protein.* Mol Cell Biol, 2000. **20**(9): p. 3079-85.

377. Klock, C., T.R. Diraimondo, and C. Khosla, *Role of transglutaminase 2 in celiac disease pathogenesis.* Semin Immunopathol, 2012. **34**(4): p. 513-22.

378. McConkey, D.J. and S. Orrenius, *The role of calcium in the regulation of apoptosis.* Biochem Biophys Res Commun, 1997. **239**(2): p. 357-66.

379. Circu, M.L. and T.Y. Aw, *Reactive oxygen species, cellular redox systems, and apoptosis.* Free Radic Biol Med, 2010. **48**(6): p. 749-62.

380. Valko, M., et al., *Free radicals, metals and antioxidants in oxidative stress-induced cancer.* Chem Biol Interact, 2006. **160**(1): p. 1-40.

381. Dufour, S., Mellon, Leandri, Jouannet, Rougeot, *Opiorphin Secretion Pattern in Healthy Volunteers: Gender difference and Organ specificity.* Biochemistry & Analytical Biochemistry, 2013. **2**.

382. D'Souza, S. and L. Tong, *Practical issues concerning tear protein assays in dry eye.* Eye Vis (Lond), 2014. **1**: p. 6.

383. Glasgow, B.J., et al., *Tear lipocalin: structure, function and molecular mechanisms of action.* Adv Exp Med Biol, 2002. **506**(Pt A): p. 555-65.

384. Hassan, M.I., et al., *Prolactin inducible protein in cancer, fertility and immunoregulation: structure, function and its clinical implications.* Cell Mol Life Sci, 2009. **66**(3): p. 447-59.

385. End, C., et al., *DMBT1 functions as pattern-recognition molecule for poly-sulfated and poly-phosphorylated ligands.* Eur J Immunol, 2009. **39**(3): p. 833-42.

386. Garrido, C., et al., *HSP27 and HSP70: potentially oncogenic apoptosis inhibitors.* Cell Cycle, 2003. **2**(6): p. 579-84.

387. De Lisle, R.C. and U. Hopfer, *Electrolyte permeabilities of pancreatic zymogen granules: implications for pancreatic secretion.* Am J Physiol, 1986. **250**(4 Pt 1): p. G489-96.

388. Fabian, T.K., et al., *Salivary defense proteins: their network and role in innate and acquired oral immunity.* Int J Mol Sci, 2012. **13**(4): p. 4295-320.

389. Märk, T.D. and G.H. Dunn, *Electron Impact Ionization*. 2013: Springer Vienna.

390. Dai, Y.Q., R.M. Whittal, and L. Li, *Two-layer sample preparation: A method for MALDI-MS analysis of complex peptide and protein mixtures.* Analytical Chemistry, 1999. **71**(5): p. 1087-1091.

391. Nordhoff, E., et al., *Sample preparation protocols for MALDI-MS of peptides and oligonucleotides using prestructured sample supports.* International Journal of Mass Spectrometry, 2003. **226**(1): p. 163-180.

392. Koonin, E.V., *Conserved sequence pattern in a wide variety of phosphoesterases.* Protein Sci, 1994. **3**(2): p. 356-8.

393. Stastna, M. and J.E. Van Eyk, *Analysis of protein isoforms: can we do it better?* Proteomics, 2012. **12**(19-20): p. 2937-48.

8. APPENDIX

Appendix 1: Correlations of peptides for Schirmer length, TBUT, age, and gender.

	Schirmer lenght (mm)				TBUT (mm)				Age				Gender			
	r(X,Y)	r^2	T	p	r(X,Y)	r^2	t	P	r(X,Y)	r^2	t	p	t	p	Mean Male	Mean Female
A2M	-0.41	0.17	-5.56	1.12E-07	-0.23	0.05	-2.91	4.16E-03	n.s.	n.s.	n.s.	n.s.	n.s.	n.s.	n.s.	n.s.
ALB	-0.36	0.13	-4.88	2.57E-06	-0.29	0.09	-3.82	1.95E-04	n.s.	n.s.	n.s.	n.s.	n.s.	n.s.	n.s.	n.s.
ALDH1A1	-0.26	0.07	-3.36	9.66E-04	n.s.	n.s.	n.s.	n.s.	n.s.	n.s.	n.s.	n.s.	n.s.	n.s.	n.s.	n.s.
ALDH3A1	-0.60	0.36	-9.33	9.81E-17	-0.23	0.05	-2.94	3.83E-03	n.s.	n.s.	n.s.	n.s.	n.s.	n.s.	n.s.	n.s.
ANXA1	-0.20	0.04	-2.51	1.32E-02	n.s.	n.s.	n.s.	n.s.	n.s.	n.s.	n.s.	n.s.	n.s.	n.s.	n.s.	n.s.
ANXA2	-0.59	0.35	-9.24	1.70E-16	-0.19	0.04	-2.38	1.86E-02	n.s.	n.s.	n.s.	n.s.	n.s.	n.s.	n.s.	n.s.
ANXA3	-0.50	0.25	-7.18	2.73E-11	-0.26	0.07	-3.39	8.77E-04	n.s.	n.s.	n.s.	n.s.	n.s.	n.s.	n.s.	n.s.
AZGP1	n.s.	n.s.	n.s.	n.s.	n.s.	n.s.	n.s.	n.s.	n.s.	n.s.	n.s.	n.s.	n.s.	n.s.	n.s.	n.s.
C3	-0.19	0.04	-2.47	1.47E-02	-0.23	0.05	-2.98	3.31E-03	n.s.	n.s.	n.s.	n.s.	n.s.	n.s.	n.s.	n.s.
CASP14	-0.28	0.08	-3.59	4.37E-04	-0.18	0.03	-2.34	2.05E-02	n.s.	n.s.	n.s.	n.s.	n.s.	n.s.	n.s.	n.s.
CLU	0.43	0.19	5.96	1.64E-08	n.s.	n.s.	n.s.	n.s.	n.s.	n.s.	n.s.	n.s.	n.s.	n.s.	n.s.	n.s.
CP	n.s.	n.s.	n.s.	n.s.	-0.20	0.04	-2.50	1.33E-02	n.s.	n.s.	n.s.	n.s.	n.s.	n.s.	n.s.	n.s.
CST1	0.33	0.11	4.32	2.78E-05	-0.22	0.05	-2.79	5.95E-03	n.s.	n.s.	n.s.	n.s.	n.s.	n.s.	n.s.	n.s.
CST3	-0.17	0.03	-2.17	3.12E-02	-0.32	0.10	-4.15	5.43E-05	n.s.	n.s.	n.s.	n.s.	n.s.	n.s.	n.s.	n.s.
CST4	0.18	0.03	2.29	2.31E-02	-0.31	0.09	-4.03	8.83E-05	n.s.	n.s.	n.s.	n.s.	n.s.	n.s.	n.s.	n.s.
CSTB	-0.39	0.15	-5.24	5.04E-07	n.s.	n.s.	n.s.	n.s.	n.s.	n.s.	n.s.	n.s.	n.s.	n.s.	n.s.	n.s.
CTSD	n.s.	n.s.	n.s.	n.s.	-0.22	0.05	-2.86	4.79E-03	n.s.	n.s.	n.s.	n.s.	n.s.	n.s.	n.s.	n.s.
DMBT1	0.50	0.25	7.18	2.61E-11	n.s.	n.s.	n.s.	n.s.	n.s.	n.s.	n.s.	n.s.	n.s.	n.s.	n.s.	n.s.
ENO1	-0.67	0.44	-11.15	1.32E-21	-0.17	0.03	-2.20	2.90E-02	n.s.	n.s.	n.s.	n.s.	n.s.	n.s.	n.s.	n.s.
EZR	n.s.	n.s.	n.s.	n.s.	-0.21	0.04	-2.69	7.85E-03	n.s.	n.s.	n.s.	n.s.	n.s.	n.s.	n.s.	n.s.
GPI	-0.69	0.47	-11.76	3.00E-23	-0.41	0.17	-5.58	1.02E-07	n.s.	n.s.	n.s.	n.s.	n.s.	n.s.	n.s.	n.s.
GSN	n.s.	n.s.	n.s.	n.s.	n.s.	n.s.	n.s.	n.s.	n.s.	n.s.	n.s.	n.s.	n.s.	n.s.	n.s.	n.s.

Appendix 1: (continued)

	Schirmer lenght (mm)				TBUT (mm)				Age				Gender			
	r(X,Y)	r²	T	p	r(X,Y)	r²	t	P	r(X,Y)	r²	t	p	t	p	Mean Male	Mean Female
GSTP1	-0.29	0.08	-3.75	2.51E-04	n.s.	n.s.	n.s.	n.s.	n.s.	n.s.	n.s.	n.s.	n.s.	n.s.	n.s.	n.s.
HEBP2	-0.46	0.21	-6.38	1.88E-09	n.s.	n.s.	n.s.	n.s.	n.s.	n.s.	n.s.	n.s.	n.s.	n.s.	n.s.	n.s.
HP	n.s.	n.s.	n.s.	n.s.	n.s.	n.s.	n.s.	n.s.	n.s.	n.s.	n.s.	n.s.	n.s.	n.s.	n.s.	n.s.
HPX	-0.47	0.22	-6.62	5.35E-10	-0.20	0.04	-2.49	1.39E-02	n.s.	n.s.	n.s.	n.s.	n.s.	n.s.	n.s.	n.s.
HSPA8	-0.35	0.12	-4.63	7.74E-06	-0.34	0.12	-4.55	1.09E-05	n.s.	n.s.	n.s.	n.s.	-2.23	3.05E-02	15.15	16.11
HSPB1	n.s.	n.s.	n.s.	n.s.	n.s.	n.s.	n.s.	n.s.	n.s.	n.s.	n.s.	n.s.	n.s.	n.s.	n.s.	n.s.
IGHA1	0.21	0.04	2.67	8.28E-03	0.17	0.03	2.12	3.54E-02	-0.34	0.12	-2.47	1.73E-02	n.s.	n.s.	n.s.	n.s.
IGKC	n.s.	n.s.	n.s.	n.s.	-0.29	0.08	-3.75	2.53E-04	n.s.	n.s.	n.s.	n.s.	n.s.	n.s.	n.s.	n.s.
IgLambda	n.s.	n.s.	n.s.	n.s.	-0.35	0.13	-4.73	4.93E-06	n.s.	n.s.	n.s.	n.s.	n.s.	n.s.	n.s.	n.s.
LACRT	0.25	0.06	3.18	1.76E-03	0.24	0.06	3.07	2.49E-03	n.s.	n.s.	n.s.	n.s.	2.46	1.76E-02	25.75	23.76
LCN1	n.s.	n.s.	n.s.	n.s.	n.s.	n.s.	n.s.	n.s.	n.s.	n.s.	n.s.	n.s.	n.s.	n.s.	n.s.	n.s.
LCN2	n.s.	n.s.	n.s.	n.s.	-0.17	0.03	-2.16	3.22E-02	0.37	0.13	2.66	1.06E-02	n.s.	n.s.	n.s.	n.s.
LDHA	-0.18	0.03	-2.32	2.18E-02	-0.23	0.05	-2.94	3.77E-03	n.s.	n.s.	n.s.	n.s.	n.s.	n.s.	n.s.	n.s.
LGALS3	-0.16	0.03	-2.00	4.69E-02	n.s.	n.s.	n.s.	n.s.	-0.30	0.09	-2.11	4.01E-02	n.s.	n.s.	n.s.	n.s.
LTF	0.17	0.03	2.15	3.31E-02	0.17	0.03	2.16	3.27E-02	n.s.	n.s.	n.s.	n.s.	n.s.	n.s.	n.s.	n.s.
LYZ	n.s.	n.s.	n.s.	n.s.	n.s.	n.s.	n.s.	n.s.	n.s.	n.s.	n.s.	n.s.	n.s.	n.s.	n.s.	n.s.
MSLN	0.39	0.15	5.33	3.41E-07	n.s.	n.s.	n.s.	n.s.	-0.30	0.09	-2.16	3.57E-02	n.s.	n.s.	n.s.	n.s.
P4HB	-0.25	0.06	-3.19	1.74E-03	-0.29	0.08	-3.77	2.29E-04	n.s.	n.s.	n.s.	n.s.	n.s.	n.s.	n.s.	n.s.
PEBP1	-0.56	0.32	-8.53	1.17E-14	-0.23	0.05	-2.97	3.40E-03	n.s.	n.s.	n.s.	n.s.	n.s.	n.s.	n.s.	n.s.
PFN1	-0.28	0.08	-3.69	3.07E-04	n.s.	n.s.	n.s.	n.s.	n.s.	n.s.	n.s.	n.s.	n.s.	n.s.	n.s.	n.s.
PIGR	0.18	0.03	2.26	2.50E-02	-0.23	0.05	-2.90	4.33E-03	n.s.	n.s.	n.s.	n.s.	n.s.	n.s.	n.s.	n.s.
PIP	0.32	0.10	4.21	4.34E-05	n.s.	n.s.	n.s.	n.s.	-0.42	0.18	-3.18	2.63E-03	n.s.	n.s.	n.s.	n.s.
PKM	-0.24	0.06	-3.06	2.57E-03	-0.27	0.07	-3.49	6.25E-04	n.s.	n.s.	n.s.	n.s.	n.s.	n.s.	n.s.	n.s.
PPIA	-0.52	0.27	-7.65	1.89E-12	-0.26	0.07	-3.34	1.05E-03	n.s.	n.s.	n.s.	n.s.	n.s.	n.s.	n.s.	n.s.
PRDX1	-0.25	0.06	-3.29	1.23E-03	-0.24	0.06	-3.09	2.37E-03	n.s.	n.s.	n.s.	n.s.	n.s.	n.s.	n.s.	n.s.

Appendix 1: (continued)

	Schirmer lenght (mm)				TBUT (mm)				Age				Gender			
	r(X,Y)	r²	T	p	r(X,Y)	r²	t	P	r(X,Y)	r²	t	p	t	p	Mean Male	Mean Female
PRDX5	-0.33	0.11	-4.31	2.90E-05	-0.17	0.03	-2.17	3.14E-02	n.s.	n.s.	n.s.	n.s.	n.s.	n.s.	n.s.	n.s.
PRDX6	-0.33	0.11	-4.32	2.74E-05	n.s.	n.s.	n.s.	n.s.	n.s.	n.s.	n.s.	n.s.	n.s.	n.s.	n.s.	n.s.
PROL1	0.54	0.29	8.00	2.71E-13	n.s.	n.s.	n.s.	n.s.	n.s.	n.s.	n.s.	n.s.	n.s.	n.s.	n.s.	n.s.
PRR4_N1	n.s.	n.s.	n.s.	n.s.	n.s.	n.s.	n.s.	n.s.	-0.25	0.06	-3.18	1.79E-03	n.s.	n.s.	n.s.	n.s.
PRR4_N2	0.24	0.06	3.05	2.72E-03	n.s.	n.s.	n.s.	n.s.	n.s.	n.s.	n.s.	n.s.	n.s.	n.s.	n.s.	n.s.
PRR4_N3	n.s.	n.s.	n.s.	n.s.	n.s.	n.s.	n.s.	n.s.	n.s.	n.s.	n.s.	n.s.	n.s.	n.s.	n.s.	n.s.
PRR4_N4	n.s.	n.s.	n.s.	n.s.	n.s.	n.s.	n.s.	n.s.	-0.38	0.14	-2.78	7.77E-03	n.s.	n.s.	n.s.	n.s.
PRR4_SUM	0.35	0.13	4.73	4.90E-06	n.s.	n.s.	n.s.	n.s.	n.s.	n.s.	n.s.	n.s.	2.45	1.82E-02	27.16	26.09
RNASE4	0.24	0.06	3.15	1.93E-03	-0.20	0.04	-2.58	1.07E-02	n.s.	n.s.	n.s.	n.s.	n.s.	n.s.	n.s.	n.s.
S100A11	-0.22	0.05	-2.75	6.66E-03	-0.27	0.07	-3.50	6.07E-04	n.s.	n.s.	n.s.	n.s.	n.s.	n.s.	n.s.	n.s.
S100A4	n.s.	n.s.	n.s.	n.s.	-0.18	0.03	-2.34	2.07E-02	n.s.	n.s.	n.s.	n.s.	n.s.	n.s.	n.s.	n.s.
S100A8	n.s.	n.s.	n.s.	n.s.	-0.36	0.13	-4.79	3.79E-06	n.s.	n.s.	n.s.	n.s.	n.s.	n.s.	n.s.	n.s.
S100A9	-0.31	0.10	-4.12	6.09E-05	-0.38	0.14	-5.08	1.07E-06	n.s.	n.s.	n.s.	n.s.	n.s.	n.s.	n.s.	n.s.
S100P	n.s.	n.s.	n.s.	n.s.	n.s.	n.s.	n.s.	n.s.	n.s.	n.s.	n.s.	n.s.	n.s.	n.s.	n.s.	n.s.
SCGB1D1	0.22	0.05	2.87	4.66E-03	n.s.	n.s.	n.s.	n.s.	-0.39	0.16	-2.91	5.57E-03	n.s.	n.s.	n.s.	n.s.
SCGB2A1	0.35	0.13	4.74	4.76E-06	n.s.	n.s.	n.s.	n.s.	-0.33	0.11	-2.37	2.18E-02	n.s.	n.s.	n.s.	n.s.
SCUBE2	-0.17	0.03	-2.19	2.98E-02	-0.27	0.07	-3.51	5.78E-04	n.s.	n.s.	n.s.	n.s.	-2.15	3.72E-02	16.59	17.88
SELENBP1	-0.32	0.10	-4.16	5.22E-05	n.s.	n.s.	n.s.	n.s.	n.s.	n.s.	n.s.	n.s.	n.s.	n.s.	n.s.	n.s.
SERPINA3	n.s.	n.s.	n.s.	n.s.	n.s.	n.s.	n.s.	n.s.	0.29	0.09	2.08	4.31E-02	n.s.	n.s.	n.s.	n.s.
TCN1	0.24	0.06	3.12	2.15E-03	n.s.	n.s.	n.s.	n.s.	n.s.	n.s.	n.s.	n.s.	n.s.	n.s.	n.s.	n.s.
TGM2	-0.37	0.14	-4.97	1.71E-06	n.s.	n.s.	n.s.	n.s.	n.s.	n.s.	n.s.	n.s.	n.s.	n.s.	n.s.	n.s.
TKT	-0.51	0.27	-7.50	4.53E-12	n.s.	n.s.	n.s.	n.s.	n.s.	n.s.	n.s.	n.s.	n.s.	n.s.	n.s.	n.s.
TXN	n.s.	n.s.	n.s.	n.s.	-0.35	0.12	-4.67	6.38E-06	n.s.	n.s.	n.s.	n.s.	n.s.	n.s.	n.s.	n.s.
UBA52	-0.33	0.11	-4.37	2.27E-05	-0.28	0.08	-3.68	3.21E-04	n.s.	n.s.	n.s.	n.s.	n.s.	n.s.	n.s.	n.s.
YWHAB	-0.33	0.11	-4.44	1.71E-05	-0.20	0.04	-2.49	1.39E-02	n.s.	n.s.	n.s.	n.s.	n.s.	n.s.	n.s.	n.s.
YWHAZ	-0.26	0.07	-3.30	1.20E-03	-0.21	0.04	-2.68	8.11E-03	n.s.	n.s.	n.s.	n.s.	n.s.	n.s.	n.s.	n.s.
ZG16B	0.64	0.40	10.27	3.23E-19	n.s.	n.s.	n.s.	n.s.	-0.36	0.13	-2.59	1.27E-02	n.s.	n.s.	n.s.	n.s.

Negative correlations factors of significant proteins are marked in blue, positive ones in red. **n.s.** = not significant.

Appendix 2: -log Benjamini-Hochberg p values for IPA analyses of diseases and biological functions, canonical pathways, and upstream regulators.

	(-log(Benjamini-Hochberg p-value)					
Diseases and Biological Functions	**DRYlip vs. CTRL**	**DRYaq vs. CTRL**	**DRYaqlip vs. CTRL**	**DRYaq vs. DRYlip**	**DRYaqlip vs. DRYlip**	**DRYaqlip vs. DRYaq**
Degranulation of cells	0.00	7.13	11.37	3.04	2.99	6.83
Apoptosis	5.11	5.52	8.40	1.77	1.63	4.11
Cell movement	7.67	4.98	9.50	2.55	1.97	4.43
Quantity of reactive oxygen species	1.90	4.93	5.74	0.00	1.30	3.20
Allergy	8.39	4.66	8.19	2.37	0.00	3.00
Necrosis	5.07	4.18	6.05	1.77	1.60	4.11
Keratoconjunctivitis sicca	0.00	2.23	2.35	1.29	1.36	0.00
Inflammatory response	2.54	2.10	2.48	1.40	0.00	0.00
Dry eye	2.12	1.80	2.86	1.86	1.12	0.00
Eosinophilic inflammation	7.33	0.00	7.16	2.50	0.00	2.62
Immune response of cells	4.00	0.00	4.01	1.72	1.16	2.43
Viral Infection	3.96	0.00	3.92	1.59	1.39	2.08
Antibacterial response	3.16	0.00	2.50	0.00	1.46	1.68
Evaporative dry eye disease	1.62	0.00	0.00	0.00	0.00	0.00
Sjögren syndrome	1.58	0.00	2.00	0.00	0.00	0.00
Canonical Pathways						
Glycolysis I	2.2	1.9	3.1	1.2	1.1	2.5
Clathrin-mediated Endocytosis Signaling	2.5	1.0	3.1	1.2	0.7	2.2
LXR/RXR Activation	1.4	1.9	3.5	1.2	0.8	1.6
Acute Phase Response Signaling	0.7	2.1	3.1	0.0	0.7	3.2
FXR/RXR Activation	0.7	1.9	2.7	0.8	0.8	0.9
Gluconeogenesis I	2.2	1.9	1.8	1.2	1.1	1.3
Upstream regulators						
Lipopolysaccharide	8.37	5.26	7.74	2.51	1.78	6.44
TNF	3.72	1.98	5.08	2.51	2.48	7.73
Beta-estradiol	2.51	4.23	3.37	2.51	2.73	5.08
IL22	2.32	2.63	3.76	1.24	1.37	2.58
IL15	2.65	1.94	4.13	1.55	1.35	1.70
IL6	1.43	1.79	2.74	0.00	0.99	3.05
Progesterone	2.93	0.00	1.99	0.00	0.00	2.05

DANKSAGUNG

Zuerst gilt mein Dank meinem Doktorvater für die Möglichkeit meine Dissertation unter seiner Leitung schreiben zu dürfen und hierdurch wertvolle Erfahrungen in der wissenschaftlichen Forschung zu sammeln.

Darüber hinaus danke ich meinem Betreuer ohne dessen fachliche Anleitung, motivierenden Worte und Freundschaft diese Arbeit wohl nicht dieselbe gewesen wäre.

Vielen Dank auch an die Arbeitsgruppe der experimentellen Ophthalmologie, für ihre Anregungen und Korrekturen in allen Phasen dieser Arbeit.

Gewidmet ist diese Dissertation den Menschen, die nicht nur die turbulenten Höhen und Tiefen des Studiums, sondern auch dieser Arbeit maßgeblich miterlebt haben, auf verschiedenste Art und Weise.

Meinem Freund, der im Zuge dieser Arbeit unter meinen schwächelnden Deutschkenntnissen zu leiden hatte, wenn ich mich mal wieder zu tief im Englischen verlor und der zu meinen Ecken und Kanten passt wie kein anderer.

Meiner Familie, auf deren Unterstützung ich zu jeder Zeit zählen konnte und ohne die dieses Studium so sicherlich nicht möglich gewesen wäre.

Meinen Freunden – im wahrsten Sinne des Wortes Mitstreitern in allen Lebenslagen.